

UNIVERSITA' DEGLI STUDI DI VERONA

DEPARTMENT OF

SURGERY, DENTISTRY, PAEDIATRICS AND GYNAECOLOGY

GRADUATE SCHOOL OF

LIFE AND HEALTH SCIENCE

DOCTORAL PROGRAM IN

CARDIOVASCULAR SCIENCE

WITH THE FINANCIAL CONTRIBUTION OF

UNIVERSITY OF VERONA

Cycle / year XXXIV / 2018

TITLE OF THE DOCTORAL THESIS

Utilization of IL-11 induced miRNA-27b-5p and miRNA-497-5p as potential biomarkers of cardiac fibrosis

S.S.D. MED/11

Coordinator: Prof. GIOVANNI BATTISTA LUCIANI

Signature _____

Supervisor: Prof. GIUSEPPE FAGGIAN

Signature _____

Tutor: Prof.ssa JULIA GORELIK

Signature _____

Tutor: Prof.ssa COSTANZA EMANUELI

Signature _____

Tutor: Dott. FABIO MARTELLI

Signature _____

Tutor: Dott. BENEDICT REILLY O' DONNELL


Signature _____


Doctoral Student: Dott. ROMAN
TIKHOMIROV

Signature _____

This work is licensed under a Creative Commons Attribution-NonCommercial- NoDerivs 3.0 Unported License, Italy. To read a copy of the licence, visit the web page:

<http://creativecommons.org/licenses/by-nc-nd/3.0/>

 **Attribution** — You must give appropriate credit, provide a link to the license, and indicate if changes were made. You may do so in any reasonable manner, but not in any way that suggests the licensor endorses you or your use.

 **NonCommercial** — You may not use the material for commercial purposes.

NoDerivatives — If you remix, transform, or build upon the material, you may not distribute the modified material.

Utilization of IL-11 induced miRNA-27b-5p and miRNA-497-5p as potential biomarkers of cardiac fibrosis

Roman
Tikhomirov
PhD thesis
Verona,
ISBN 12324-
5678-910

University of Verona
Research Office – National and International PhD programmes ph:
045.802.8608 – fax 045.802.8411 – Via Giardino Giusti 2 – 37129
Verona

ABSTRACT

This work focuses upon the prediction and validation of the micro ribonucleic acids (miRNAs) -27b-5p and 497-5p as key regulators of cardiac fibroblast (CFs) to myofibroblast transdifferentiation and consequently cardiac fibrosis. We have studied the expression, functional role and molecular pathways of these miRNAs in distinct in vitro models of cardiac fibrosis. We also observed the expression pattern of miRNAs-27b-5p and -497-5p in the left ventricle and blood plasma of patients characterized with extensive extracellular matrix remodeling (ECMR). The narration is organized in four main paragraphs, each with a specific introduction, relative methods and discussion. The first part describes the methodology of predicting miRNAs which regulate two crucial pro-fibrotic pathways: transforming growth factor beta 1 (TGF β 1) and interleukin-11 (IL-11). Following this, miRNA expression was tested in rat CFs treated with TGF β 1 or IL-11 and in myocardial infarction (MI) rat CFs. Consequently, the expression levels of our best candidates (miRNA-497-5p and miRNA-27b-5p) were checked in human CFs. The second chapter further investigates miRNA-27b-5p and miRNA-497-5p and potential downstream targets through analysis of RNAseq data from human CFs treated with IL-11. Consequently, in the third phase of this study we probed miRNA-27b-5p, miRNA-497-5p and their targets to establish their functional role in rat CFs. In addition, miRNA-27b-5p and its target, EGLN1, was studied in human CFs. Finally, in the fourth part we translated our cellular studies to patient samples. We studied miRNA-27b-5p and miRNA-497-5p (and their targets) expression in left ventricle (LV) of patients with cardiac fibrosis induced by hypertrophy caused by aortic valve stenosis (AVS). Moreover, we investigated miRNAs levels in blood plasma of these patients and how they correlate with clinical parameters.

Cardiac fibrosis is a pathological condition which accompanies a wide variety of heart diseases. It impairs heart function by extensive deposition of extracellular matrix (ECM) into the myocardium. CFs in their activated form — myofibroblasts, act as the main source of ECM proteins and play a crucial role in the pathology. Fibroblast to myofibroblast transition can be regulated by many factors. In this

work we focused upon two crucial determinants of cardiac fibrosis: TGF β 1 and IL-11 and in particular on the role of their downstream effector molecules: miRNAs. These molecules are short (20-22 nucleotides) non-coding endogenous RNA molecules which participate in gene regulation by messenger ribonucleic acid (mRNA) degradation or inhibition of mRNA translation. It is possible for one miRNA to have multiple targets within the same biological process or even the same pathway. Our investigation of novel miRNAs, participating in the regulation of IL-11 pathway has the potential to elucidate the molecular mechanisms of cardiac fibrosis. Consequently, these novel miRNAs could be used as therapeutic targets in treatment of the pathology or as biomarkers of the disease.

Rationale of the chapter I: In order to find novel miRNAs which are regulating IL-11 and TGF β 1 pathways we had to design a bioinformatical pipeline, which would provide reliable candidates. We predicted miRNAs by using existing databases rather than conducting miRNAseq or miRNA array for several reasons: 1) bioinformatic prediction requires less time; 2) there is no requirement for large financial investment; 3) there is no requirement for practical experimental set up; 4) Prediction tools are not limited by the experimental model or species; 5) Data can be integrated and analyzed for both rats and humans. These criteria were important for us because we would like to check the functional role of our miRNAs in rat CFs before testing it in human fibroblasts.

Despite these substantial advantages, there are several limitations to this technique. Unfortunately, the prediction tools we have chosen (MirWalk, TargetScan and miRcode) often produce a high number of false positive candidates [1]. Due to the fact, that binding affinity of the miRNA is calculated mathematically by aggregated P_{CT} and it does not take into account many other parameters which can be important for the regulation of a target by miRNA. In order to overcome this limitation, we designed a bioinformatical pipeline which included comparison of binding affinity between miRNA and its target in three existing prediction tools (MirWalk, TargetScan and miRcode) rather than just one. In order to reduce the number of false positive candidates in our prediction process we introduced special selection criteria which are described precisely in the chapter I. Another limitation of our study is that we only considered miRNAs

expressed by CFs. According to the most recent literature, it is shown that miRNAs participate in cross-talk between cell types meaning there is a high likelihood that cardiomyocytes may also contribute to regulation of TGF β 1 and IL-11 pathways in CFs.

Aims of chapter I: 1) Predict miRNAs which can potentially contribute to the regulation of two crucial pro-fibrotic pathways: TGF β 1 and IL-11, which is working through extracellular regulated kinase (ERK). 2) Validate miRNA modulation by TGF β 1/IL-11 treatment. 3) Validate miRNA modulation in cardiac fibrosis associated models: MI rat CFs. 4) Investigate miRNA modulation in human CFs from pathological samples characterized by ECM remodeling and myofibroblasts activation: ischemic (ICM) or dilated cardiomyopathy (DCM).

Results of chapter I: Using our bioinformatical pipeline we predicted 7 miRNAs which regulate the IL-11 and TGF β 1 pathways. Using multiple in vitro models (IL-11, TGF β 1-treated rat CFs and MI rat CFs) we characterized our 7 “best candidate” miRNAs associated with cardiac fibrosis. We identified that miRNA-27b-5p, miRNA-497-5p and miRNA-21-5p are up-regulated in MI and IL-11 treated rat CFs. We focused our work upon miRNA-27b-5p and miRNA-497-5p as they are poorly characterized. We also found that miRNA-497-5p was up-modulated in human CFs from LV of patients with ICM and DCM, while miRNA-27b-5p was not regulated.

Rationale of chapter II: miRNAs can target several genes within the same biological process or pathway. We therefore aimed to observe if our miRNAs regulated targets from the IL-11 and TGF β 1 pathways. However, in our prediction approach (described in chapter I) we used already validated targets from the KEGG network. To identify new molecular mechanisms which underlie the pro-fibrotic response we decided to re-design our approach. In order to identify the downstream targets of miRNA-27b-5p and miRNA-497-5p we constructed a network of IL-11 and TGF β 1 differentially co-expressed genes by using existing data from the work of Schafer [2] and Chen [3]. The theoretical model of genes differentially co-expressed with IL-11 was created by an analysis of the gene correlation matrix with IL-11 by application filtration criteria: false discovery

rates (FDR) < 0.05 and correlation coefficient > 0.5. To validate the resulting targets, we used public RNA-sequencing (RNAseq) dataset done on human DCM CFs treated with 5 ng/μl IL-11 for 24 hours. After that, we compared the list of IL-11 co-expressed genes with list of miRNA-27b-5p and miRNA-497-5p targets with conserved binding sites between rat and human in order to detect target genes. Gene expression under IL-11 treatment was examined in DCM human CFs. Therefore, we filtered targets which were not regulated or up-modulated by IL-11 treatment and were not connected with cardiac fibrosis in literature. Consequently, downstream targets of our miRNAs were validated by dual luciferase assay. The re-designed approach has several advantages including the ability to investigate miRNAs targets which are differentially co-expressed with IL-11, which are then down-modulated by IL-11 treatment. In other words, IL-11 stimulation which results in IL-11 autocrine production by fibroblasts leads to target gene down-regulation in an IL-11 dependent manner. So miRNA-27b-5p and miRNA-497-5p may facilitate the IL-11 pro-fibrotic pathway by down-regulation of these certain genes. Moreover, with our target prediction approach we only considered targets which contain a conserved binding site between human and rat. Consequently, suppression of predicted targets by miRNAs should be valid in all of our in vitro models. Importantly, we have not considered any other cell types involved in cardiac fibrosis beyond cardiac fibroblasts. Future work of this project would include analysis of the IL-11 differential co-expression network in other cell types such as immune cells, cardiomyocytes and endothelial cells.

Aims of chapter II:

- 1) To predict targets for miRNA-497-5p and miRNA-27b-5p which are important in the regulation of the IL-11 pro-fibrotic pathway. For this to construct and characterize IL-11 and TGFβ1 stimulated differential co-expression network of genes.
- 2) To predict target genes in this network based on the binding affinity between miRNA and gene by using TargetScan 8.0.
- 3) To validate target gene suppression by miRNAs via dual luciferase assay.

4) To test predicted targets expression in rat cardiac fibroblasts treated with IL-11 and in MI rat cardiac fibroblasts.

Results of the chapter II: Using our bioinformatical approach we were able to construct an IL-11 differential co-expression network of genes based upon RNAseq from human DCM CFs. The resulting network consisted of 677 genes which have significant (FDR < 0.05) correlation with IL-11 autocrine expression in these CFs ($r > 0.5$ for positive correlation; $r < - 0.5$ for negative). This network was then integrated with an already existing network from (Chen et al. 2019) which produced a list of 1313 genes. Next, we constructed a protein-protein interaction network, based on data obtained for the IL11 and TGF β 1 pro-fibrotic networks. The resulting protein networks established themselves as a useful tool to identify novel pathways and to gain knowledge of disease-related pathways. The protein interaction network was organized using 'STRING v.11'. In STRING protein interaction is ranked by confidence level: in our study we required a medium or high confidence of association (> 0.4). The network obtained via STRING v.11 was imported in Cytoscape 3_7_1 to generate a network visualization graph. Cytoscape is very powerful software for topological analysis and network visualisation. In the resulting network graph, we applied continuous mapping of average log₂ (expression fold change) for nodes by color, in order to understand gene regulation under IL-11 treatment. We analyzed Gene Ontology (GO) enrichment of genes associated with a certain biological process or pathway. Consequently, we validated the significant enrichment of genes involved in MAPK and TGF β 1 pathways. To our surprise we also observed significant enrichment in genes associated with hypoxia (p-value < 0.00005). In order to experimentally validate the theoretical network, we conducted RNAseq on human DCM CFs treated with IL-11 5ng/ μ l for 24 hours. RNAseq data was normalized and differential expression (DE) fold change was calculated in Rstudio. Afterwards, we performed gene set enrichment analysis (GSEA). GSEA was conducted with default settings. As a result, we observed IL-11 treatment significantly up-regulated the IL-11 co-expression network we had constructed with a normalized enrichment score of 1.45 and FDR values below 0.05. As a next step, we compared a list of IL-11 co-expressed genes (1313 genes) with a list

of targets with binding sites conserved in human and rat for our miRNAs. This resulted in a list of targets for miRNA-27b-5p (28 genes) and for miRNA-497-5p (14 genes). Following this, we checked each target's gene expression under IL-11 treatment in human DCM CFs and investigated their functional role on UniProt. We found that the target of miRNA-27b-5p EGLN1 was decreased by IL-11 treatment (Gene Rank = -0.52). Moreover, recent studies by (Zhiu et al. 2021) demonstrated that loss of EGLN1 leads to hypertrophy and cardiac fibrosis. At the same time, we discovered that TRABD2B (target of miRNA-497-5p) is down-regulated by IL-11 treatment in human DCM CFs (Rank = -1.4). TRABD2B is a protein which acts as a negative regulator of WNT3A and WNT5A, which were considered to be pro-fibrotic proteins. Following our prediction, we constructed plasmids containing wild type (WT) and mutated (MUT) binding sites in EGLN1 and TRABD2B. HEK293FT cells were co-transfected with these plasmids and miRNA-27b-5p stem loop or miRNA-497-5p stem loop containing plasmids. We then performed a dual luciferase assay. Through this methodology, we were able to validate the interaction of miRNA-27b-5p with EGLN1. Unfortunately, TRABD2B and miRNA-497-5p did not demonstrate the same pattern. RLU, although decreased (RLU = 0.89), was not significant from the control and MUT conditions, suggesting that the interaction is not strong. For this reason, TRABD2B was not included as our gene of interest in further chapters.

Rationale of chapter III: In chapter III we overexpressed and inhibited miRNA-27b-5p or miRNA-497-5p in different in vitro models: rat CFs, MI rat CFs, human donor CFs, human ICM and DCM CFs. In each of the in vitro models we transfected cells with nucleotides, mimics and inhibitors. mimics are short double-strand nucleotides which mimic miRNA function. Inhibitors are single strand nucleotides which bind the miRNA of interest preventing the endogenous miRNA from exerting its normal function. This approach is preferable in miRNA function studies rather than a simple transfection with miRNA expression plasmids. Transfection with mimics and inhibitors is a faster and cheaper way to gain insight upon miRNA function. Moreover, it allows reaching an increased concentration of miRNA which cannot be reached in endogenous conditions with

plasmid transfection. Transient transfection can efficiently deliver miRNA mimics and inhibitors into *in vitro* cultured mammalian cells. Overall, we tested the functional role of miRNA-27b-5p and miRNA-497-5p with two techniques in CFs originating from different models associated with cardiac fibrosis. The functional role of miRNAs was estimated by myofibroblast markers namely ECM proteins their gene expression. In addition, CFs phenotype was characterized by immunostaining against alpha smooth muscle actin α -SMA, which is considered to be a marker of myofibroblasts [4].

Aim of chapter III: According to the literature miRNA-27b and miRNA-497-5p are known pro-fibrotic miRNAs in settings of pulmonary fibrogenesis. Moreover, data obtained on miRNA-27b-5p and miRNA-497-5p up-regulation in IL-11 treated CFs and pathological CFs from MI rats may indicate miRNAs role in induction of fibroblasts to myofibroblasts transition or in suppression of CFs anti-fibrotic mechanisms. For this we wanted:

- 1) To elucidate the effect of miRNA-27b-5p and miRNA-497-5p on gene expression and phenotype in CFs. For this to overexpress/inhibit each miRNA separately in healthy rat/human CFs and CFs from a pathological condition (MI rat, human DCM, human ICM).
- 2) To validate relevance of EGLN1 repression by miRNA-27b-5p in cardiac pathologies like: MI, DCM and ICM

Results of chapter III: In this chapter we show that both miRNA-27b-5p and miRNA-497-5p are pro-fibrotic in CFs. Overexpression of each miRNA in CFs from both rat and human, including healthy, MI rat, DCM and ICM CFs lead to an increased number of myofibroblasts in cell culture detected with immunostaining. Interestingly, miRNA-27b-5p and miRNA-497-5p inhibition did not reverse the cellular phenotype. This observation suggests that both miRNAs induce fibroblast to myofibroblast transition rather than preventing anti-fibrotic mechanisms.

However, analysis of changes in gene expression induced by miRNA-27b-5p or miRNA-497-5p overexpression/inhibition revealed significant differences in gene expression in different pathologies. As we demonstrated, miRNA-27b-5p and miRNA-497-5p overexpression in rat and MI rat CFs increase expression of ACTA2, gene encoding α -SMA, and COL1A1, gene encoding collagen I. Both

genes are usually up-modulated in myofibroblasts and increase the ability of myofibroblasts to produce stress fibers and ECM, since collagen I is a main type of proteins in ECM. Moreover, EGLN1 was modulated significantly when miRNA-27b-5p was either overexpressed or inhibited. These results were further confirmed in human donor CFs. In addition, gene expression changes induced by miRNA-27b-5p overexpression in human donor CFs showed significant up-regulation of HIF1 α /HIF2 α which may indicate that miRNA is facilitating hypoxia signaling in CFs. On the other hand, miRNA-27b-5p overexpression in human ICM CFs lead to up-regulation of ACTA2, suggesting that miRNA-27b-5p participated in fibroblast to myofibroblast transition. However, EGLN1 was not modulated significantly by miRNA-27b-5p overexpression, whereas HIF2 α was up-regulated. Finally, gene expression of several genes (ACTA2, HIF1 α , HIF2 α , EGLN1) was not affected by miRNA-27b-5p inhibition/overexpression. These differences can be potentially explained by other molecular mechanism for miRNA-27b-5p which can potentially be involved in cardiomyopathies or due to the genetic mutations which accompany dilated cardiomyopathy.

Rationale of chapter IV: As we have identified that both miRNA-27b-5p and miRNA-497-5p have a pro-fibrotic role we aimed to identify the potential utilization of these miRNAs as circulating biomarkers of cardiac fibrosis. The rationale behind this aim was that IL-11 is up-modulated in heart pathologies which are accompanied by cardiac fibrosis and inflammation such as myocardial infarction, pressure-overload and heart failure. Cardiac fibrosis can be precisely detected with cardiac magnetic resonance; however, this is an extremely expensive procedure. In addition, it is not always prescribed to asymptomatic patients with preserved ejection fraction. This is an important issue for asymptomatic patients with aortic valve stenosis (AVS), as when they begin to experience severe symptoms survival rates decrease dramatically. Aortic valve replacement (AVR) surgery is performed to improve heart function and reverse interstitial fibrosis but not replacement fibrosis in patients. For this reason, reliable blood biomarkers which reflect cardiac fibrosis progression could be a useful tool to make a clinical decision upon AVR in asymptomatic AVS patients.

Aim of chapter IV:

We aimed at studying the potential of utilizing miRNA-27b-5p and miRNA-497-5p as circulating biomarkers of cardiac fibrosis in AVS patients with preserved ejection fraction. For this we wanted to achieve several aims:

- 1). Characterize clinical parameters of patients from aortic valve stenosis and control group.
- 2). Characterize left ventricle remodeling in aortic valve stenosis patients.
- 3). Measure miRNA-27b-5p, miRNA-497-5p and EGLN1 expression in left ventricle of aortic valve stenosis patients.
- 4). Measure miRNA-27b-5p and miRNA-497-5p levels in peripheral blood plasma of aortic valve stenosis patients.
- 5). Characterize extracellular vesicles from peripheral blood of aortic valve stenosis patients and measure miRNA-27b-5p and miRNA-497-5p expression in extracellular vesicles.
- 6). Plot receiver operating characteristics curves for miRNA-27b-5p and miRNA-497-5p expression in peripheral blood of aortic valve stenosis patients.
- 7). Study correlations of miRNA-27b-5p and miRNA-497-5p expression with left ventricle remodeling and other clinical parameters

Results of chapter IV: We recruited 30 patients with SAVS and preserved ejection fraction undergoing transaortic valve myectomy and compared them with 35 healthy donors. In our selection criteria we avoided patients with previous MI, coronary artery disease and history of arrhythmia. However, the resulting cohort of patients was significantly older than the control group. Moreover, the AVS exhibited more patients with dyslipidemia and hypertension due to their age. For this reason, we performed a sub-analysis on measured values in LV and blood plasma (BP) of AVS patients with hypertension or dyslipidemia and histological analysis of LV of AVS patients with demonstrated significant ECM remodeling and collagens accumulation which is accruing in these patients. We observed significant increase in collagens area (%) in sections cut from LV biopsies of AVS patients. Since we previously showed that miRNA-27b-5p and miRNA-497-5p altered colla1 expression in rat CFs we performed immunostaining upon collagen I in LV of AVS patients. We found collagen I was accumulated in LV biopsies from AVS patients. In addition, LV biopsies were characterized with a

significant up-regulation of CCN2, gene encoding CTGF, an important protein which is orchestrating ECM remodeling and pro-fibrotic signaling. Our experiments also showed that both miRNA-27b-5p and miRNA-497-5p are significantly up-modulated in the LV of AVS patients. At the same time, EGLN1, a target of miRNA-27b-5p was strongly down-regulated in LV of AVS patients. RT-qPCR analysis of BP from AVS patients demonstrated a significant increase of miRNA-27b-5p and miRNA-497-5p. We hypothesized that increased expression of miRNA-27b-5p and miRNA-497-5p in BP of AVS patients could be potentially explained by miRNAs released from myofibroblasts and damaged cardiomyocytes in fibrotic LV. According to literature, miRNAs can circulate in blood in complex with proteins like Ago2, lipids like HDL or encapsulated in extracellular vesicles (EVs). We were able to isolate EVs from BP of AVS patients and characterized them with transmission electron microscopy. Correlation plot revealed that miRNA-27b-5p and miRNA-497-5p in BP are mostly present by encapsulated form. We plotted ROC Curves based on miRNAs expression from EVs in BP of AVS and healthy donor patients. Both miRNA-27b-5p and miRNA-497-5p were proven to be sensitive and specific biomarkers of AVS as suggested by significantly high area under the curve (AUC) for each miRNA. Following this, we tested Pearson correlations between miRNAs expression in LV, BP and EVs from BP with other parameters, such as histology data, CTGF expression and measured clinical parameters in patients. As a result, we observed that miRNA-497-5p expression in LV positively correlated with ECM Area (%) in LV measured by histology, with CTGF expression in LV and with miRNA-27b-5p expression in LV. At the same time, miRNA-27b-5p expression in LV of AVS patients positively correlated with the interventricular septum (IVS) in these patients. This can be explained by pro-hypertrophic role of this particular miRNA. Also, the expression of the target of miRNA-27b-5p, EGLN1, correlated negatively with ECM Area (%) in LV and with CTGF expression in LV. Unfortunately, miRNA expression in blood plasma did not show any significant correlation with the measured parameters, but miRNA-27b-5p and miRNA-497-5p derived from EVs in BP of AVS patients positively

correlated with aortic peak gradient in AVS patients. Increased aortic peak gradient is one of the parameters which characterize severity of AVS in patients. In addition, we tested how co-morbidities like age, hypertension and dyslipidemia are affecting miRNA-27b-5p and miRNA-497-5 expression in LV, BP and EVs from BP of AVS patients. As a result, we found that these co-morbidities did not affect miRNA expression. However, miRNA-497-5p from EVs in BP of AVS patients demonstrated dependence on patient age.

This is the first study to report on potential utilization of miRNA-497-5p and miRNA-27b-5p as biomarker of cardiac fibrosis in AVS patients with preserved ejection fraction. Both miRNAs are activating fibroblasts to myofibroblasts transition and collagen I production. We believe that this part of our study can be used for the decision-making process of cardiac surgery in AVS patients. Moreover, miRNAs are released in peripheral blood where they can be easily detected. Importantly, we found that both miRNAs are critical component of the IL-11 pro-fibrotic mechanisms. In particular, we found that EGLN1 suppression by miRNA-27b-5p represents a novel mechanism which underlies IL-11 signaling in CFs. Thus, this study may serve as a starting point for further investigation on EGLN1 and hypoxia signaling in IL-11 activation of CFs.

Table of Contents

ABSTRACT	4
Table of Contents	15
ABBREVIATIONS	22
CHAPTER I.....	23
1. INTRODUCTION I	23
1.1 The heart anatomy and functions	23
1.2 Cardiac fibroblasts: key players in cardiac fibrosis and extracellular matrix remodeling.....	25
1.3 Cardiac fibroblasts in myocardial infarction.....	26
1.4 Molecular mechanisms of cardiac fibrosis	26
TGFβ canonical and non-canonical pathways in cardiac fibroblasts transdifferentiation.....	28
Wnt pathway in cardiac fibrosis.....	29
IL-11 signaling pathway is a novel player in cardiac fibrosis?	29
1.5 miRNAs in cardiac fibrosis: potential down-stream effectors of IL-11	30
2. AIMS OF THE STUDY I	32
3. METHODS I.....	33
3.1 Animal models and cell culture	33
3.2 Cultivation of human cardiac fibroblasts.....	33
3.3 Immunostaining against vimentin and α-SMA	34
3.4 Image acquisition and analysis for immunostaining in cell culture.....	34
3.5 RT-qPCR	35
RNA extraction from cells.....	35
Reverse transcription of RNA	36
3.6 Prediction of miRNAs involved in regulation of TGFβ1 and IL-11 (ERK) pathways with designed bioinformatical pipeline	38
3.7 Statistics	40
4. RESULTS I.....	41
4.1 IL-11 and TGFβ1 treatment causes an increased expression of α-SMA and Col1a1 in rat cardiac fibroblasts as well as MI rat cardiac fibroblasts	41

4.2 IL-11 and TGFβ1 treatment causes an increased number of myofibroblasts in rat cardiac fibroblasts comparable with fibroblasts from myocardial infarction rats.....	44
4.3 miRNA-497-5p and miRNA-27b-5p predicted to be involved in regulation of TGFβ1 and ERK pathways.....	46
4.4 miRNA-497-5p and miRNA-27b-5p are up-modulated in cardiac fibroblasts from myocardial infarction rats and in IL-11 treatment model of cardiac fibrosis.....	48
4.5 Remaining predicted miRNAs regulation under IL-11 treatment and in myocardial infarction rat cardiac fibroblasts	50
4.6 Characterization of human cardiac fibroblasts from patients with dilated and ischemic cardiomyopathies	51
4.7 miRNA-27b-5p and miRNA-497-5p expression in cardiac fibroblasts from left ventricle of patients with dilated and ischemic cardiomyopathy	52
5. DISCUSSION I.....	54
6. REFERENCES I	56
CHAPTER II.....	67
1. INTRODUCTION II.....	67
1.1 An overview on miRNAs: biology and functions	67
miRNAs biogenesis	67
miRNAs functions.....	68
1.2 miRNAs and their targets prediction.....	69
1.3 miRNA-27b-5p: current knowledge.....	70
1.4 miRNA-497-5p: current knowledge.....	71
2. AIMS OF THE STUDY II.....	72
3. METHODS II	73
3.1 Bioinformatic analysis of Human RNA-seq data.....	73
Code in RStudio 4.0.2 for IL-11 differential co-expression network construction	74
3.2 Gene set enrichment analysis.....	75
3.3 Protein-protein interaction network construction.....	75
3.4 Network analysis with Cytoscape 3_7_1.....	76

3.5 miRNAs targets prediction	76
3.6 Constructs preparation	76
3.7 Bacterial transformation	77
3.8 Constructs amplification	78
3.9 HEK293FT cell culture	78
3.10 3'UTR luciferase assays to demonstrate miRNA direct binding to the predicted target genes.....	78
3.11 RT-qPCR	79
3.12 Statistics	79
4. RESULTS II	80
4.1 IL-11 diferential co-expression network characterization.....	80
4.2 Application of RNAseq data done in human dilated cardiomyopathy cardiac fibroblasts treated with IL-11 on IL-11 co-expression network	80
4.3 EGLN1 is down-regulated in vitro by miRNA-27b-5p as a target.....	82
4.4 TRABD2B is not regulated in vitro as miRNA-497-5p target	85
4.5 Validation of the construct presence by gel electrophoresis and DNA-sequencing.....	88
5. DISCUSSION II	89
6. RFERENCES II	92
CHAPTER III	100
1. INTRODUCTION III.....	100
1.1 Myocardial infarction, ischemic cardiomyopathy: etiology, mechanisms of extracellular matrix remodeling, heart failure progression	
100	
1.2 Etiology	100
1.3 ECM remodeling in post-myocardial infarction/ischemic cardiomyopathy	100
1.4 HF progression after MI or ICM: molecular mechanisms	102
1.5 Dilated cardiomyopathy: etiology, mechanisms of extracellular matrix remodeling, heart failure progression.....	102
1.6 Etiology	102
1.7 ECM remodeling in DCM patients	103

1.8 ECM remodeling in post-myocardial infarction/ischemic cardiomyopathy	103
2. AIMS OF THE STUDY III	104
3. METHODS III.....	105
3.1 Animal models and cell culture	105
3.2 Cultivation of human cardiac fibroblasts.....	105
3.3 miRNA-27b-5p and miRNA-497-5p gain/loss of functions in rat cardiac fibroblasts	106
3.4 miRNA-27b-5p gain/loss of functions in human cardiac fibroblasts from donor, DCM and ICM patients	106
Transfection of cardiac fibroblasts with oligonucleotides and Lipofectamine 3000.....	106
3.5 Immunostaining against Vimentin and α -SMA	107
3.6 Image acquisition and analysis for immunostaining in cell culture....	107
3.7 RNA isolation and reverse transcription polymerase chain reaction on transfected cardiac fibroblasts	108
3.8 Validation of transfection with RT-qPCR on miRNA-27b-5p and miRNA-497-5p in cardiac fibroblasts	108
3.9 Statistics	109
4. RESULTS III.....	110
4.1 In vitro modulation of miRNA-27b-5p and miRNA-497-5p in rat cardiac fibroblasts.....	110
4.2 miRNA-27b-5p and miRNA-497-5p overexpression leads a significant increase in the number of α -SMA and Vimentin positive cells in rat cardiac fibroblasts	111
4.3 miRNA-27b-5p and miRNA-497-5p gain and loss of functions causing gene expression changes in myofibroblasts associated markers in rat cardiac fibroblasts.....	112
4.4 miRNA-27b-5p and miRNA-497-5p overexpression leads a significant increase in the number of α -SMA and Vimentin positive cells in MI rat cardiac fibroblasts.....	115

4.5 miRNA-27b-5p and miRNA-497-5p gain and loss of functions causing gene expression changes in myofibroblasts associated markers in MI rat cardiac fibroblasts.....	116
4.6 In vitro modulation of miRNA-27b-5p in human cardiac fibroblasts.	119
4.7 miRNA-27b-5p function in human donor cardiac fibroblasts.	120
4.8 miRNA-27b-5p gain and loss of functions causing gene expression changes in myofibroblasts and hypoxia associated markers in human donor cardiac fibroblasts.....	121
4.9 miRNA-27b-5p effect on the phenotype of cardiac fibroblasts from ICM patients.....	122
4.10 miRNA-27b-5p gain and loss of functions causing gene expression changes in myofibroblasts but not hypoxia associated markers in cardiac fibroblasts from ICM patients.	123
4.11 miRNA-27b-5p effect on the phenotype of cardiac fibroblasts from DCM patients.	125
4.12 miRNA-27b-5p gain and loss of functions does not cause any changes in gene expression of myofibroblasts and hypoxia related markers in cardiac fibroblasts from DCM patients	125
5. DISCUSSION III.....	128
6. REFERENCES III	131
CHAPTER IV.....	137
1. INTRODUCTION IV	137
1.1 Aortic valve: biomechanics, functions and composition	137
1.2 Aortic valve stenosis.....	138
1.3 Current diagnostic tools used for aortic valve stenosis detection.....	139
Cardiac imaging.....	139
BNP as a biomarker in AVS patients.....	140
LV remodeling biomarkers in AVS patients.....	141
2. AIMS OF THE STUDY IV	143
3. METHODS IV	144
3.1 Patient populations	144
3.2 Histology and morphometric analysis.....	145

3.3 miRNA isolation from patient’s blood plasma with Nucleospin ^R miRNA Plasma kit	146
3.4 Extracellular vesicles isolation from patient’s blood plasma with Exospin blood kit	148
3.5 Transmission electron microscopy for validation of extracellular vesicles preparation	148
3.6 RNA isolation and reverse transcription polymerase chain reaction in left ventricle biopsies	149
3.7 Reverse transcription polymerase chain reaction on miRNAs.....	149
3.8 Statistics	150
4. RESULTS IV	151
4.1 Patients baseline characteristics	151
4.2 Left ventricle biopsies were characterized with increased collagens area and CTGF expression.....	151
4.3 miRNA-497-5p, miRNA-27b-5p and its target EGLN1 expression in left ventricle of aortic valve stenosis patients.....	153
4.4 miRNA-497-5p and miRNA-27b-5p expression in peripheral blood plasma of aortic valve stenosis patients	154
4.5 Co-morbidities effect on miRNA-27b-5p, miRNA-497-5p and EGLN1 expression in left ventricle biopsies from aortic valve stenosis patients ...	154
4.6 miRNA-27b-5p and miRNA-497-5p are transferred via extracellular vesicles and can be potentially utilized as circulating biomarkers of cardiac fibrosis in aortic valve stenosis patients.....	156
4.7 miRNA-27b-5p, miRNA-497-5p and EGLN1 correlations with extracellular remodeling characterized by histology, RT-qPCR and echo	157
4.8 Co-morbidities effect on miRNA-27b-5p and miRNA-497-5p expression in peripheral blood plasma from patients with aortic valve stenosis.....	159
5. DISCUSSION IV	163
6. REFERENCES IV	165
CONCLUSIONS	172
PHD COURSE ACTIVITIES	174

PUBLICATIONS	174
CONFERENCES	175
ACKNOWLEDGMENTS	176

ABBREVIATIONS

ACTA2	actin alpha 2
CFs	cardiac fibroblasts
Col1a1	Collagen type I alpha 1 chain
Col3a1	Collagen type III alpha 1 chain
CTGF	connective tissue growth factor
DCM	dilated cardiomyopathy
DNA	deoxyribonucleic acid
ECM	extracellular matrix
ERK	extracellular signal-regulated kinase
HF	heart failure
ICM	ischemic cardiomyopathy
IL-11	interleukin 11
IL-11RA1	interleukin 11 receptor
LA	left atrium
LAPs	latency-associated peptides
LV	left ventricle
MAPK	mitogen-activated protein kinase
MI	myocardial infarction
miRNA	microRNA
RA	right atrium
RNA	ribonucleic acid
RT-qPCR	Reverse transcription quantitative polymerase chain reaction
RV	right ventricle
TGF β 1	transforming growth factor β 1
α -SMA	α -smooth muscle actin

CHAPTER I

1. INTRODUCTION I

1.1 The heart anatomy and functions

The heart is a multicellular organ which main function is to pump the blood enriched in oxygen and nutrition to each cell in the organism. The mammalian heart is divided in two main sections: i) the right one sustains the pulmonary circulation, ii) while the left one is responsible for the systemic circulation. Both sections contain two chambers which are named accordingly: atrium and ventricle. Atria in the right section, right atrium (RA), and in the left section, left atrium (LA), constitute the heart base. Two ventricles fuse at the levels of the cardiac apex. Right and left atria are divided by the inter-atrial septum while the interface between atria and ventricles is delimited by the atrioventricular valves the tricuspid valve for the right section and the mitral valve for the left section, which guarantee unidirectional flow of the blood from the atria to the ventricles. The semilunar valves are located at the interface between the ventricles and great arteries and ensure blood flow from the ventricle to the arteries while tricuspid and mitral valves are fastened to *chordae tendineae* a fibrous structure which is connecting the valve leaflet to papillary muscles and which maintains the correct valve plane during the heart cycle.

Blood runs through the right stream, enters through pulmonary valve which is organized of three fibrous cusps. They are closed during diastole, process of relaxation all atrium and ventricular muscles. When blood is oxygenated in lungs, it is transported through pulmonary veins into the LA. LA is separated from LV by mitral valve. LV is the biggest in size and muscle mass among all 4 chambers, since it is surrounded by thick muscular wall. Its contraction provides enough pressure to pump the blood across the body through aorta. In diastole aorta is separated from LV by aortic valve. LV and RV are separated from each other by inter-ventricular septum (**Figure 1.1**) [5].

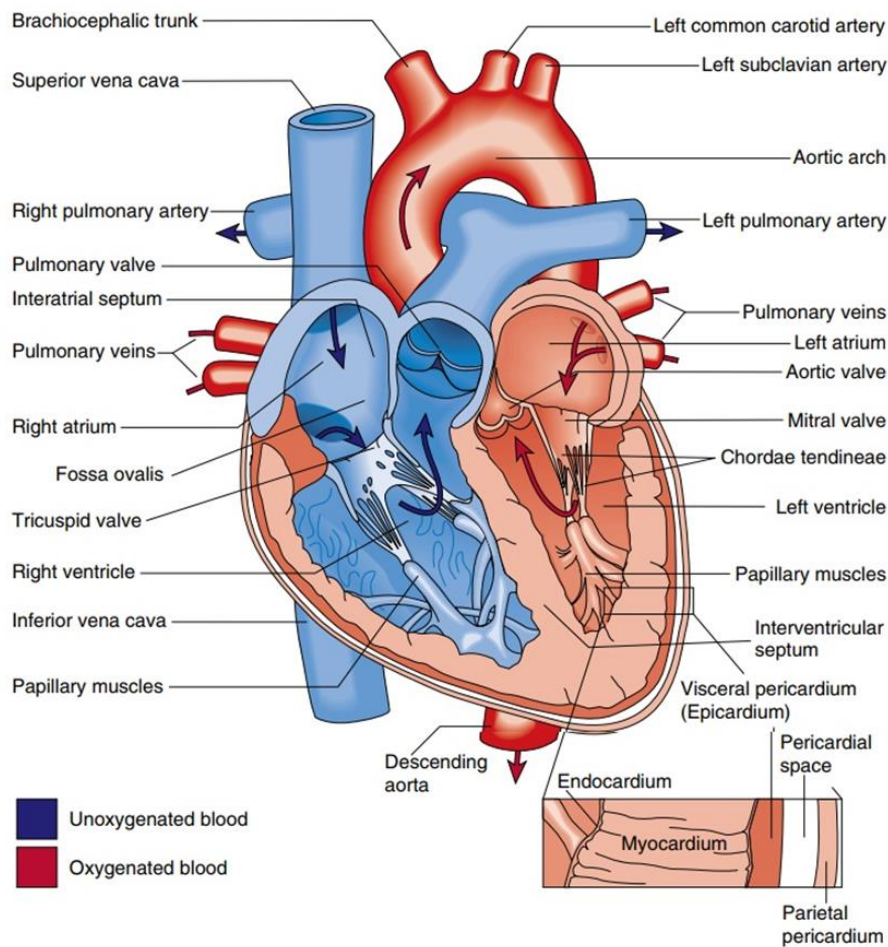


Figure 1.1 The internal structures of the heart [5].

Cardiac fibrosis is an adaptive or pathological process caused by remodeling and extension of collagens based ECM [6-7]. This process is associated with many forms of cardiac diseases and leads to cardiac remodeling. Historically, the term “remodeling” was used in context of LV [8]. Remodeling is associated with morphological changes in the cavity diameter and mass (hypertrophy), in the heart geometry (heart wall thickness or heart shape), scar formation after MI, inflammatory cells infiltration and fibrosis [9]. The process of cardiac remodeling leads to cardiac dysfunction. The process involves changes in gene expression in response to cardiac injury. Following this, molecular and cellular changes which are taking place into injured heart enhance loss of ventricular function [10]. Left ventricular dysfunction desperately influences patient’s prognosis. Almost 50% of patients would not survive in five years, 40% of patients would die in the first year after hospitalization [11]. That fact highlights an extreme importance on

investigation of reliable biomarkers of cardiac remodeling before it turns into cardiac dysfunction [12].

1.2 Cardiac fibroblasts: key players in cardiac fibrosis and extracellular matrix remodeling

The myocardium is an involuntary, striated muscle constituting the main tissue mass of the heart walls build up with cardiomyocytes. Another important cell type is cardiac fibroblasts (CFs). Under homeostatic conditions, the fibroblast-produced ECM proteins which provide a structural scaffold for cardiomyocytes, distributes mechanical forces through the cardiac tissue, and mediates electric conduction [13]. During heart injury, loss of cardiomyocytes leads to an adaptive process: infiltration of inflammatory cells, activation of CFs, which are named as myofibroblasts, beginning of endothelial to mesenchymal cells transition [14]. Due to the low-regeneration capacity of mammalian heart, dead cells are removed and myofibroblasts, pericytes and endothelial cells are forming a scar, acting to preserve structural and functional integrity of the myocardium [15]. Long inflammation, hypoxia and hypertrophy are followed by maladaptive fibrosis, when myofibroblasts are actively producing, α -SMA, CTGF, Collagen I, Angiotensin II, TGF β 1, IL-11 etc (Figure 1.2) [16]. Therefore, activated fibroblasts degrade current ECM and produce new one, which intervenes in healthy myocardium. As a consequence, heart is losing its integrity and cannot sustain its normal functions [17]. Myofibroblasts produce alpha smooth muscle actin (α -SMA) and myosin, which form connections with focal adhesion proteins, bridging cellular actin filaments with the ECM. Mechanical stress can provoke further expression of α -, β - and γ -fibers, connected to focal adhesion proteins [18].

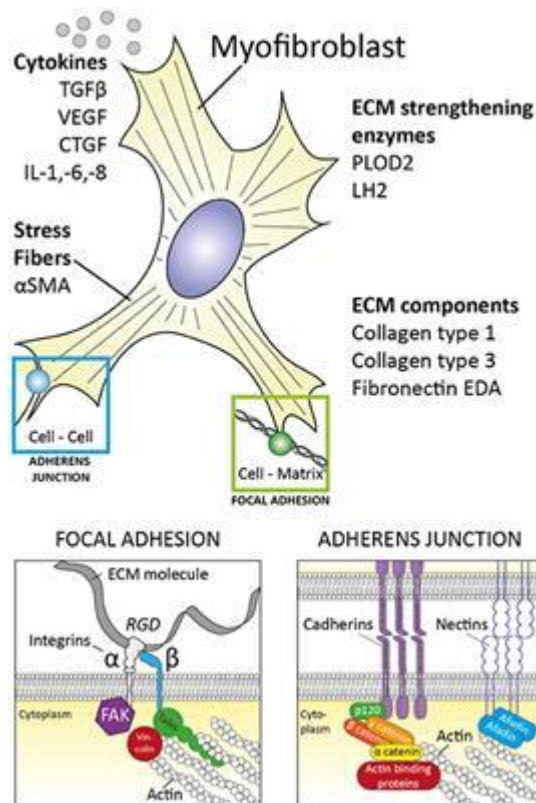


Figure 1.2 Myofibroblasts: phenotype and genotype [16].

1.3 Cardiac fibroblasts in myocardial infarction

Under homeostatic conditions, the fibroblast-produced ECM provides a structural scaffold for cardiomyocytes, distributes mechanical forces through the cardiac tissue, and mediates electric conduction. The post-natal Mammalian heart has very limited regenerative capacity after injury. Following an MI, cardiomyocyte necrosis triggers an inflammatory phase guided by neutrophils, which leads to activation of cardiac fibroblasts to become myofibroblasts. The myofibroblasts then form a scar, acting to preserve structural and functional integrity of the myocardium [19].

1.4 Molecular mechanisms of cardiac fibrosis

Several molecular mechanisms regulate cardiac fibrosis. A summary of related mechanisms in this thesis can be viewed in Figure 1.3.

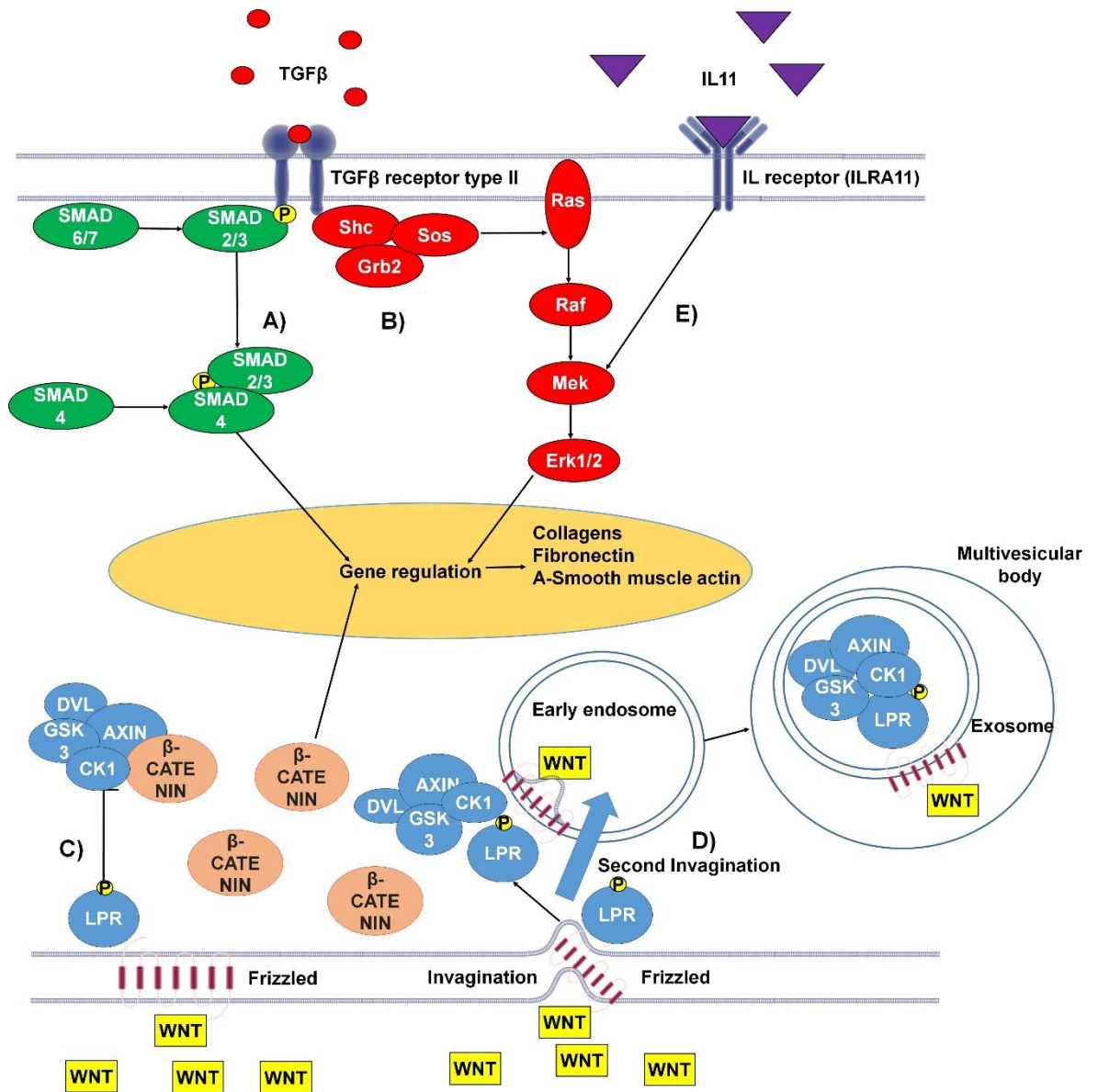


Figure 1.4 The canonical and non-canonical pro-fibrotic pathways of TGFβ and Wnt and the pro-fibrotic IL-11 pathway. **A)** Canonical TGFβ pathway: TGFβ – Transforming growth factor β binds to the type I/II TGFβ receptor. The Smad2/3 complex is then phosphorylated, at this point the pathway can be inhibited by Smad6/7. In the cytoplasm Smad2/3 binds Smad4 and the whole complex transfers to the nucleus, where it binds to GAGAC motifs, promoting gene expression. **B)** Non-canonical TGFβ pathway: TGFβ binds the TGFβ receptor type I/II, resulting in tyrosine residues and Shc (Src homology 2 domain containing) transforming protein are phosphorylation. This promotes the binding of Grb2 (Growth factor receptor-bound protein 2) and Sos (son of sevenless). This complex can activate Ras, launching the MAPK cascade and further gene regulation. **C)** Wnt canonical pathway: Wnt (Wingless-related integration site) binds

transmembrane protein frizzled (Fz). Fz bound WNT can then bind LPR5/6 protein (low-density-lipoprotein-related protein) which undergoes phosphorylation of its tail by GSK3 and CK1 proteins. Following this, LRP interacts with Dishevelled (DVL), Axin and GSK3 via Pro-Pro-Pro-(Ser/Tyr)-Pro repeats. This complex is responsible for β -catenin attenuation. D) Wnt non-canonical pathway: Wnt binds transmembrane protein Fz at the site of a membrane invagination. The complex then becomes part of the membrane of an early endosome. LPR5/6 is phosphorylated at its tail by GSK3 and CK1 proteins. Following this, LRP interacts with DVL, Axin and GSK3 via Pro-Pro-Pro-(Ser/Tyr)-Pro repeats. The membrane of the early endosome can form a second invagination, eventually leading to the whole complex being locked down inside a multivesicular body. E) The IL-11 signaling pathway activates the MAPK cascade, promoting gene regulation. [2,20-22].

TGF β canonical and non-canonical pathways in cardiac fibroblasts transdifferentiation

Transforming growth factor β (TGF β) is a multifunctional cytokine, which is considered a main driver of cardiac fibrosis. Under pathological conditions, TGF β is released from the ECM, where it is stored in complex with latency-associated peptides (LAPs) and latent TGF β binding proteins [23]. There are two membrane bound TGF β receptors (types I and II), when activated by TGF β the receptors activate the Smad pathway [20]. In the cytoplasm, phosphorylated Smad2/3 forms a heteromeric complex with Smad4; following this, the complex associates with DNA-binding proteins and is transported to the nucleus where GAGAC motifs are bound to initiate extensive expression of target genes [24]. Such a cascade can be interrupted at the step of Smad2/3 phosphorylation due to inhibition by Smad6/7 [25]. Inhibition of the TGF β - signaling pathways does not completely attenuate the progression of fibrosis, indicating that other pathways are also involved [26]. Evidence for non-canonical pathways of TGF β -signaling include activation of the MAPK pathway as demonstrated in work of Lu Xie and colleagues [27]. Briefly, this proposed pathway begins with the phosphorylation and activation of TGF β binding receptors type I and II, which consequently activates Shc. Shc forms a complex with Grb2 and Son of sevenless (Sos) protein [28]. Consequently, the complex activates membrane embedded Ras leading to step by step activation of Raf, Mek and Erk with a further involvement of MAPK cascades [29]. As a result,

Erk and Smad signaling influence expression of genes associated with fibrosis [30].

Wnt pathway in cardiac fibrosis

Nowadays, the Wnt pathway is extensively studied. This has led to the identification of canonical and non-canonical Wnt- β -catenin pathways [21]. The Wnt pathways have been identified as participating strongly in the development of cardiac fibrosis [30]. Wnt3a causes upregulation of both TGF β and Smad2 and induces proliferation of cultured mouse fibroblasts [30]. Additional connections between the Wnt canonical pathway and TGF β pathway have been confirmed in other investigations [31, 32]. The canonical Wnt pathway works through negative regulation of the complex which binds and inhibits β -catenin (which was found to be important in the promotion of fibrosis). The loss of function of β -catenin was reported to reduce interstitial fibrosis suppressing Col3a1 [33]. Signaling begins when Wnt binds to the transmembrane receptor Frizzled (Fz). Afterwards the receptor can interact with a low-density-lipoprotein-related protein (LRP5/6) with further phosphorylation of LRP tail by GSK3 and CK1 proteins [34]. Following this, LRP interacts with Dishevelled (DVL), Axin and GSK3 via Pro-Pro-Pro-(Ser/Tyr)-Pro repeats [35]. This complex is responsible for β -catenin attenuation through interaction with phosphorylated LRP. As a result, β -catenin translocates into the nucleus where, in a complex with T-cell factor/lymphoid enhancer-binding factor-1 (TCF/Lef-1), transcription factors and co-factors; it can regulate gene transcription [36]. Wnt is also closely connected to the biogenesis of extracellular vesicles, what would be extensively studied in the Chapter IV. Following binding between Wnt and Frizzled (transmembrane receptor), a membrane invagination occurs and early endosome forms [37]. During the maturation of endosome, the multivesicular body (MVB) formation leads to trapping of the β -catenin inhibiting complex inside MVB. This complex can be released in the extracellular space with the extracellular vesicles [38].

IL-11 signaling pathway is a novel player in cardiac fibrosis?

Interleukin 11 (IL11) is a cytokine which was found to be upregulated in response of TGF β 1 stimulation of cardiac fibroblasts. The laboratory of Stuart Cook showed that IL11 binds interleukin receptor (ILRA11) and acts through ERK to regulate gene expression, in order to produce ECM proteins [2]. This group also showed that activation of SMAD cascade through TGF β 1 results in high release of IL11 cytokine [2] and that IL11 stimulates lung fibroblasts and leads to generation of α -smooth muscle actin and collagens in an ERK-dependent posttranscriptional manner [39]. Similar results were observed in liver fibrosis in the model of nonalcoholic steatohepatitis mouse [40]. A recent study demonstrated that IL-11 was significantly increased in a mouse model of pressure-overload mice, and that *IL-11ra* knockout mice were protected from developing fibrosis [2]. Moreover, mRNA levels of IL-11 were significantly increased in the infarct and remote zones of mice with myocardial infarction [41]. Plasma IL-11 levels were also increased in patients with heart failure (HF) in comparison with healthy donors [42]. The clinical relevance of these findings was demonstrated by work on clinical samples, showing increased IL-11 in aortic tissue samples and peripheral blood plasma of patients with acute thoracic aortic dissection [43]. Taken together, these studies situate IL-11 as a universal activator of cardiac fibrosis in various diseases. However, the role of downstream effectors and non-canonical signaling pathways triggered by IL-11 stimulation of CFs remains unclear [44]. One class of molecules which could be an effective downstream effector of IL-11 in CFs are miRNAs, the most studied class of small non-coding RNAs.

1.5 miRNAs in cardiac fibrosis: potential down-stream effectors of IL-11

miRNAs are small endogenous oligonucleotides of 21-25 nucleotides, which are found in both animals and plants. miRNAs play an important role in post-transcriptional gene regulation by binding and generally inhibiting target mRNAs [45]. The interaction with the mRNA is usually mediated by a “seed” sequence near the 5'-terminus of the miRNA. The “seed” sequence consists of 6-8 nucleotides and can be highly conserved among species. Since the regulation of miRNAs is dependent upon sequence, the complementary principle indicates that

one mRNA can be silenced by several miRNAs and one miRNA can target various mRNAs. There are a number of miRNAs which are produced by the cardiac cell types which could contribute to or alleviate a variety of pathologies, including cardiac fibrosis [46,47]. TGF β 1 has previously been shown to induce miRNAs such as miRNA-21-5p, miRNA-125b, miRNA-181b, which facilitate fibroblast to myofibroblast transition and collagen production [48-50]. However, the role of miRNAs in the fibrotic response to IL-11 is still unknown.

2. AIMS OF THE STUDY I

Aims:

- 1) Establish an in vitro model of IL-11 treatment of rat CFs by analyzing CFs phenotype and Col1a1, Col3a1 and α -SMA gene expression. This model will be compared with well-established TGF β 1 treatment model of rat CFs and CFs derived from MI rat.**
- 2) Predict miRNAs which can potentially contribute in to the regulation of two crucial pro-fibrotic pathways: TGF β 1 and IL-11, which is working through extracellular regulated kinase (ERK).**
- 2) Validate miRNA modulation by TGF β 1/IL-11 treatment.**
- 3) Validate miRNA modulation in cardiac fibrosis associated models: MI rat CFs.**
- 4) Investigate miRNA modulation in human CFs from pathological conditions samples characterized by ECM remodeling and myofibroblasts activation: ischemic (ICM) or dilated cardiomyopathy (DCM).**

3. METHODS I

3.1 Animal models and cell culture

All animal models were established and used in the United Kingdom (UK) with established standards for the care of animal subjects written by the UK Home Office (ASPA1986 Amendments Regulations 2012) incorporating the EU directive 2010/63/EU. Ethics was approved by committee of Imperial College London.

Age-matched male Sprague-Dawley rats were used as a control group to rat with MI. In order to induce MI in rat's coronary artery ligation was performed. After 16 weeks, animals were sacrificed when end stage heart failure (HF) develops [51]. These animal experiments were approved by the Animal Welfare and Ethical Review Board (AWERB) of Imperial College London, UK and carried out in accordance with the UK Animals (Scientific Procedures) Act 1986, incorporating the European Union Directive 2010/63/EU.

CFs were isolated with Langendorff technique with following enzymatic digestion of rats LV [52]. Following this, cells were centrifuged at low gradients in order to remove cardiomyocytes (CMs). After that, CFs were pelleted and plated in high-glucose (4500 mg/l) Dulbecco's Modified Eagle Medium supplemented with 10% Fetal Bovine Serum and 1% of penicillin/streptomycin. Cells were cultured 20 day's maximum after fixation or lysis at 37 °C and 5% CO₂. Confluent T-25 flask of CFs was treated with IL11 (5 ng/μl) or TGFβ1 (100 ng/μl). After 24 hours, first treatments cells were washed with 2.5 ml of PBS and used for further experiments.

3.2 Cultivation of human cardiac fibroblasts

Human cardiac fibroblasts from healthy donor (N = 1, biological replicates = 4), DCM (N = 4, biological replicates = 2) and ICM (N = 4, biological replicates = 2) patients were obtained from LV organotypic culture [53]. LV pieces were fixed in the 6-well plate covered with fibronectin. Cardiac fibroblasts were growing from pieces for 2-3 weeks in 20% Fetal Bovine Serum and 1% of

penicillin/streptomycin at 37 °C and 5% CO₂. Following this, cells were seeded equally in 12-well plate for further experiments. Ethics was approved by the NHS committee (REC reference 19/SC/0257; IRAS project ID:264059).

3.3 Immunostaining against vimentin and α -SMA

CFs were fixed with 4% paraformaldehyde with further permeabilization with 0.05% TritonX-100 diluted in PBS. Any non-specific binding was prevented by blocking of fixed cells with 5% (w/v) BSA for 1 hour at room temperature. After that, cells were stained with primary antibodies overnight at 4°C: α -SMA mouse monoclonal DAKO antibody (M0851) and vimentin chicken polyclonal antibody from Invitrogen (PA1-16759). On the next day, coverslips were washed three times with PBS and incubated for three hours at room temperature in a dark place with secondary antibodies: anti-mouse donkey polyclonal AlexaFluor-488 from Invitrogen (A21202) and anti-chicken goat polyclonal AlexaFluor-546 from Invitrogen (A11040). After that, coverslips were washed in PBS three times and mounted onto the labelled slides, using hard-set mounting medium (ProlongTM Gold Antifade reagent with DAPI) [54]. Slides were then stored under aluminium foil at 4°C until imaging.

3.4 Image acquisition and analysis for immunostaining in cell culture

CFs and MI CFs that were stained according to 3.2 were analyzed with the optical system [Nikon Eclipse Ti with pE-4000 light source (Cool LED) and ORCA-Flash 4 camera (Hamamatsu)]. With 20x magnification we collected 5-7 images for one coverslip with ~10 cells per image. Images processing was done in Fiji (ImageJ). In order to distinguish α -smooth muscle actin positive cells (α -SMA) from healthy CFs images were thresholded to control condition. Raw images in DAPI and Vimentin channels were uploaded in ImageJ and turned to 16-bit images where cells were manually highlighted and mean fluorescence for each cell was detected in α -SMA channel with help of ROI Manager. After that, mean fluorescence from each cell was used for distribution analysis, where 90th percentile was chosen as a threshold value for all conditions. Fibers morphology was also considered as important criteria for α -SMA positive cell detection [55].

3.5 RT-qPCR

Reverse transcription-polymerase chain reaction (RT-PCR) involves the same process as ordinary polymerase chain reaction (PCR) — cycling temperature to amplify nucleic acids.

The difference between PCR and RT-PCR is that in the first case there is amplification only of deoxyribonucleic acids (DNA), and in the second case there is the amplification of ribonucleic acids (RNA) through the formation of complementary DNA (cDNA) by using specialized enzymes, known as reverse transcriptase (RT). By using specific primers, it is possible to control the exact part of cDNA which will be amplified. Designed primers in order to detect genes of interest are present in table 3.5.1.

Table 3.5.1 List of primers

Gene name	Species	Forward primer sequence 5'→3'	Reverse primer sequence 5'→3'
α-SMA	rat	ACCATCGGGAATGAACGCTT	CTGTCAGCAATGCCTGGGTA
Col1a1	rat	CCCAGCCGCAAAGAGTCTAC	CAGGTTCCACGTCTCACCA
Col3a1	rat	CCACCCTGAACTCAAGAGCG	ACAGTCATGGGACTGGCATT
Gapdh	rat	TGATTCTACCCACGGCAAGTT	TGATGGGTTCCATTGATGA

RNA extraction from cells

The total RNA was isolated following the manufacturer's TRIzol™ Reagent protocol (ThermoFisher scientific). CFs grown in a monolayer were treated with Trizol on ice under the hood and incubated for 5 min in order to complete lysis. After that, lysate was pipetted up and down several times and was transferred to clear 1.5 ml tube. As a next step, we added chloroform equals 0.2 of Trizol volume. Mixture was homogenized by inversion and incubated on ice for 3 minutes. Following this, tubes were centrifuged at 12 000xg for 15 minutes at 4 °C. Therefore, mixture separates in three layers, where RNA is present in the top aqueous phase, which was transferred to a new tube, where it was resuspended in isopropanol 0.5 of Trizol volume. This was then followed by 10 minutes incubation on ice and further centrifugation at 12 000xg 10 minutes at 4°C. As a result, white gel pellet can be observed on the bottom of a tube. Isopropanol was carefully aspirated and pellet was resuspended in 75% ethanol equal volume of Trizol used in the beginning. Sample was vortexed and spun at 7 500xg 5 minutes

4°C. In order to remove any remaining ethanol, it was carefully aspirated and pellet was air dried for 15 minutes. After that it was diluted in 20 µl of Nuclease free water.

Quality of RNA isolations was observed with usage of NanoDrop™ One/OneC Microvolume UV-Vis Spectrophotometer. Absorbance of nucleic acids on 260 nm was related to absorbance on 280 nm in order to determine protein contamination and to 230 nm in order to detect phenol contamination. We considered isolations with A260/280 and A260/230 ratios more than 1.75.

Reverse transcription of RNA

Total RNA was converted into cDNA, using the GoScript™ Reverse Transcription kit (Promega). An hour before experiment RNA aliquots were thawed on ice. GoScript™ Reverse Transcriptase allows to generate cDNA based on RNA. After that, cDNA was used as a matrix in polymerase chain reaction to measure gene expression. Then stock RNA was diluted to 250 ng in 10 µl of Nuclease Free water with 2 µl of random primers. After that reaction master mix was prepared according to GoScript™ Reverse Transcription kit protocol. 8 µl GoScript™ 5X Reaction Buffer, 2 µl of MgCl₂ (25 mM), 2 µl of PCR Nucleotide Mix, 1 µl of Recombinant Rnasine Ribonucelase Inhibitor, and 2 µl of GoScript™ Reverse Transcriptase, making-up a volume of 30 µl of master mix per RNA sample. Volumes were multiplied according to the number of samples. After that 30 µl of master mix was mixed with RNA sample by gentle pipetting. Reverse transcription reaction was performed on Bio-Rad Thermocycler according to manufacturer's protocol: 25°C for 5 mins, 42°C for another 60 mins, and for a final 15 mins at 70°C by a Thermal Cycler, proceeding it to finally cool down to 4°C, marking the end of the reverse transcription reaction.

Quantitative PCR (qPCR) or Real Time PCR for mRNA

This step is used to detect and quantify nucleic acids for numerous applications. In standard PCR, DNA is amplified by 3 repeating steps: denaturation, annealing and elongation. In dye-based qPCR due to fluorescence labeling it is possible to

quantify the amount of the amplified DNA by measuring proportional increases of fluorescence signal during each cycle as DNA replicates, according DNA is quantified in “real time”. In this work we used SYBR® Green is the most commonly used dye for non-specific detection. The dye emits at 520 nm and fluorescence emitted can be detected and related to the amount of targeted DNA. Gene expression was detected by StepOnePlus™ Real-Time PCR System with by mixing prepared cDNA with the Universal SYBR Green Supermix (dilution factor 1:20). Forward and reverse primers were pre-mixed together and diluted 1:20. Primers were designed for RT-qPCR by using NCBI Blast (Table 3.5.1). Negative control reaction with primers but without cDNA was performed. Reaction was performed in two stages: hold stage at 95 °C for 10 minutes and PCR stage (95 °C for 15 seconds; 60 °C for 1 minute). Data was analyzed with $-\Delta\Delta Ct$ method. Gene of interest expression was normalized to the expression of endogenous housekeeper gene (GAPDH). After that, $-\Delta Ct$ for control group was calculated as average and all samples were normalized to this $-\Delta Ct$, what gives us a $-\Delta\Delta Ct$ for each sample.

Quantitative PCR (qPCR) or Real Time PCR for miRNA

MicroRNAs and U6 small nuclear RNA (table 3.5.2) were polyadenylated and converted into cDNA with the use of TaqMan™ MicroRNA Reverse Transcription (RT) kit (Thermo Fisher Scientific, 4366596). Briefly, 3.4 ng of total RNA was mixed with 1.06 μ l of Nuclease-free water, 0.5 μ l of 10X RT Buffer, 0.05 μ l of dNTP mix w/dTTP (100M Total), 0.06 μ l of RNase inhibitor (20U/ μ L), and 0.33 μ l of MultiScribe™ RT enzyme (50U/ μ L). Finally, 3 μ l of RT primer was added (table 2), to make-up a total volume of 15 μ l. Reverse transcription was then performed by a Thermal Cycler according to the following reaction starting at 16°C for 30 mins, 42°C for another 30 mins, and for final 5 mins at 85°C, proceeding the machine to then cool down to 4°C, marking the end of the reaction.

Expression of miRNAs and U6 was then quantified by using StepOnePlus™ Real-Time PCR System and TaqMan™ Fast Universal PCR Master Mix (2X) kit. The reaction was performed in the final volume of 20 μ l, containing 4 μ l of prepared

cDNA, 15 μ l TaqManTM PCR master mix, and 1 μ l of TaqMan primers for RNU6, and miRNA of interest Table 3.4.2. Data was analyzed with $-\Delta\Delta C_t$ method. Gene of interest expression was normalized to the expression of endogenous housekeeper u6. After that, $-\Delta C_t$ for control group was calculated as average and all samples were normalized to this $-\Delta C_t$, what gives us a $-\Delta\Delta C_t$ for each sample.

Table 3.5.2 List of miRNAs analyzed in this research

miRNA	Mature miRNA sequence	Species	Assay ID
rno-miR-27b-5p	AGAGCUUAGCUGAUUGGUGAACAG	rat	4440886
rno-miR-497-5p	CAGCAGCACACUGUGGUUUGUA	mouse, rat	001346
rno-miR-214-3p	ACAGCAGGCACAGACAGGCAG	rat	000517
rno-miR-16-5p	UAGCAGCACGUAAAUAUUGGCG	mouse, rat, human	000391
rno-let-7e-5p	UGAGGUAGGAGGUUGUAUAGUU	mouse, rat, human	002406
rno-miR-21-5p	UAGCUUAUCAGACUGAUGUUGA	mouse, rat, human	000397
rno-miR-351-5p	UCCUGAGGAGCCCUUUGAGCCUGA	rat	002063
hsa-miRNA-27b-5p	AGAGCUUAGCUGAUUGGUGAAC	mouse, human	002174
hsa-miRNA-497-5p	CAGCAGCACACUGUGGUUUGU	human	001043
U6		mouse, rat, human	001973

3.6 Prediction of miRNAs involved in regulation of TGF β 1 and IL-11 (ERK) pathways with designed bioinformatical pipeline

In order to predict miRNAs expressed in rat and human CFs which can regulate IL-11 (ERK) and TGF β 1 signaling pathways we designed a specific bioinformatical pipeline. We believe that our selection criteria and filtration step allowed us to decrease false positive results in our prediction. From the database generated by Claudia's Bang group (Geo Gene Expression Omnibus Query DataSets for GSE76175) we found 728 miRNAs expressed in rat cardiac fibroblasts (CFs) and in extracellular vesicles derived from these cells [56]. From KEGG databases we picked up genes involved in TGF β 1 pathway and ERK signaling pathway [57, 58]. The next step was to check if some miRNAs were already validated by RT-qPCR or microarray. We found that 226 miRNAs were validated. Remaining 502 miRNAs were sorted by their expression in CFs and 25 % of the most expressed miRNAs (127 miRs) were used for further analysis with 226 validated miRNAs. After that, we checked the presence of binding site for

353 miRNAs in each gene from TGFβ1 and ERK pathways in three databases: TargetScan, MiRwalk and MirCode [59-61]. Our selection criteria were: 3-UTR miRNAs which were predicted to target genes from two crucial fibrotic pathways in all three databases. Moreover, predicted binding site should be conserved between rat and human. These criteria were used in order to eliminate false positive non-coding nucleic acids from our prediction. Finally, we obtained 68 miRNAs that showed affinity to one or more targets in two pathways. Graphical representation of discussed pipeline can be found on figure 3.5.1

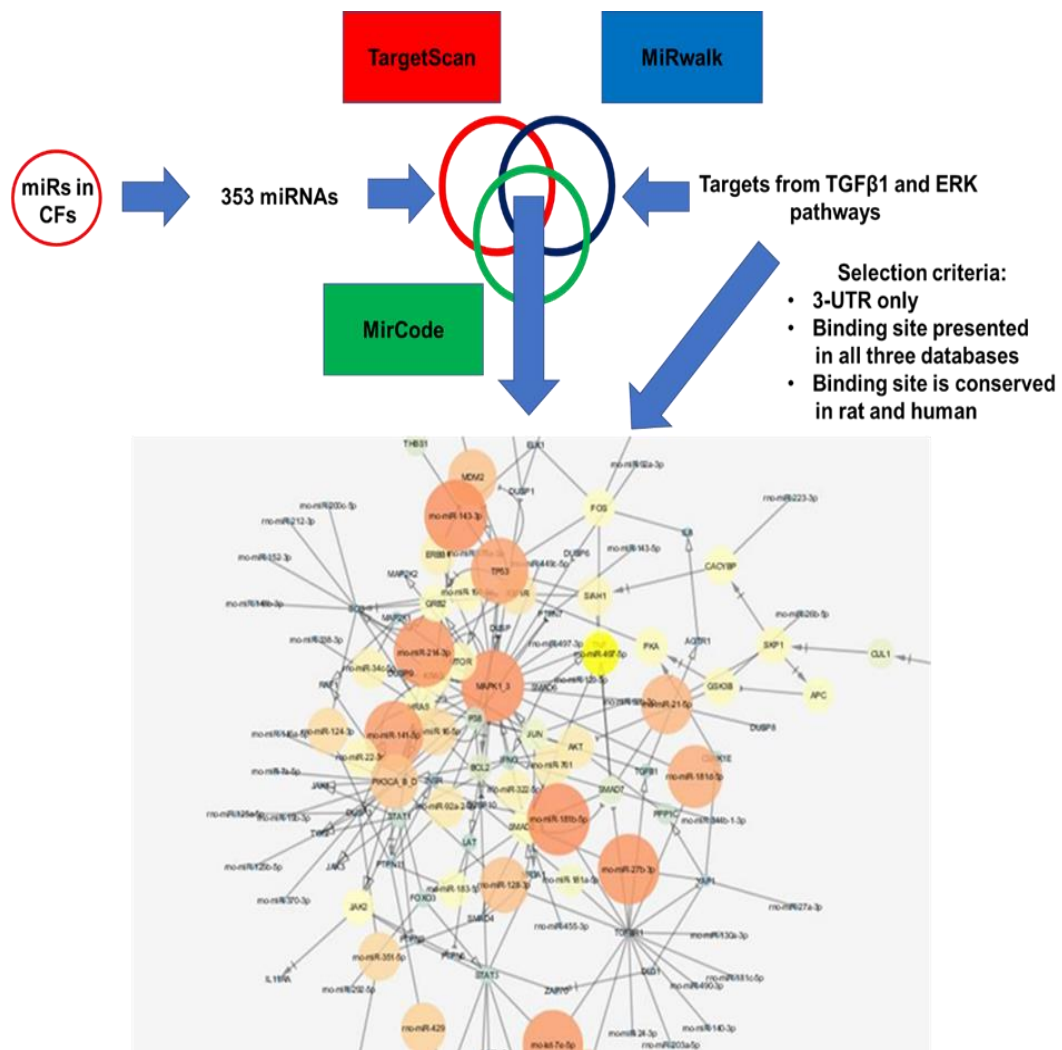


Figure 3.5 Bioinformatical pipeline for prediction of miRNAs regulated in cardiac fibrosis. 353 miRNAs expressed in rat CFs were analyzed for binding ability with genes from TGFβ1 and ERK signaling pathways. 68 miRNAs that satisfied selection criteria were used for network construction.

However, further analysis was required in order to pick up “best candidates”. For this reason, remaining miRNAs and their targets were used for network construction in cytoscape [62]. We sorted out nodes in the network by the number of their connections and set up a threshold: miRNA which have 3 or more targets in the network was considered a “good candidate”. As a result, we ended up with 7 miRNAs that have 3 and more targets in TGF β 1 and IL11 pathways.

3.7 Statistics

Statistic was done in Origin 8 Pro for all experiments. In vitro experiments on rat CFs (Immunostaining, RT-qPCR) was performed for $N \geq 3$ animals in biological duplicates with at least (2-3) technical replicates. Normal distribution was checked by Shapiro-Wilk test. For Immunostaining Data One-Way Anova followed by a Šídák’s multiple comparison test was performed. For RT-qPCR data Student’s t-test was performed. For all data present as Mean \pm SEM. P values <0.05 were considered statistically significant.

4. RESULTS I

4.1 IL-11 and TGF β 1 treatment causes an increased expression of α -SMA and Colla1 in rat cardiac fibroblasts as well as MI rat cardiac fibroblasts

In the work of Schafer et al. 2017 [2] a pro-fibrotic role of IL-11 cytokine was extensively discussed for human cardiac fibroblasts. We decided to prove that IL-11 stimulation can also be used for differentiation into myofibroblasts and further use as a cell culture model of cardiac fibrosis in cells derived from rats LV. In order to reproduce existing data in rat cardiac fibroblasts isolated from LV we prepared three T-25 flasks with equal number of cells. As a positive control of stimulation of fibroblasts with pro-fibrotic factors we introduced treatment with TGF β 1, which is known as master regulator of cardiac fibrosis [20]. Another flask, was stimulated with IL-11 itself. The last one remained untreated. Experiment was repeated for three animals in triplicates, as described in chapter (3.4).

First of all, we were aiming to observe if IL-11 causes changes in gene expression of Acta2, gene encoding α -SMA, which is considered to be one of the markers of myofibroblasts [4]. In 24 h IL-11 should up-regulate expression of genes associated with ECM deposition, like Colla1, and myofibroblasts differentiation through ERK signaling. On Figure 4.1.A we can observe an increase in α -SMA expression (9.8 ± 1.3) of rat cardiac fibroblasts treated with 5 ng/ul of IL-11. Gene expression was normalized to Gapdh expression. The effect was comparable with TGF β treatment (100 ng/ul) Figure 4.1.B. Stimulation with TGF β 1 leads to a significant increase of α -SMA expression up to (7.6 ± 1.6). Student's t-test was applied since normal distribution was assumed. *p-value<0.05.

Next, we decided to check how IL-11 stimulation in rat cardiac fibroblasts affects expression of ECM proteins, like collagens. For this purpose, we analyzed expression of Colla1 and Col3a1, since they are the most presented collagen types in ECM [63]. On the figure 4.1.D it is shown that 5ng/ μ l treatment significantly boosts Colla1 expression (8.3 ± 1.9) in rat cardiac fibroblasts (N=3). At the same time, TGF β 1 stimulation also results in growing expression of Colla1

(11.7 ± 1.2) in rat cardiac fibroblasts (N=3). These results support current knowledge about IL-11 and TGF β 1 stimulation. Moreover, we have measured expression of Col3a1, which is known to be the second prevalent type of collagen in ECM. Unfortunately, we did not observe any significant regulation of Col3a1 under both treatments in rat cardiac fibroblasts (N=3) Figure 4.1.G-H. There is a point of view that Collagen III is an important ECM protein which is well expressed by cells around vessels [64]. In this case, treatment models of healthy CFs won't be able to mimic conditions and state of cells forming vessels.

Treatment models stimulated with different pro-fibrotic factors are not representing all processes which underlie fibrosis events in heart. It also doesn't distinguish between different types of fibrosis. For this reason, we decided to include in our research an animal model which would mimics cardiac events associated with development of fibrosis. Myocardial infarction model was chosen as an event which leads to scar formation and fibrosis progression as described in introduction. We compared wild-type rat CFs with MI rat CFs which were cultivated in parallel. When cells reached confluence we isolated RNA and conducted RT-qPCR. Experiment was done for three animals (N =3) in triplicates. Results of RT-qPCR for α -SMA (Figure 4.1.C), Col1a1 (Figure 4.1.F) and Col3a1 (Figure 4.1.I) referred to endogenous control Gapdh indicate significant up-regulation of all three genes. In other words, MI causes changes in expression of genes associated with formation of stress fibers and main elements of ECM, what was expected from MI rat model.

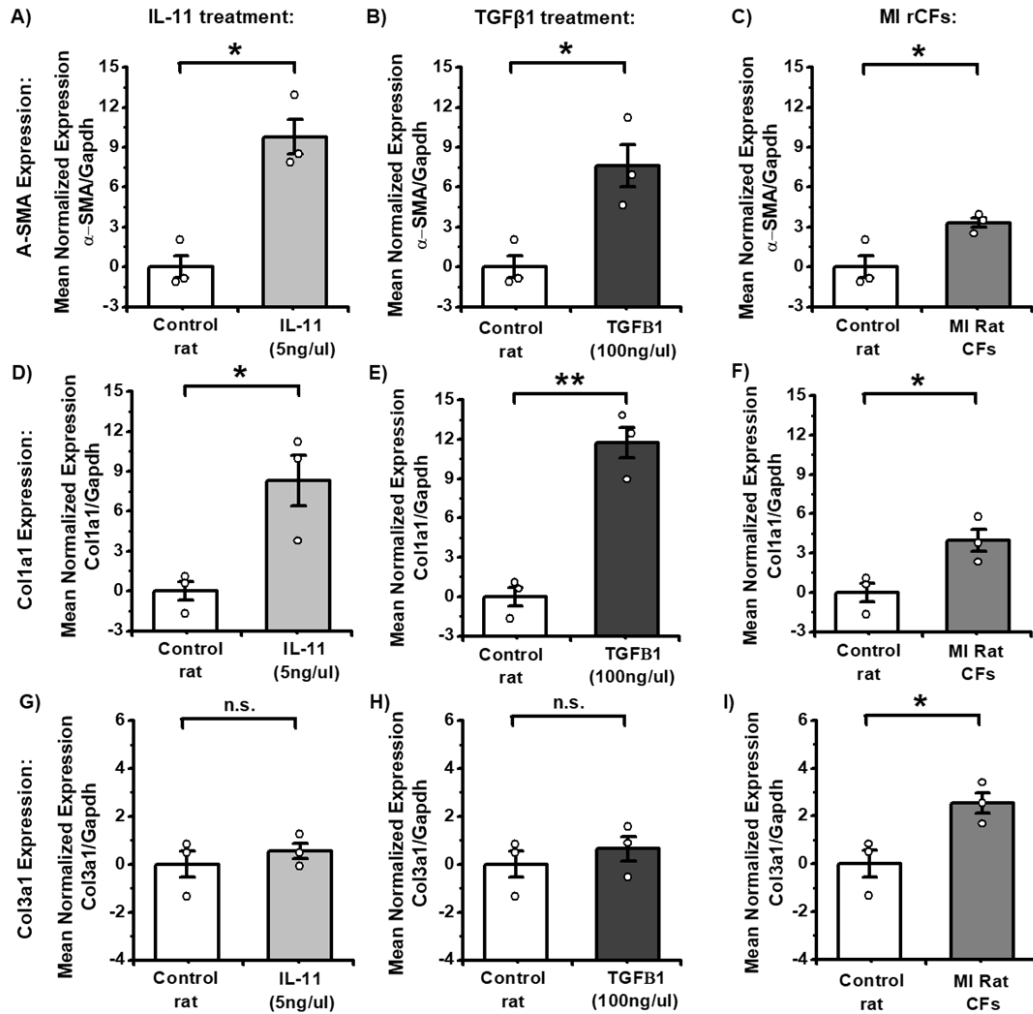


Figure 4.1 IL-11 (5 ng/μl) and TGFβ1 (100 ng/μl) treatment models and MI model validation by RT-qPCR. RT-qPCR results are calculated with $-\Delta\Delta CT$ method, normalized to Gapdh expression and referred to control group (A-I). Data present as Mean $-\Delta\Delta CT$ values \pm SEM (A-I). **A)** A-Sma expression in rCFs treated with IL-11 (5 ng/μl). **B)** A-Sma expression in rCFs treated with TGFβ1 (100 ng/μl). **C)** A-Sma expression in MI CFs. **D)** Col1a1 expression in rCFs treated with IL-11 (5 ng/μl). **E)** Col1a1 expression in rCFs treated with TGFβ1 (100 ng/μl). **F)** Col1a1 expression in MI CFs. **G)** Col3a1 expression in rCFs treated with IL-11 (5 ng/μl). **H)** Col3a1 expression in rCFs treated with TGFβ1 (100 ng/μl). **I)** Col3a1 expression in MI CFs. Expression was compared with the control rat CFs. Student's t-test was used to determine significant difference between control group and pathological model. *p-value<0.05, **p-value<0.01; ns – not significant.

Overall, results of our first experiment indicate that IL-11 treatment mimics caused by TGFβ1 treatment gene expression patterns. Even though, both TGFβ1

and IL-11 did not affect Col3a1 expression like CFs from MI they were causing transcriptional changes in ACTA2 (encoding α -SMA) and Col1a1. That results indicate that in vitro models were representing transcriptional changes associated with cardiac fibrosis.

4.2 IL-11 and TGF β 1 treatment causes an increased number of myofibroblasts in rat cardiac fibroblasts comparable with fibroblasts from myocardial infarction rats

To investigate the role of IL-11 and TGF β 1 treatment on the phenotype rat CFs from LV we repeated experiment described in previous paragraph. However, this time rat CFs were utilized for immunostaining against vimentin and α -SMA. As we already, mentioned α -SMA is the hallmark of mature myofibroblasts, it helps to remodel ECM and keep heart contractility in the area of scar in MI. At the same time, vimentin is an intermediate filament protein which usually presented in mesenchymal lineages. According to the literature, vimentin is the most sensitive marker to detect CFs [65]. However, there are other cell types which are expressing this protein: endothelial cells, smooth muscle cells, neurons and pericytes. Interestingly, that α -SMA is also presented in endothelial cells [66]. For this reason, we were considering that IL-11 or TGF β 1 treatment may stimulate some remaining endothelial cells in vitro, what remains a limitation of this experiment.

Equal number of cells were seeded in 12-well flask (100 000 cells/well) for 24 h at 37 °C and 5% CO₂. Two wells were treated with IL-11 (5 ng/ μ l), other two wells were treated with TGF β 1 (100 ng/ μ l) for 24 h and the remaining wells were untreated and used as a control condition. On the next day, we proceeded with Immunostaining described in chapters 3.2-3.3. In parallel, rat CFs from LV of MI rats were seeded equally with healthy rat CFs. On the next day, they were used for Immunostaining.

With immunostaining we observed a massive increase in numbers of α -SMA and vimentin cells with recognizable stress fibers, what indicates that these healthy rat CFs are already myofibroblasts under IL-11 treatment and TGF β 1 treatment. On

the Figure 4.2 (A-C) representative images can be observed. In comparison to control cells (A), cells stimulated with IL-11 (B) and TGF β 1 (C) have a strong signal in green channel (α -SMA). Furthermore, stress fibers can be appreciated. Quantification on α -SMA and vimentin positive rat CFs (Figure 4.2.1.D) revealed significant accumulation of the myofibroblasts in rat CFs treated with IL-11 (Percentage of α -SMA positive cells = 62.6 ± 4.2 , p-value = 0.01) and with TGF β 1 (Percentage of α -SMA positive cells = 70.4 ± 3.7 , p-value = 0.001).

As we expected comparison of CFs from healthy and MI rats showed an increased intensity of α -SMA in cells derived from pathological rats. Having a closer look on rat CFs (Figure 4.2 E) we can observe few α -SMA positive cells while pathological rat CFs present α -SMA in all of them. Quantification over α -SMA positive cells in healthy and MI rat CFs (213 cells vs 161 cells in total, respectively) demonstrated significantly higher presence of myofibroblasts in cells derived from MI rat CFs (Percentage of α -SMA positive cells = 67.9 ± 2.1 , p-value = 0.01).

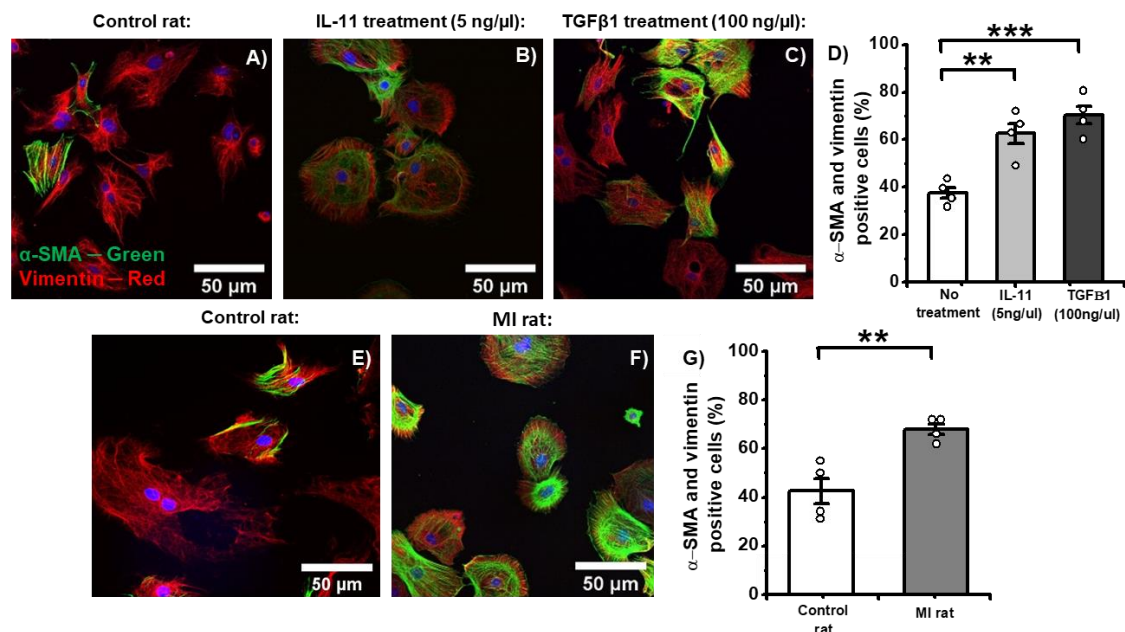


Figure 4.2 IL-11 (5 ng/ μ l), TGF β 1 (100 ng/ μ l) and MI rat CFs exhibit more α -SMA and vimentin positive cells in comparison with rat CFs from healthy rats. A) Through D), rat CFs were treated with IL-11 or TGF β 1 for 24 hours in 10% FBS DMEM medium supplemented with 1% of penicillin and streptomycin. After treatment, rat CFs were washed with PBS, fixed in paraformaldehyde, and permeabilized with Triton 100.

After blocking, cells were incubated with primary and secondary antibodies. DAPI was used to stain the nucleus. **D)** Quantitative analysis suggests that both IL-11 and TGF β 1 treatment significantly induce the number of myofibroblasts (α -SMA and vimentin positive cells). **E)** through **F)** rat CFs were compared with MI rat CFs (cells isolated after 16 weeks when coronary artery ligation was performed), both of them were cultivated in 10% FBS DMEM medium supplemented with 1% of penicillin and streptomycin. **G)** Quantitative analysis indicates that MI rat model results in significant boost of myofibroblasts number in cell culture. Red represents vimentin, green – α -SMA and blue – DAPI. Six fields of view were imaged per coverslip using a 20x magnification with ~20 cells for image. All results are presented as mean \pm standard error of mean (SEM) with (N = 4) The statistical analysis of the immunostaining data was assessed using One-Way analysis of variance (ANOVA), followed by a Šídák's multiple comparison test, **p<0.01, ***p<0.001.

Overall, with this experiment we demonstrated that treatment models (TGF β 1, IL-11) as well as MI rat CFs are characterized not only by up-regulation of fibrotic markers but also by presence of significantly higher number of myofibroblasts in vitro.

4.3 miRNA-497-5p and miRNA-27b-5p predicted to be involved in regulation of TGF β 1 and ERK pathways

As we were aiming to find miRNAs which are acting as down-stream effectors of IL-11 we designed bioinformatical pipeline described in methods. Since IL-11 production in cardiac fibroblasts is strongly dependent on TGF β 1 pathway activation we decided to use both ERK and TGF β 1 pathways for prediction. In this study we tested 353 miRNAs which are expressed in rat CFs (Figure 4.3) for the binding affinity with a list of targets for TGF β 1 and ERK pathway which were obtained from KEGG. After the filtration step, we got 68 miRNAs that showed an affinity for a binding site to one or more targets in pathways. Consequently, we removed miRNAs that have less than 3 targets. miRNA-27b-5p and miRNA-497-5p which were extensively studied in this research are highlighted in yellow while other miRNAs are colored with cyan (Figure 4.3).

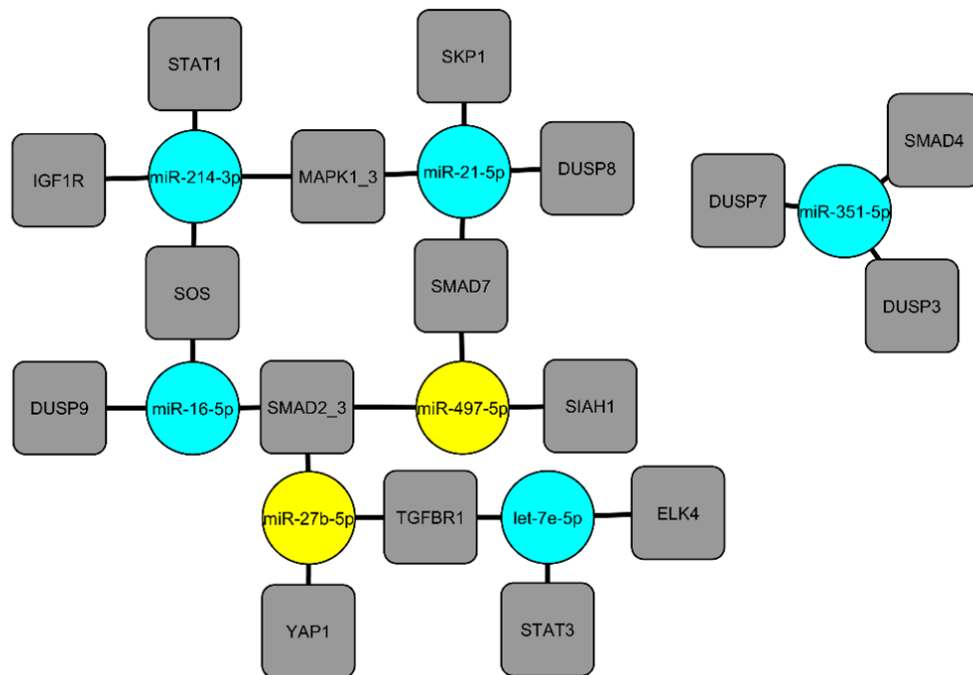


Figure 4.3 Prediction of miRNAs expressed in cardiac fibroblasts and associated with cardiac fibrosis through regulation of IL-11 and TGFβ1 pathways. Prediction pipeline for miRNAs that can be associated with cardiac fibrosis by their regulation of IL-11 and TGFβ1 pathways. 728 miRNAs were used for the analysis from public dataset (Geo Gene Expression Omnibus Query DataSets for GSE76175). From KEGG databases we picked up genes involved in TGFβ1 pathway and ERK signaling pathway. 226 miRNAs were already validated, from remaining 502 miRNAs (25%) of the most expressed miRNAs were also included. 353 miRNAs in total were checked for a binding site within a list of targets from KEGG in TargetScan, MiRwalk and MirCode. Best candidates were selected according to selection criteria. miRNAs of interest are highlighted with yellow, remaining miRNAs colored with cyan and target genes with grey.

Interestingly that among seven predicted “candidates” miRNA-214-3p, miRNA-21-5p, miRNA-27b-5p are known to participate in regulation of molecular mechanisms of cardiac fibrosis.

4.4 miRNA-497-5p and miRNA-27b-5p are up-modulated in cardiac fibroblasts from myocardial infarction rats and in IL-11 treatment model of cardiac fibrosis

In order to narrow down the number of candidates we conducted RT-qPCR on miRNAs in rat CFs treated with IL-11 (5 ng/ μ l) or TGF β 1 (100 ng/ μ l) and in MI CFs. Our results demonstrate that both miRNA-27b-5p and miRNA-497-5p are significantly up-regulated ($-\Delta\Delta$ CT miRNA-27b-5p = 2.7 ± 0.5 ; $-\Delta\Delta$ CT miRNA-497-5p = 2.9 ± 0.1 ; p-value < 0.01) in IL-11 treated (Figure 4.4 A, B) rat CFs and in MI rat CFs (Figure 4.4 C, D) but not in TGF β 1 (Figure 4.4 E, F) treated rat CFs.

Up-regulation of miRNA-27b-5p and miRNA-497-5p by IL-11 treatment may indicate their role as down-stream effectors of that pro-fibrotic cytokine. It is supported by the fact of IL-11 up-modulation in border zone of MI patients [29]. In addition, we observed up-regulation of both miRNAs in CFs derived from rats with MI. Interestingly, that TGF β 1 did not demonstrate any significant effect on miRNAs expression. That can be explained, by regulation of miRNAs expression through Smad independent manner. Alternatively, TGF β 1 stimulation for 24h may be insufficient to induce significant changes in miRNAs expression.

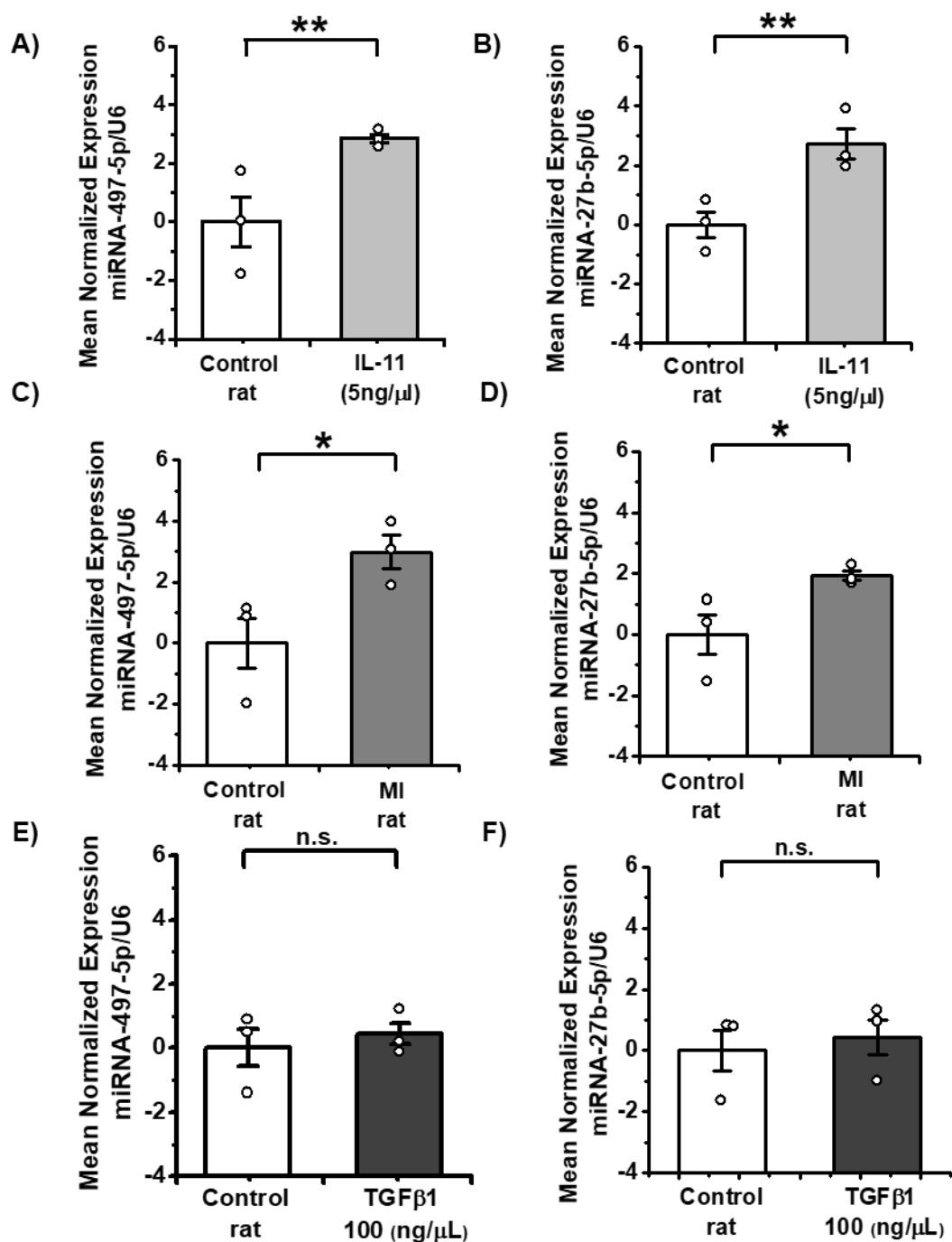


Figure 4.4 Validation experiments for miRNAs expressed in cardiac fibroblasts and associated with cardiac fibrosis through regulation of IL-11 and TGFβ1 pathways. RT-qPCRs of miRNA expression in control rat CFs (white bar), rat CFs treated with IL-11 (5ng/μl, 24hrs) (light grey) with TGFβ1 treated (100ng/μl) and in MI rat CFs (grey). miRNA-497-5p expression in IL-11 treated rat CFs **A**), MI rat CFs **C**) and in TGFβ1 treated rat CFs **E**). miRNA-27b-5p expression in IL-11 treated rat CFs (**B**), MI rat CFs (**D**) and in TGFβ1 treated rat CFs **F**). Data presented as mean $-\Delta\Delta\text{CT}$ values \pm SEM (N=3, n

=3). Student's t-test was used to determine significant difference between groups. *p<0.05, **p<0.01, n.s. = non-significant (p>0.05).

4.5 Remaining predicted miRNAs regulation under IL-11 treatment and in myocardial infarction rat cardiac fibroblasts

The expression of the 5 remaining predicted miRNAs was determined in rat CFs treated with IL-11 (5ng/μl), or in MI rat model (Figure 4.5). miRNA let-7e-5p, miRNA-16-5p and miRNA-214-3p were not regulated by IL-11 treatment or in MI model (Figure 4.5 A-C). From remaining miRNAs only miRNA-21-5p was also significantly (p-value<0.05) up-regulated in IL-11 and MI model (Figure 4.5 D), while miRNA-351 was up-modulated only in MI rat CFs (p-value<0.05). We decided to focus on miRNA-27b-5p and miRNA-497-5p in our research since their less studied than miRNA-21-5p not only in terms of molecular mechanism [67] but also as potential circulating biomarkers [68].

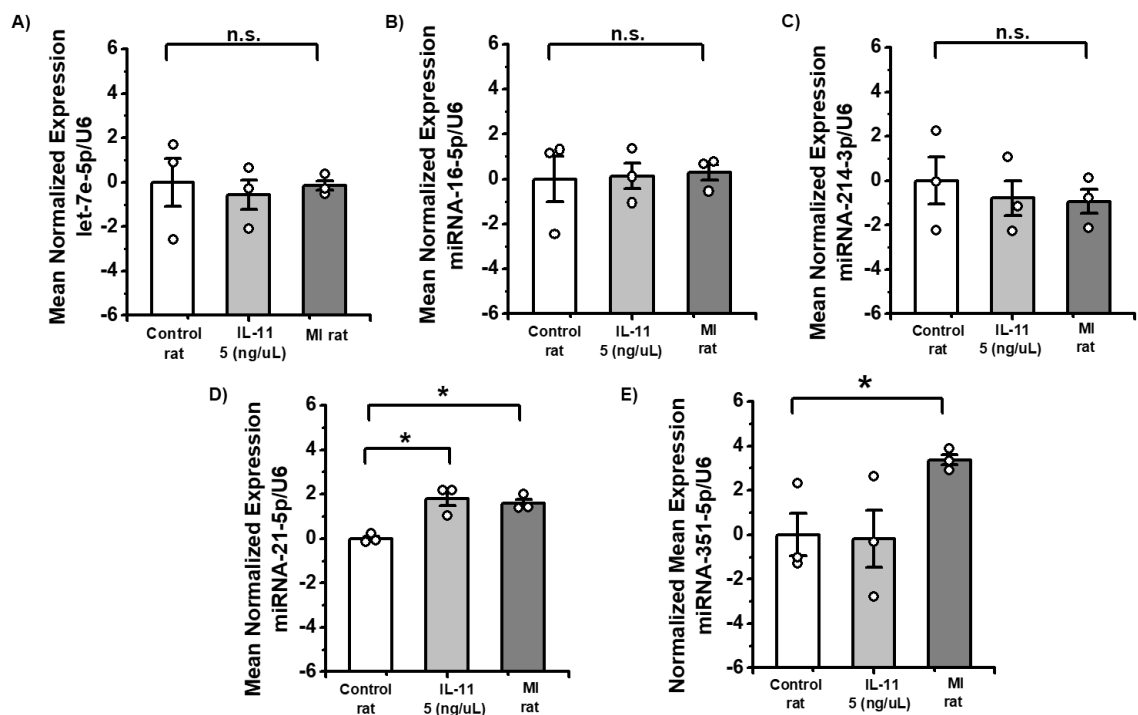


Figure 4.5 Predicted miRNAs expression under IL-11 treatment (5 ng/μl) and MI models. A), B), C) indicate that predicted miRNA-214, miRNA-16 and let-7e were not regulated in IL-11 (5 ng/μl, 24h) and MI models. D) shows that miRNA-21 was up-

regulated in IL-11 (grey bar) treatment and MI (blue bar) rat models in comparison to control condition. **E)** indicates that miRNA-351 was not affected by IL-11 treatment for 24h but was significantly up-modulated in MI model in comparison to control rat. RT-qPCR data is calculated with $-\Delta\Delta\text{CT}$ method. miRNAs expression was normalized to u6 expression and referred to the control group. All results are presented as mean \pm standard error of mean (SEM) with (N = 3). Student's t-test was used to determine significant difference between control group and pathological model for figures * $p < 0.05$.

4.6 Characterization of human cardiac fibroblasts from patients with dilated and ischemic cardiomyopathies

In order to test miRNA-27b-5p and miRNA-497-5p expression in CFs derived from patients with cardiac fibrosis we characterized available patients with dilated and ischemic cardiomyopathies (DCM and ICM respectively) (Figure 4.6). Unfortunately, we were limited in number of patients (N = 3 for DCM/ICM patients and N = 1 for donor heart rejected for transplantation). However, we were able to detect significant up-regulation of α -SMA expression accompanied by patterns for up-regulation in CTGF levels (Figure 4.6 A, B) in CFs from ICM patients but not DCM patients. Data on gene expression was also confirmed by Immunostaining against α -SMA positive cells, which were significantly more present in cell culture from ICM patients in comparison with donors but, again, not in DCM patients. These results suggest that ICM CFs in vitro pathological model is more preferable and comparable with our previous models rather than DCM. Also we considered our limitation in sample number and genetic variance which is present in DCM patients [69].

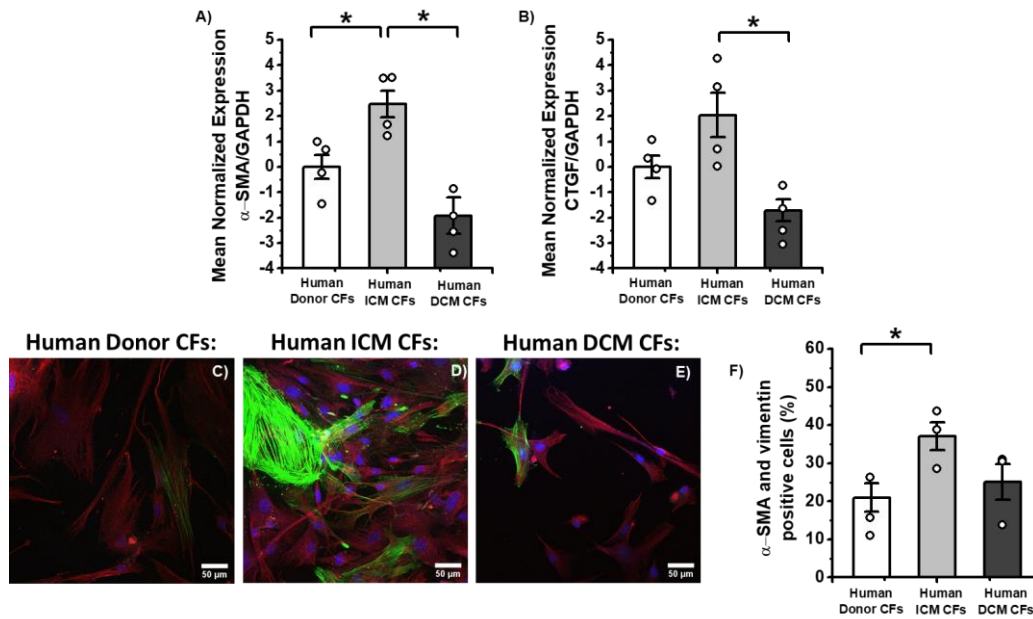


Figure 4.6 Characterization of CFs from donor, ICM and DCM patients. Gene expression in human CFs from donor (white bar), ICM patients (light grey) and DCM patients (dark grey). **A)** α -SMA expression. **B)** CTGF expression. Representative images of human CFs stained against α -SMA (green), vimentin (red) and DAPI (blue) from donor **C)**, ICM patients **D)**, DCM patients **E)**. Quantification of α -SMA positive cells (%) in human CFs from donor (white bar), ICM patients (light grey) and DCM patients (dark grey). Data presented as mean \pm SEM. N =1, n =4 for donor and N =4 n = 2 for patients with ICM or DCM. Data was assessed using one-way ANOVA, followed by a Tukey's multiple comparison test, * $p < 0.05$.

4.7 miRNA-27b-5p and miRNA-497-5p expression in cardiac fibroblasts from left ventricle of patients with dilated and ischemic cardiomyopathy

Finally, we tested miRNA-27b-5p (Figure 4.7 A) and miRNA-497-5 (Figure 4.7 B) expression in human CFs from ICM and DCM patients. We demonstrated that in human patients with cardiomyopathies miRNA-27b-5p was not regulated. While miRNA-497-5p had patterns for up-regulation in ICM patients and was significantly increased in levels in CFs from DCM patients ($-\Delta\Delta CT = 1.8 \pm 0.4$, p -value < 0.05). For this reason, we continued our research on miRNA-497-5p in next chapters and kept an eye on miRNA-27b-5p.

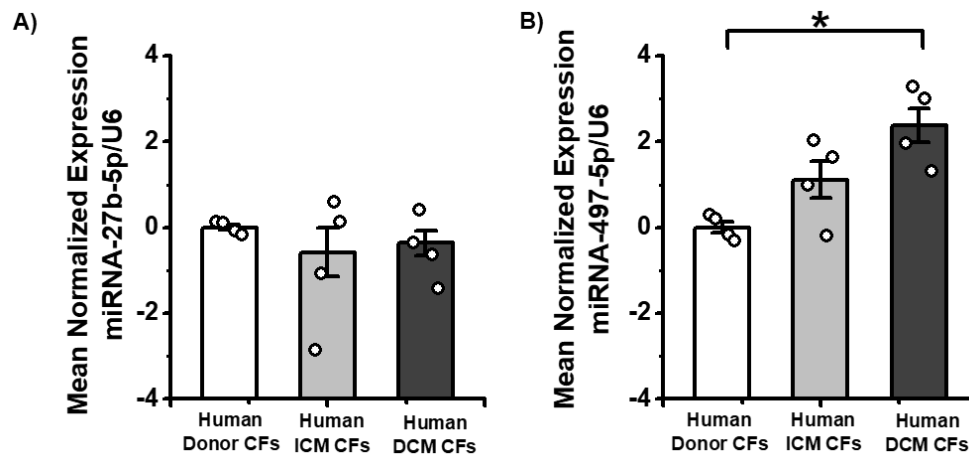


Figure 4.7 miRNA-27b-5p and miRNA-497-5p expression in human donor, ICM and DCM CFs. miRNA expression in human CFs from donor (white bar), ICM patients (light grey) and DCM patients (dark grey). **A)** miRNA-27b-5p expression. **B)** miRNA-497-5p expression. Data presented as mean \pm SEM. N =1, n =4 for donor and N =4 n = 2 for patients with ICM or DCM. Data was assessed using one-way ANOVA, followed by a Tukey's multiple comparison test, *p<0.05.

5. DISCUSSION I

In this study we predicted and validated miRNA-27b-5p and miRNA-497-5p up-regulation in response to IL-11 treatment.

Myofibroblasts as main drivers of the pathological cardiac fibrosis in heart can be activated by various stimulus depends on the context and model [70,71]. Among various context/model dependent pro-fibrotic factors and stimulus like ANGII, TIMP, TNF α e.t.c. TGF β 1 and IL-11 are considered to be essential regulators of myofibroblasts activation [2, 72]. Here we demonstrated effect of IL-11 on rat CFs. It was characterized with increased myofibroblasts markers: α -SMA and Colla1 expression and increase of number of myofibroblasts in vitro. This effect was comparable with TGF β 1 treatment and CFs derived from MI rats.

In the past decade, several studies have emphasized that beside of activation of pro-fibrotic genes by TGF β 1 it can functionally repress anti-fibrotic mechanisms via miRNAs [73, 74]. Unlike TGF β 1, IL-11 down-stream activation of miRNAs is less studied, especially in cardiac fibrosis [75]. In this work we were aiming to predict and validate miRNAs activated by IL-11. We considered that usually IL-11 autocrine production in CFs is activated by TGF β 1 [2]. In addition, IL-11 increase pro-fibrotic gene expression through ERK signaling. For this reason, we assessed binding affinity of 353 miRNAs expressed in CFs with targets from TGF β 1 and ERK pathways in 3 miRNAs targets prediction tools. Narrowing it down, we ended up with 7 potential candidates among which we found miRNA-27b-5p and miRNA-497-5p-5 as IL-11 effectors. Interestingly, that both miRNAs were also up-regulated pathologically in MI rat CFs but were not affected by TGF β 1 treatment. Up-regulation of IL-11 activated miRNAs in MI model is reasonable since this cytokine was reported to be an important up-modulated pro-fibrotic regulator in this model [41]. At the same time, TGF β 1 24 hours treatment maybe insufficient in order to increase IL-11 expression and consequently further expression of its down-stream effectors, miRNA-27b-5p and miRNA-497-5p.

Despite the fact that, we also observed an IL-11 effect on miRNA-21-5p (among 7 predicted candidates) expression we decided to continue research on miRNA-27b-5p and miRNA-497-5p since their less studied [67,68]. miRNA-21-5p is a well-known driver of cardiac fibrosis which is working through regulation of TGF β 1 (targeting SMAD7) pathway [76] and ERK pathway (targeting Spry1) [77]. At the same time, it is known that miRNA-27b expression can be repressed by TGF β 1 and its overexpression in CMs leads to cardiac hypertrophy and dysfunction by targeting PPAR- γ in transgenic mice [78]. Moreover, miRNA-27b can accelerate angiogenesis by regulating translation of Dll4/Notch axis, PPAR γ and its downstream effectors [79]. Alternatively, miRNA-497-5p in the literature is known for its anti-hypertrophic effect through regulation of Sirt4 expression both in vitro and in vivo [80]. Furthermore, miRNA-497-5p was studied in pulmonary fibrogenesis processes where it was inducing fibrosis through RECK inhibition and further ECM reorganization through MMP2/9 [81].

In this chapter we also evaluated miRNA-27b-5p and miRNA-497-5p expression in CFs from patients with ICM and DCM. Cardiomyopathies are usually accompanied by cardiac fibrosis and lead to HF [82]. However, etiologies for DCM and ICM are different what leads to different consequences [83]. ICM is caused by long-term myocardial ischemia [84] while DCM can be originated by autoimmune diseases, viral infections or by a genetic factor [84]. DCM characterized by dilation of the ventricle and systolic dysfunction accompanied by diffused cardiac fibrosis [85]. Unfortunately, due to the limited number of patients or maybe due to the genetic variability in DCM patients [86] we were not able to characterize CFs with increased α -SMA and CTGF expression, while ICM were described with increased numbers of α -SMA positive cells and α -SMA expression. According to our RT-qPCR results we observed up-regulation of miRNA-497-5p in DCM CFs. While miRNA-27b-5p was not regulated in CFs from both ICM and DCM.

6. REFERENCES I

1. Pinzón N, Li B, Martinez L, et al. microRNA target prediction programs predict many false positives. *Genome Res.* **2017**;27(2):234-245. doi:10.1101/gr.205146.116
2. Schafer S, Viswanathan S, Widjaja AA, et al. IL-11 is a crucial determinant of cardiovascular fibrosis. *Nature.* **2017**;552(7683):110-115. doi:10.1038/nature24676
3. Chen H, Moreno-Moral A, Pesce F, et al. WWP2 regulates pathological cardiac fibrosis by modulating SMAD2 signaling [published correction appears in *Nat Commun.* 2019 Sep 9;10(1):4085]. *Nat Commun.* **2019**;10(1):3616. Published 2019 Aug 9. doi:10.1038/s41467-019-11551-9
4. Shinde AV, Humeres C, Frangogiannis NG. The role of α -smooth muscle actin in fibroblast-mediated matrix contraction and remodeling. *Biochim Biophys Acta Mol Basis Dis.* **2017**;1863(1):298-309. doi:10.1016/j.bbadis.2016.11.006
5. Zhuang X, Rhode KS, Razavi RS, Hawkes DJ, Ourselin S. A registration-based propagation framework for automatic whole heart segmentation of cardiac MRI. *IEEE Trans Med Imaging.* **2010**;29(9):1612-1625. doi:10.1109/TMI.2010.2047112
6. Frangogiannis NG. Cardiac fibrosis. *Cardiovasc Res.* **2021**;117(6):1450-1488. doi:10.1093/cvr/cvaa324
7. Berk BC, Fujiwara K, Lehoux S. ECM remodeling in hypertensive heart disease. *J Clin Invest.* **2007**;117(3):568-575. doi:10.1172/JCI31044
8. Azevedo PS, Polegato BF, Minicucci MF, Paiva SA, Zornoff LA. Cardiac Remodeling: Concepts, Clinical Impact, Pathophysiological Mechanisms and Pharmacologic Treatment. *Arq Bras Cardiol.* **2016**;106(1):62-69. doi:10.5935/abc.20160005

9. O'Grady H, Mostafa K, Zafar H, Lohan D, Morris L, Sharif F. Changes in left ventricular shape and morphology in the presence of heart failure: a four-dimensional quantitative and qualitative analysis. *Int J Comput Assist Radiol Surg.* **2019**;14(8):1415-1430. doi:10.1007/s11548-019-01985-3
10. Ahmad F, Seidman JG, Seidman CE. The genetic basis for cardiac remodeling. *Annu Rev Genomics Hum Genet.* **2005**;6:185-216. doi:10.1146/annurev.genom.6.080604.162132
11. Richard Hobbs FD, Andrea K. Roalfe, Russell C. Davis, Michael K. Davies, Rachel Hare, and the Midlands Research Practices Consortium (MidReC), Prognosis of all-cause heart failure and borderline left ventricular systolic dysfunction: 5 year mortality follow-up of the Echocardiographic Heart of England Screening Study (ECHOES), *European Heart Journal*, Volume 28, Issue 9, May **2007**;28:1128-1134.
12. Ding Y, Wang Y, Zhang W, et al. Roles of Biomarkers in Myocardial Fibrosis. *Aging Dis.* **2020**;11(5):1157-1174. Published 2020 Oct 1. doi:10.14336/AD.2020.0604
13. Hausmann C, Zoschke C, Wolff C, et al. Fibroblast origin shapes tissue homeostasis, epidermal differentiation, and drug uptake. *Sci Rep.* **2019**;9(1):2913. Published 2019 Feb 27. doi:10.1038/s41598-019-39770-6
14. Orogo AM, Gustafsson ÅB. Cell death in the myocardium: my heart won't go on. *IUBMB Life.* **2013**;65(8):651-656. doi:10.1002/iub.1180
15. Alex L, Frangogiannis NG. Pericytes in the infarcted heart. *Vasc Biol.* **2019**;1(1):H23-H31. Published 2019 Apr 25. doi:10.1530/VB-19-0007
16. van Caam A, Vonk M, van den Hoogen F, van Lent P, van der Kraan P. Unraveling SSc Pathophysiology; The Myofibroblast. *Front Immunol.* **2018**;9:2452. Published 2018 Nov 13. doi:10.3389/fimmu.2018.02452
17. Cole MA, Quan T, Voorhees JJ, Fisher GJ. Extracellular matrix regulation of fibroblast function: redefining our perspective on skin aging. *J Cell Commun Signal.* **2018**;12(1):35-43. doi:10.1007/s12079-018-0459-1

18. Herum KM, Choppe J, Kumar A, Engler AJ, McCulloch AD. Mechanical regulation of cardiac fibroblast profibrotic phenotypes. *Mol Biol Cell*. **2017**, 28 (14):1871–1882.
19. van der Slot A.J, Zuurmond A.M, van den Bogaerd A.J, Ulrich M.M, Middelkoop E, Boers W, et al. Increased formation of pyridinoline cross-links due to higher telopeptide lysyl hydroxylase levels is a general fibrotic phenomenon. *Matrix Biol* **2004**, 23:251–7.
20. Zhang YE. Non-Smad pathways in TGF-beta signaling. *Cell Res*. **2009**, 19 (1):128–139.
21. Fu WB, Wang WE, Zeng CY. Wnt signaling pathways in myocardial infarction and the therapeutic effects of Wnt pathway inhibitors. *Acta Pharmacol Sin*. **2019**, 40(1):9–12.
22. Tikhomirov R, Reilly-O'Donnell B, Catapano F, Faggian G, Gorelik J, Martelli F, & Emanuelli C. EVs: From Potential Culprits to New Therapeutic Promise in the Setting of Cardiac Fibrosis. *In Cells*, **2020**;9(3) <https://doi.org/10.3390/cells9030592>
23. Zilberberg L, Todorovic V, Dabovic B, Horiguchi M, Couroussé T, Sakai LY, et al. Specificity of latent TGF- β binding protein (LTBP) incorporation into matrix: role of fibrillins and fibronectin. *J Cell Physiol* **2012**, 227:3828–36.
24. Itoh Y, Koinuma D, Omata C, et al. A comparative analysis of Smad-responsive motifs identifies multiple regulatory inputs for TGF- β transcriptional activation. *J Biol Chem*. **2019**;294(42):15466-15479. doi:10.1074/jbc.RA119.009877
25. Miyazawa K, Miyazono K. Regulation of TGF- β Family Signaling by Inhibitory Smads. *Cold Spring Harb Perspect Biol*. **2017**;9(3):a022095. Published 2017 Mar 1. doi:10.1101/cshperspect.a022095
26. Piersma B, Bank RA, Boersema M. Signaling in Fibrosis: TGF- β , WNT, and YAP/TAZ Converge. *Front Med (Lausanne)*. **2015**;2:59. Published 2015 Sep 3. doi:10.3389/fmed.2015.00059

27. Xie L, Law BK, Chytil AM, Brown KA, Aakre ME, Moses HL. Activation of the Erk pathway is required for TGF-beta1-induced EMT in vitro. *Neoplasia*. **2004**, 6 (5):603–610.
28. Harmer SL, DeFranco AL. Shc contains two Grb2 binding sites needed for efficient formation of complexes with SOS in B lymphocytes. *Mol Cell Biol*. **1997**;17(7):4087-4095. doi:10.1128/MCB.17.7.4087
29. Plotnikov A, Zehorai E, Procaccia S, Seger R. The MAPK cascades: signaling components, nuclear roles and mechanisms of nuclear translocation. *Biochim Biophys Acta*. **2011**;1813(9):1619-1633. doi:10.1016/j.bbamcr.2010.12.012
30. Carthy JM, Garmaroudi FS, Luo Z, McManus BM. Wnt3a induces myofibroblast differentiation by upregulating TGF- β signaling through SMAD2 in a β -catenin-dependent manner. *PLoS One*. **2011**, 6(5):e19809.
31. Hermans KCM, Daskalopoulos E., Blankesteyn WM. The Janus face of myofibroblasts in the remodeling heart. *J Mol Cell Cardiol*. **2016**, 91:35–41.
32. Blyszczuk P, Müller-Edenborn B, Valenta T, Osto E, Stellato M, Behnke S, et al. Transforming growth factor- β -dependent Wnt secretion controls myofibroblast formation and myocardial fibrosis progression in experimental autoimmune myocarditis. *Eur Heart J*. **2017**, 38:1413–25.
33. Xiang FL, Fang M, Yutzey KE. Loss of β -catenin in resident cardiac fibroblasts attenuates fibrosis induced by pressure overload in mice. *Nat Commun*. **2017**, 8(1):712.
34. MacDonald BT, Tamai K, He X. Wnt/beta-catenin signaling: components, mechanisms, and diseases. *Dev Cell*. **2009**;17(1):9-26. doi:10.1016/j.devcel.2009.06.016
35. Zeng X, Huang H, Tamai K, et al. Initiation of Wnt signaling: control of Wnt coreceptor Lrp6 phosphorylation/activation via frizzled, dishevelled and axin functions. *Development*. **2008**;135(2):367-375. doi:10.1242/dev.013540

36. Davidson G, Wu W, Shen J, Bilic J, Fenger U, Stanek P, et al. Casein kinase 1 gamma couples Wnt receptor activation to cytoplasmic signal transduction. *Nature* **2005**, 438:867–72.
37. Blitzer JT, Nusse R. A critical role for endocytosis in Wnt signaling. *BMC Cell Biol.* **2006**;7:28. Published 2006 Jul 6. doi:10.1186/1471-2121-7-28
38. Taelman VF, Dobrowolski R, Plouhinec JL, Fuentealba LC, Vorwald PP, Gumper I, et al. Wnt signaling requires sequestration of glycogen synthase kinase 3 inside multivesicular endosomes. *Cell* **2010**, 143:1136–48.
39. Ng B, Dong J, D'Agostino G. et al Interleukin-11 is a therapeutic target in idiopathic pulmonary fibrosis. *Sci. Transl. Med.* **2019**, 11(511): eaaw1237.
40. Anissa A. Widjaja, Brijesh K. Singh, Eleonora Adami, et al Inhibiting Interleukin 11 Signaling Reduces Hepatocyte Death and Liver Fibrosis, Inflammation, and Steatosis in Mouse Model of Nonalcoholic Steatohepatitis. *Gastroenterology* **2019**, 157: 777-792.
41. Obana M, Maeda M, Takeda K, et al. Therapeutic activation of signal transducer and activator of transcription 3 by interleukin-11 ameliorates cardiac fibrosis after myocardial infarction. *Circulation.* **2010**;121(5):684-691. doi:10.1161/CIRCULATIONAHA.109.893677
42. Ye J, Wang Z, Ye D, et al. Increased Interleukin-11 Levels Are Correlated with Cardiac Events in Patients with Chronic Heart Failure. *Mediators Inflamm.* **2019**;2019:1575410. Published 2019 Jan 8. doi:10.1155/2019/1575410
43. Xu Y, Ye J, Wang M, et al. Increased interleukin-11 levels in thoracic aorta and plasma from patients with acute thoracic aortic dissection. *Clin Chim Acta.* **2018**;481:193-199. doi:10.1016/j.cca.2018.03.014
44. Corden B, Adami E, Sweeney M, Schafer S, Cook SA. IL-11 in cardiac and renal fibrosis: Late to the party but a central player. *Br J Pharmacol.* **2020**;177(8):1695-1708. doi:10.1111/bph.15013

45. Pu M, Chen J, Tao Z, Miao L, Qi X, Wang Y. and Ren J. Regulatory network of miRNA on its target: coordination between transcriptional and post-transcriptional regulation of gene expression. *Cell Mol Life Sci.* **2019**, 76:441-451.
46. Greco S, Gorospe M, Martelli F. Noncoding RNA in age-related cardiovascular diseases. *J Mol Cell Cardiol.* **2015**, 83:142–155.
47. Dutka M, Bobiński R, Korbecki J. The relevance of microRNA in post-infarction left ventricular remodelling and heart failure. *Heart Fail Rev.* **2019**, 24(4):575–586.
48. Yuan J, Chen H, Ge D, et al. Mir-21 Promotes Cardiac Fibrosis After Myocardial Infarction Via Targeting Smad7. *Cell Physiol Biochem.* **2017**;42(6):2207-2219. doi:10.1159/000479995
49. Nagpal V, Rai R, Place AT, Murphy SB, Verma SK, Ghosh, AK, & Vaughan DE. MiR-125b Is Critical for Fibroblast-to-Myofibroblast Transition and Cardiac Fibrosis. *Circulation.* **2016**;133(3), 291–301. doi:10.1161/CIRCULATIONAHA.115.018174
50. Chen C, Ponnusamy M, Liu C, Gao J, Wang K, Li P. MicroRNA as a Therapeutic Target in Cardiac Remodeling. *Biomed Res Int.* **2017**;2017:1278436. doi:10.1155/2017/1278436
51. Liu YH, Yang XP, Nass O, Sabbah HN, Peterson E, Carretero OA. Chronic heart failure induced by coronary artery ligation in Lewis inbred rats. *Am J Physiol.* **1997**;272(2 Pt 2):H722-7. doi: 10.1152/ajpheart.1997.272.2.H722. PMID: 9124430.
52. Watanabe M, Okada T. Langendorff Perfusion Method as an Ex Vivo Model to Evaluate Heart Function in Rats. *Methods Mol Biol.* **2018**;1816:107-116. doi: 10.1007/978-1-4939-8597-5_8. PMID: 29987814.
53. Brandenburger M, Wenzel J, Bogdan R, Richardt D, Nguemo F, Reppel M, Hescheler J, Terlau H, Dendorfer A. Organotypic slice culture from human

- adult ventricular myocardium. *Cardiovasc Res.* **2012**;93(1):50-9. doi: 10.1093/cvr/cvr259. Epub 2011 Oct 4. PMID: 21972180.
54. Schultz F, Hasan A, Alvarez-Laviada A, Miragoli M, Bhogal N, Wells S, Poulet C, Chambers J, Williamson C, Gorelik J. The protective effect of ursodeoxycholic acid in an in vitro model of the human fetal heart occurs via targeting cardiac fibroblasts. *Prog Biophys Mol Biol.* **2016**;120(1-3):149-63. doi: 10.1016/j.pbiomolbio.2016.01.003. Epub 2016 Jan 8. PMID: 26777584.
55. Reilly-O'Donnell B, Ferraro E, Tikhomirov R, Nunez-Toldra R, Shchendrygina A, Patel L, Wu Y, Mitchell AL, Endo A, Adorini L, Chowdhury RA, Srivastava PK, Ng FS, Terracciano CM, Williamson C, Gorelik J. UDCA and INT-777 suppress cardiac fibrosis triggered by IL-11 through involvement of TGR5. *MedRxiv*, **2022**;2022.05.11.22274945. <https://doi.org/10.1101/2022.05.11.22274945>
56. Bang C, Batkai S, Dangwal S, Gupta SK, Foinquinos A, Holzmann A, Just A, Remke J, Zimmer K, Zeug A, Ponimaskin E, Schmiedl A, Yin X, Mayr M, Halder R, Fischer A, Engelhardt S, Wei Y, Schober A, Fiedler J, Thum T. Cardiac fibroblast-derived microRNA passenger strand-enriched extracellular vesicles mediate cardiomyocyte hypertrophy. *J Clin Invest.* **2014**;124(5):2136-46. doi: 10.1172/JCI70577. Epub 2014 Apr 17. PMID: 24743145; PMCID: PMC4001534.
57. Turner MD, Nedjai B, Hurst T, & Pennington D J. Cytokines and chemokines: At the crossroads of cell signalling and inflammatory disease. *Biochimica et Biophysica Acta (BBA) - Molecular Cell Research*, **2014**;1843(11), 2563–2582. <https://doi.org/https://doi.org/10.1016/j.bbamcr.2014.05.014>
58. Samad TA, Rebbapragada, A, Bell E, Zhang Y, Sidis Y, Jeong SJ, Campagna JA, Perusini S, Fabrizio DA, Schneyer AL, Lin HY, Brivanlou AH, Attisano L, & Woolf CJ. DRAGON, a Bone Morphogenetic Protein Co-receptor *. *Journal of Biological Chemistry*, **2005**;280(14), 14122–14129. <https://doi.org/10.1074/jbc.M410034200>

59. McGeary SE, Lin KS, Shi CY, Pham TM, Bisaria N, Kelley GM, Bartel DP. The biochemical basis of microRNA targeting efficacy. *Science*. **2019**;366(6472):eaav1741. doi: 10.1126/science.aav1741. Epub 2019 Dec 5. PMID: 31806698; PMCID: PMC7051167.
60. Sticht C, De La Torre C, Parveen A, Gretz N. miRWalk: An online resource for prediction of microRNA binding sites. *PLoS One*. **2018**;18;13(10):e0206239. doi: 10.1371/journal.pone.0206239. PMID: 30335862; PMCID: PMC6193719.
61. Jeggari A, Marks DS, Larsson E. miRcode: a map of putative microRNA target sites in the long non-coding transcriptome. *Bioinformatics*. **2012**;28(15):2062-3. doi: 10.1093/bioinformatics/bts344. Epub 2012 Jun 19. PMID: 22718787; PMCID: PMC3400968
62. León LE, Calligaris SD. Visualization and Analysis of MiRNA-Targets Interactions Networks. *Methods Mol Biol*. **2017**;1509:209-220. doi: 10.1007/978-1-4939-6524-3_19. PMID: 27826930.
63. Frantz C, Stewart KM, Weaver VM. The extracellular matrix at a glance. *J Cell Sci*. **2010**;123(Pt 24):4195-4200. doi:10.1242/jcs.023820
64. Kuivaniemi H, Tromp G. Type III collagen (COL3A1): Gene and protein structure, tissue distribution, and associated diseases. *Gene*. **2019**;707:151-171. doi:10.1016/j.gene.2019.05.003
65. Sliogeryte K, Gavara N. Vimentin Plays a Crucial Role in Fibroblast Ageing by Regulating Biophysical Properties and Cell Migration. *Cells*. **2019**;8(10):1164. Published 2019 Sep 27. doi:10.3390/cells8101164
66. Lu X, Dunn J, Dickinson AM, Gillespie JI, Baudouin SV. Smooth muscle alpha-actin expression in endothelial cells derived from CD34+ human cord blood cells. *Stem Cells Dev*. **2004**;13(5):521-527. doi:10.1089/scd.2004.13.521
67. Das S, Shah R, Dimmeler S, Freedman JE, Holley C, Lee J-M, Moore K, Musunuru K, Wang D-Z, Xiao J, Yin K-J, & null, null. Noncoding RNAs in

- Cardiovascular Disease: Current Knowledge, Tools and Technologies for Investigation, and Future Directions: A Scientific Statement From the American Heart Association. *Circulation: Genomic and Precision Medicine*, **2020**;13(4), e000062. <https://doi.org/10.1161/HCG.0000000000000062>
68. Biener M, Giannitsis E, Thum T, et al. Diagnostic value of circulating microRNAs compared to high-sensitivity troponin T for the detection of non-ST-segment elevation myocardial infarction. *Eur Heart J Acute Cardiovasc Care*. 2021;10(6):653-660. doi:10.1093/ehjacc/zuaa034
69. Pugh TJ, Kelly MA, Gowrisankar S, et al. The landscape of genetic variation in dilated cardiomyopathy as surveyed by clinical DNA sequencing. *Genet Med*. **2014**;16(8):601-608. doi:10.1038/gim.2013.204
70. Fu X, Liu Q, Li C, Li Y, & Wang L. Cardiac Fibrosis and Cardiac Fibroblast Lineage-Tracing: Recent Advances *In Frontiers in Physiology*, **2020**; 11. <https://www.frontiersin.org/article/10.3389/fphys.2020.00416>
71. Aujla P K, & Kassiri Z. Diverse origins and activation of fibroblasts in cardiac fibrosis. *Cellular Signalling*, **2021**;78, 109869. <https://doi.org/10.1016/j.cellsig.2020.109869>
72. Kim KK, Sheppard D, Chapman HA. TGF- β 1 Signaling and Tissue Fibrosis. *Cold Spring Harb Perspect Biol*. **2018**;10(4):a022293. doi:10.1101/cshperspect.a022293. PMID: 28432134; PMCID: PMC5880172.
73. Kang H. Role of MicroRNAs in TGF- β Signaling Pathway-Mediated Pulmonary Fibrosis. *Int J Mol Sci*. **2017**;25;18(12):2527. doi:10.3390/ijms18122527. PMID: 29186838; PMCID: PMC5751130.
74. Miscianinov V, Martello A, Rose L, et al. MicroRNA-148b Targets the TGF- β Pathway to Regulate Angiogenesis and Endothelial-to-Mesenchymal Transition during Skin Wound Healing. *Mol Ther*. **2018**;26(8):1996-2007. doi:10.1016/j.ymthe.2018.05.002

75. O'Reilly S. MicroRNAs in fibrosis: opportunities and challenges. *Arthritis Res Ther.* **2016**;13;18:11. doi: 10.1186/s13075-016-0929-x. PMID: 26762516; PMCID: PMC4718015.
76. Yuan J, Chen H, Ge D, et al. Mir-21 Promotes Cardiac Fibrosis After Myocardial Infarction Via Targeting Smad7. *Cell Physiol Biochem.* **2017**;42(6):2207-2219. doi:10.1159/000479995
77. Thum T, Gross C, Fiedler J, et al. MicroRNA-21 contributes to myocardial disease by stimulating MAP kinase signalling in fibroblasts. *Nature.* **2008**;456(7224):980-984. doi:10.1038/nature07511
78. Wang, J., Song, Y., Zhang, Y. et al. Cardiomyocyte overexpression of miR-27b induces cardiac hypertrophy and dysfunction in mice. *Cell Res.* **2021**;2 22, 516–527. doi:10.1038/cr.2011.132
79. Veliceasa D, Biyashev D, Qin G, et al. Therapeutic manipulation of angiogenesis with miR-27b. *Vasc Cell.* **2015**;7:6. Published 2015 Jun 24. doi:10.1186/s13221-015-0031-1
80. Xiao Y, Zhang X, Fan S, Cui G, Shen Z. MicroRNA-497 Inhibits Cardiac Hypertrophy by Targeting Sirt4. *PLoS One.* **2016**;11(12):e0168078. Published 2016 Dec 16. doi:10.1371/journal.pone.0168078
81. Chen, X., Shi, C., Wang, C. et al. The role of miR-497-5p in myofibroblast differentiation of LR-MSCs and pulmonary fibrogenesis. *Sci Rep.* **2017**; 7, 40958 (2017). doi:10.1038/srep40958
82. Eijgenraam TR, Silljé HHW, de Boer RA. Current understanding of fibrosis in genetic cardiomyopathies. *Trends Cardiovasc Med.* **2020**;30(6):353-361. doi:10.1016/j.tcm.2019.09.003
83. Sisakian H. Cardiomyopathies: Evolution of pathogenesis concepts and potential for new therapies. *World J Cardiol.* **2014**;6(6):478-494. doi:10.4330/wjc.v6.i6.478

84. Lu D, Xia Y, Chen Z, et al. Cardiac Proteome Profiling in Ischemic and Dilated Cardiomyopathy Mouse Models. *Front Physiol.* **2019**;10:750. Published 2019 Jun 18. doi:10.3389/fphys.2019.00750
85. Liu T, Song D, Dong J, et al. Current Understanding of the Pathophysiology of Myocardial Fibrosis and Its Quantitative Assessment in Heart Failure. *Front Physiol.* **2017**;8:238. Published 2017 Apr 24. doi:10.3389/fphys.2017.00238
86. Pugh TJ, Kelly MA, Gowrisankar S, et al. The landscape of genetic variation in dilated cardiomyopathy as surveyed by clinical DNA sequencing. *Genet Med.* 2014;16(8):601-608. doi:10.1038/gim.2013.204

CHAPTER II

1. INTRODUCTION II

1.1 An overview on miRNAs: biology and functions

miRNAs biogenesis

miRNAs belong to the class of small (~21-25 nucleotides) non-coding RNAs which is present in viruses, bacteria, plants and animals [1]. The production of a miRNA begins in the nuclei where it is synthesized as a long primary transcript (pri-miRNA) from its non-coding gene or from an intron of a protein-coding gene by RNA-polymerase II [2]. pri-miRNA appears in its folded form, hairpin, in which it is recognized by a member of RNase III family of enzymes, Drosha [3]. Drosha forms a complex with DGCR8 and cleaves the primary transcript of miRNA in order to remove miRNA precursor (~70 nucleotides) [3, 4]. With the help of exportin-5 cleaved pre-miRNA is transferred to the cytoplasm [5] where it binds to another member of RNase III family of enzymes, Dicer [6]. It further processes pre-miRNA into the mature miRNA duplex of ~20 base pairs without the terminal loop. The directionality of the miRNA strand determines the name of the mature miRNA form. The 5p strand arises from the 5' end of the pre-miRNA hairpin while the 3p strand originates from the 3' end. The mature miRNA can be further loaded into the Argonaute (AGO) family of proteins in the ATP-dependent manner [7]. The choice between 3p or 5p strands depends on the thermodynamic stability at the 5' end of miRNA duplex [8]. The unloaded strand which is called passenger strand unbinds from the guide strand. Further, it would be cleaved by AGO2 and cellular machinery [9]. This biogenesis pathway is considered as a canonical pathway.

There are several non-canonical pathways that have been described. They can be classified as Drosha or Dicer independent pathways [10]. In the Drosha-independent pathway pre-miRNAs resemble Dicer substrates. The best examples of that biogenesis are mirtrons. Mirtrons are produced from the introns of mRNA during the splicing [11]. Other examples are snoRNA derived pathway, tRNA derived pathway, shRNA derived pathway, tRNaseZ dependent pathway and pre-

esiRNA derived pathway [12]. In the Dicer-independent pathway miRNAs are affected by Drosha from endogenous short hairpin RNA transcripts [13]. These miRNAs require Ago2 in order to complete their maturation. Canonical and non-canonical pathways are summarized in the Figure 1.1.1.

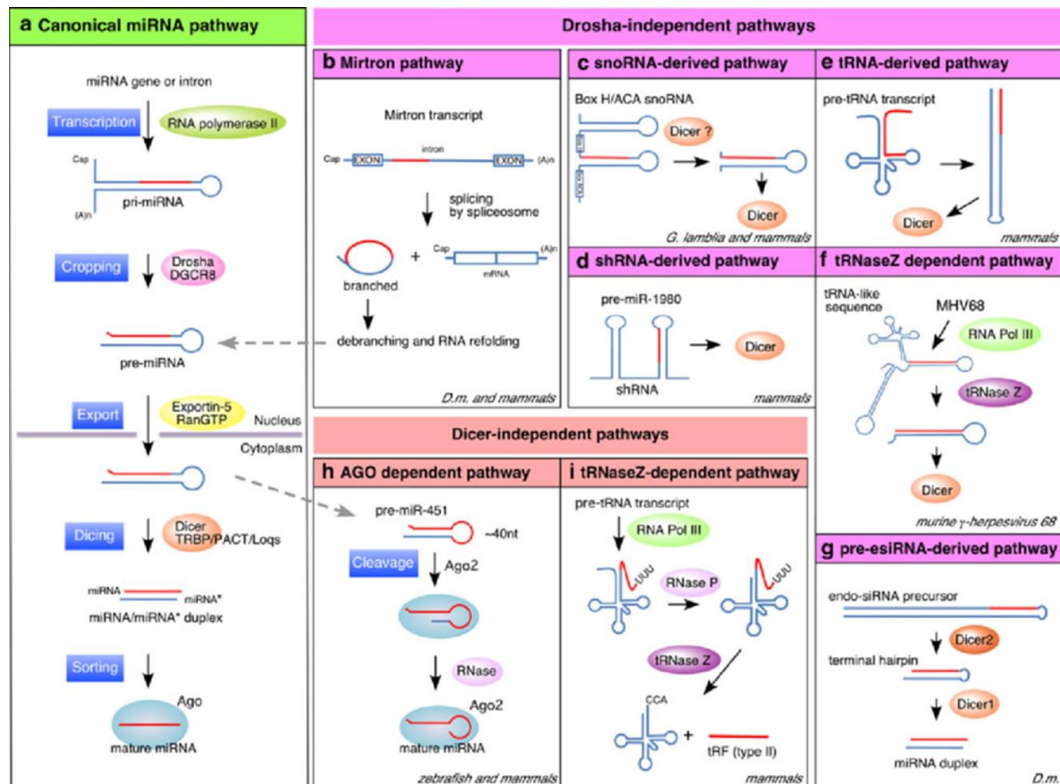


Figure 1.1.1 Canonical and non-canonical miRNAs biogenesis pathways [12].

miRNAs functions

Most of miRNAs bind to a specific sequence, binding site, at the 3'-UTR of their target [14]. Consequently, miRNA triggers translational repression and mRNA deadenylation and decapping [14, 15]. However, binding sites for miRNAs were also found in the 5'-UTR, coding sequence and in promoter regions [16]. To date, interaction of miRNAs with these binding sites requires an additional research.

Guiding miRNA strand in complex with AGO2 forms the minimal miRNA-induced silencing complex (miRISC) [17]. Specificity is determined by complementary sequence on the target mRNA [18]. Full complementarity of miRISC with a target sequence will result in increased AGO2 endonuclease activity and targets mRNA cleavage [18]. Most miRISC-target sequence

interactions are not fully complementary. In that case, AGO2 acts as a mediator of RNA interference [19]. miRISC complex can shuttle between nuclei and cytoplasm [20]. Enrichment of miRNA at actively transcribed genes may suggest that miRISC interacts with target mRNA co-/post-transcriptionally [21].

Several studies reported an induction of translational activity by miRNAs [22,23]. For example, Fragile-x-mental retardation related protein 1 (FXR1) was associated with AGO2 and miRNAs to activate translation at the moment of cell cycle arrest [24].

1.2 miRNAs and their targets prediction

In the absence of high-throughput biological approaches to identify miRNA targets, many computational methods, such as TargetScan [25], miRWalk [26], miRCode [27] and miRanda [28] were developed.

Target prediction tools can use various parameters and criteria in their algorithms to assess interaction between a miRNA and its potential binding site [29]. However, search of the binding site is based on the sequence complementarity [29]. Class of sites with ideal complementarity to the 5'-UTR of miRNA is called 'seed region'. It is located at positions 2-7 in miRNA sequence. This region is sufficient for a miRNA to suppress its potential target. Another class of binding sites has non-ideal complementarity, which is compensated by additional base pairings in the 3'-UTR of the miRNAs [30]. Unfortunately, the length of miRNAs is a limiting factor, so prediction cannot be based on standard sequence analysis, such as Karlin–Altschul statistics [31]. For this reason, most of the modern algorithms are created to detect the cross-species conservation requirement in order to decrease the number of false positives [32]. Nevertheless, these algorithms have a precision of ~50% with a sensitivity that ranges from 6 to 12% [33].

However, these prediction tools also contain databases with annotated miRNAs and mRNAs (targets). In addition, most of them provide a functional enrichment

analysis on miRNAs which facilitate the search of a ‘promising miRNA’ [29] (Figure 1.2).

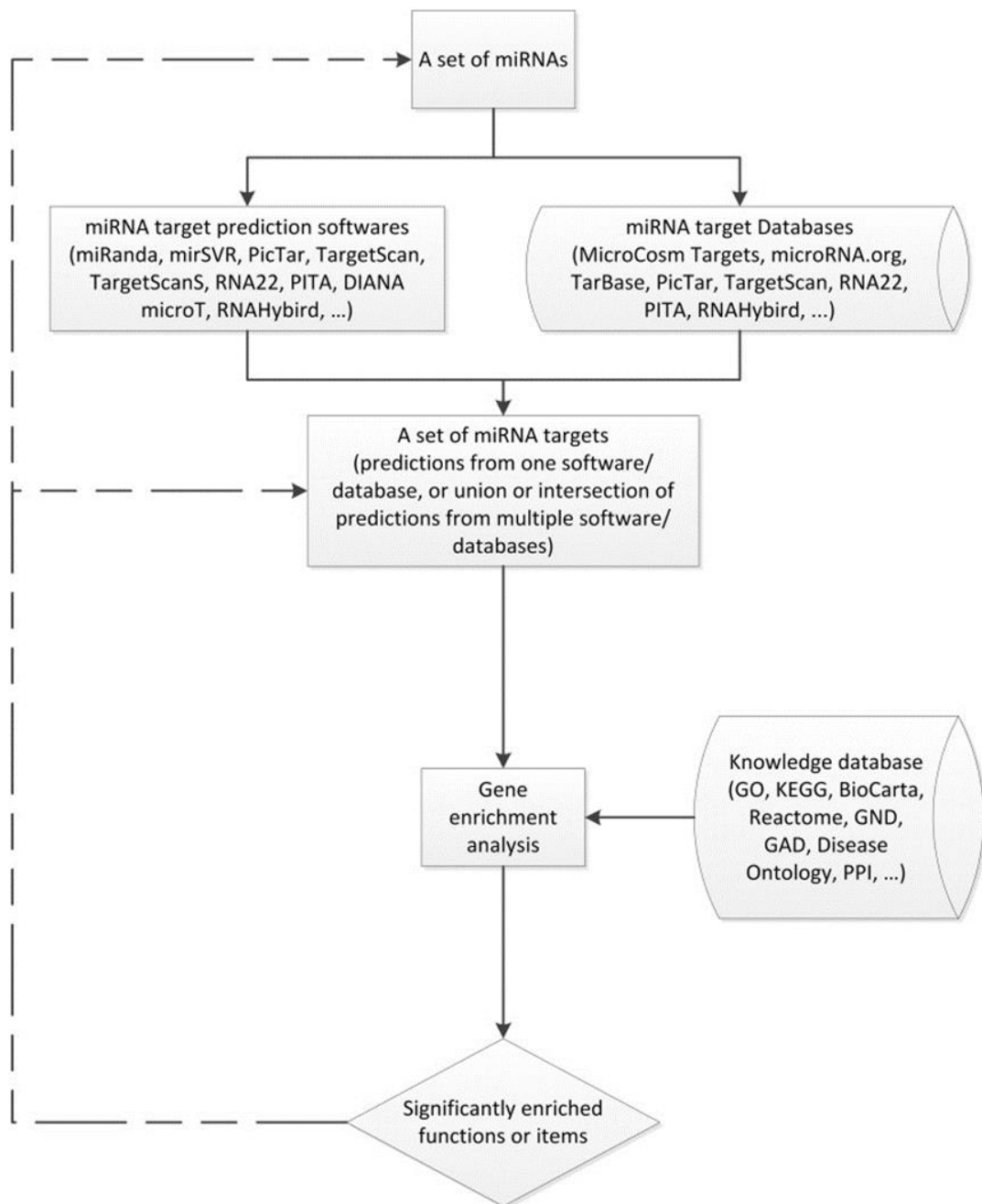


Figure 1.2 Framework of miRNA functional annotation [29]

1.3 miRNA-27b-5p: current knowledge

Animals and humans express miRNA-27b which belongs to a miRNA-27 family. This miRNA family is known for its role in cholesterol homeostasis [34] and fatty acid metabolism [35]. It was widely investigated in adipocytes [36] and

osteoblasts [37]. In the first cell type it acts as a negative regulator of adipocyte differentiation through regulation of the peroxisome proliferator-activated receptor gamma (PPAR γ) post-transcriptionally [38], as well as C/EBP alpha in the case of miRNA-27b [39]. In osteoblasts miRNA-27 has been found to target and inhibit gene expression of the adenomatous polyposis coli (APC) protein, enabling it to regulate osteoblast differentiation.

Recently, in the work of Qiang Fu et al. [40] miRNA-27b was examined in rat MI CFs and in pressure-overload system where it enhanced fibrosis through repression of FBW7 and further accumulation of Snail. At the same time, it is known that miRNA-27b expression can be repressed by TGF β 1 and its overexpression in CMs leads to cardiac hypertrophy and dysfunction by targeting PPAR- γ in transgenic mice [41]. Moreover, miRNA-27b can accelerate angiogenesis by regulating translation of Dll4/Notch axis, PPAR γ and its downstream effectors [42]. Overall, knowledge on miRNA-27b in heart is still limited. However, works [40, 41] indicate an important potential pro-fibrotic role of miRNA-27b in HF.

1.4 miRNA-497-5p: current knowledge

A member of the miR-15/16/195/424/497 family, miRNA-497-5p, has the same 3'-untranslated (UTR) binding seed sequence (AGCAGCA) as other member of the family [42]. Currently, miRNA-497-5p is famous for its anti-proliferative role and down-regulation across many cancer types [43].

In cardiovascular science miRNA-497-5p is known for its anti-hypertrophic effect through regulation of Sirt4 expression both in vitro and in vivo [44]. Furthermore, miRNA-497-5p was studied in pulmonary fibrogenesis processes where it induces fibrosis through RECK inhibition and further ECM reorganization through MMP2/9 [45].

2. AIMS OF THE STUDY II

- 1) To predict targets for miRNA-497-5p and miRNA-27b-5p which are important in the regulation of the IL-11 pro-fibrotic pathway. For this to construct and characterize IL-11 and TGF β 1 stimulated differential co-expression network of genes.**
- 2) To predict target genes in this network based on the binding affinity between miRNA and gene by using TargetScan 8.0.**
- 3) To validate target gene suppression by miRNAs via dual luciferase assay.**
- 4) To test predicted targets expression in rat cardiac fibroblasts treated with IL-11 and in MI rat cardiac fibroblasts.**

3. METHODS II

3.1 Bioinformatic analysis of Human RNA-seq data

The data set was obtained from the open source GEO dataset: GSE97358, which was published through the research of Schafer et al. [47] and GSE133017 which was published through the research of Chen et al. [48]. This expression data set consists of RNA-sequencing in 168 primary cardiac FB derived from patients (84 control samples and 84 treated with TGF- β). The data set consisted of 64254 genes and was uploaded to R (v4.0.2) and then transformed into expression data using the edgeR package [49]. The resulting matrix was filtered to remove minimally- expressed genes. Genes with a $\log_{10}(\text{expression})$ value less than 0 in at least 90% (>74) of all samples were removed. The resulting dataset contained 14203 genes. The filtered dataset was then separated by culture conditions (control and TGF- β treated). Using the 'gtools' package we were able to compare (TGF- β treated vs. control) the expression fold change of all expressed genes in the 84 paired samples [50]. The average expression fold change of each gene was then calculated ($\text{Log}_2(\text{expression fold change})$) and applied to the network described below (all NaN and Inf values were replaced with 0). We then created a correlation matrix of genes which will include; correlation coefficients, p-values and false discovery rate (FDR) using the Hmisc package [51]. We extracted a list of 14203 genes and their correlation data for the IL11 gene and then removed matches with FDR greater than 0.05, resulting in 4853 genes with significant adjusted p-values. To further filter our data, we applied another threshold based upon correlation coefficients (where $r \geq \pm 0.5$), in this dataset values varied between -0.78 and +0.75. The majority of our results were observed to have a low to moderate correlation. For this reason, we applied a cut off for values with a low correlation value. We considered values $\geq \pm 0.5$ to have a strong correlation [52]. This analysis identified 677 genes which were used to build a protein-protein network. In order to cover other fibrotic related genes we united our IL-11 co-expression network with a recently constructed WWP2 network (683 genes), from

cluster of genes which was found to be important in fibrosis and responsible for cell adhesion [48].

Code in RStudio 4.0.2 for IL-11 differential co-expression network construction

```
library(edgeR)
library(gtools)

data<-as.matrix(read.csv(file="route to the file",row.names=1, sep=";",header=T))
data = cpm(data)

odd_indexes<-seq(1,167,2)
even_indexes<-seq(2,168,2)

datC1<-t(data[,c(odd_indexes)])
datC2<-t(data[,c(even_indexes)])

datC1[which(!is.finite(datC1))]<-0
datC2[which(!is.finite(datC2))]<-0

foldchange<-foldchange(datC1,datC2)
foldchange[which(!is.finite(foldchange))]<-0

#print(str((length(cors) - length(which(cors < .8)) - length(rownames(cors))) / 2) +
str(length(cors)))
#cors[abs(cors) < 0.8] <- NA

library(Hmisc)
mycor=rcorr(as.matrix(foldchange),type="spearman")

result<-c(mycor$r[,1622])
```

```
write.table(result, "route.txt", sep="\t", row.names=F, col.names=F, quote=F)

result<-c(mycor$P[,1622])
write.table(result, "C:route.txt", sep="\t", row.names=F, col.names=F, quote=F)

result<-p.adjust(result, method = "fdr", n = length(result))
write.table(result, "route.txt", sep="\t", row.names=F, col.names=F, quote=F)
```

3.2 Gene set enrichment analysis

In order to reveal the enriched pathways associated with the IL-11 co-expression network, we conducted gene set enrichment analysis using DAVID 6.8 [53]. Ensemble gene ids were uploaded as a gene list for Homo Sapiens with the same background. For each gene, we searched the database annotations for Gene Ontology, GO_BP_Direct and in Pathways, KEGG_Pathway. We set up the database to only highlight terms with $p\text{-value} < 0.05$ (FDR and fold enrichment were also included added as additional search terms).

3.3 Protein-protein interaction network construction

In this study, we aim to construct a protein- protein interaction network based upon genes identified from the IL-11 co-expression network. To construct this network, we used STRING v.11 ('Search Tool for Retrieval of Interacting Genes/Proteins') [54] which links proteins based on reported associations between them. In order to establish protein associations, we investigated 7 active interaction sources: text mining, experiments, databases, co-expression, neighborhood, gene fusion and co-occurrence. Each edge was then ranked based upon the confidence of the protein- protein association being true. During the construction of our protein-protein network, we searched all 7 active sources and only included pairs of genes which showed greater than 'medium' confidence behind their association (confidence > 0.4). The resulting network was exported as a table; genes were assigned the average \log_2 (expression fold change) from filtrated IL-11 dataset [55].

3.4 Network analysis with Cytoscape 3_7_1

The network which was generated in STRING v.11 was imported in Cytoscape 3_7_1 to generate a network visualization graph [56] network analysis was performed using NetworkAnalyzer [57]. In the resulting network, node colour represents the average $\text{Log}_2(\text{expression fold change})$ in IL-11 vs Non-treated conditions. The size of each node represents the degree of connectivity (i.e. the number connections with other elements of a network). In order to examine how IL-11 treatment affected our resulting network we did enrichment analysis of the network with WebGestalt. The IL-11 and WWP2/ TGF- β networks were uploaded separately. Following this we tested the networks with gene lists comparing the IL-11 vs. Control condition. Significantly regulated genes were defined as having a false discovery rate <0.05 .

3.5 miRNAs targets prediction

In order to predict miRNA targets associated with IL-11 we filtered lists of targets for miRNA-27b-5p and miRNA-497-5p from TargetScan [25], MiRWalk [26], miRcode [27] according to the following criteria: target gene should have conserved binding site for miRNA in human and rat, binding site is in 3'-UTR, target gene is present in IL-11 and TGF β 1 co-expression network and target gene is down-regulated in CFs treated with IL-11 [55], loss of target gene function is leading to fibrosis in literature. According to the designed pipeline, miRNA-27b-5p has 28 potential targets which were satisfying all criteria. The target genes of miRNA-27b-5p overlapped with IL-11 (genes = 18) and TGF β 1 (genes =9) co-expression networks. The majority of target genes for miRNA-27b-5p is down-regulated in CFs treated with IL-11. Therefore, based on the literature search EGLN1 was identified as promising target of miRNA-27b-5p [33]. Alternatively, miRNA-497-5p has only 14 targets which were fitting criteria above. Among all predicted targets, TRABD2B was found to be strongly down-regulated by IL-11 treatment, so it was investigated further. Binding sites were obtained from TargetScan [25].

3.6 Constructs preparation

Binding sites obtained from the TargetScan for miRNA-27b-5p target EGLN1 (AAGCTCA) and miRNA-497-5p target TRABD2B (TGCTGCTA) and were used for further constructs preparation for the dual luciferase assay. Oligonucleotides were ordered from Eurofins Genomics and reconstituted to the concentration equals 3 µg/µl. And were used at 1/50 (v/v) for annealing reaction.

Annealing buffer:

-100 mM NaCl

-50 mM HEPES pH=7.4

Annealing protocol:

each temperature for 4 minutes

94°C - 85°C - 82°C - 80°C - 78°C - 75°C - 70°C - 60 °C - 50°C - 40 °C - 30°C - 20 °C - 10°C - 4°C.

pMIR-REPORT-Luciferase (pLUC, Ambion) were linearized and extracted from gel. We saved cut and uncut variants of the vector. By a combination of Annealed oligonucleotides for (WT/MUT) TRABD2B and EGLN1 with linearized pMIR (0.5 µg/µl) and T4 ligase in T4 Buffer we performed ligation.

Ligation:

16°C overnight (18h)

65°C 20 min.

3.7 Bacterial transformation

By using 10 µl of ligation reactions (WT-no insert; WT-insert; Mutated-no insert; mutated-insert + vector alone) we transformed Invitrogen Top10 cells on ampicillin pre-treated agar plates. Colonies were counted and 5-10 colonies were chosen from a plate. They were amplified in 5 ml of LB Broth with Ampicilin for 8 h at 37°C under shaking. After that, DNA was isolated according to the manufacturer protocol of Mini DNA Plasmid kit from Qiagen from 3 ml in order to check the presence of the constructs with gel electrophoresis. Remaining volume was frozen with an addition of glycerol 60% (v/v).

3.8 Constructs amplification

By using flask with 250 ml of LB Broth with added Ampicilin we mixed up colonies with validated presence of the construct (5 ml) and leave it at 37⁰C under shaking for 24h. Following this, DNA was isolated MAXI Plasmid Dna extraction kit from Qiagen.

3.9 HEK293FT cell culture

HEK293FT cells from InvitrogenTM were defrozed and cultivated for the dual luciferase experiments in high-glucose DMEM supplemented 10% FBS and 1% penicillin and streptomycin. Cells were cultured for 3 days at 37 ⁰C and 5% CO₂ before further experiments.

3.10 3'UTR luciferase assays to demonstrate miRNA direct binding to the predicted target genes

Binding sites DNA sequences for wild-type (WT) EGLN1 (AAGCTCA) and TRABD2B (TGCTGCTA) were obtained from TargetScan. Cloning of miRNA-targeted sequences in its 3'UTR induces the translational inhibition of the firefly luciferase gene. Plasmids used in luciferase assays were generated by cloning oligonucleotides bearing wt or deleted miR-27b or miR-497-seed pairing sites of EGLN1 and TRABD2B genes downstream of the stop codon in pMIR-REPORT-Luciferase (pLUC, Ambion), between SpeI and Hind III restriction sites. For each gene, HEK293FT cells, plated in 96-well plate, were transfected with WT or MUT targets constructs or vector alone in combination with CmiR0001-MR04 vector (miRNA control) or with HmiR-0145-MR04 (Homo sapiens miR-27b stem-loop) or with HmiR-0271-MR04 (Homo sapiens miR-497 stem loop) and with pRL-null renilla luciferase. 48hrs after transfection, cellular lysates were tested with Dual Glo Luciferase Assay System (Promega), according to the manufacturer instructions, using a 1420 Victor3 Multilab Counter (Perkin Elmer). Renilla luminescence was used for values normalization and the ratio of firefly luminescence of each construct was calculated either in the presence or in the absence of exogenous miR-27b (GeneCopoeiaTM HmiR0145-MR04) or miR-497 (GeneCopoeiaTM HmiR-0271-MR04).

3.11 RT-qPCR

RNA was collected and converted to cDNA as it is described in chapter I 3.5. Designed primers in order to detect genes of interest are present in table 3.10.

Table 3.10 List of primers

Gene name	species	Forward primer sequence (5'->3')	Reverse primer sequence (5'->3')
Trabd2b	rat	ACAAACATCAGCGCCAAGG	TACAGGCTTCAGTGCCAGCTT
Egln1	rat	GAGACCATCGGCCTGCTCAT	CGACCATGGCTTTCGTTCCGG
Gapdh	rat	TGATTCTACCCACGGCAAGTT	TGATGGGTTTCCCATTGATGA

3.12 Statistics

Statistical tests for bioinformatics part described in Chapter II 3.1-3.5. For remaining experiments statistical analysis was performed with Origin 8 Pro. For multiple experimental groups comparison One-Way Anova with following Tukey's multiple comparison was used. N= number of patients/ animals, n= number of technical repeats. Data were presented as Mean \pm SEM. P values <0.05 were considered statistically significant.

4. RESULTS II

4.1 IL-11 differential co-expression network characterization

A network of genes differentially expressed due to IL-11 or TGF- β treatment of human FBs was constructed from the RNA-seq datasets published by Schafer et al. [47] and Chen et al. [48]. Analysis of the gene ontology enrichment of these datasets showed a high prevalence of genes clearly associated with cardiac fibrosis, in the IL-11 (Figure 4.1 A) and WWP2/ TGF- β networks (Figure 4.1 B), like TGF β 1 signaling, ECM organization etc. Interestingly, that IL-11 co-expression network was significantly enriched in genes associated with a response to hypoxia. A slice of the network with genes associated with fibrosis like CTGF, FN1, IL-11, TGF β 1 etc. is presented in the (Figure 4.1 C).

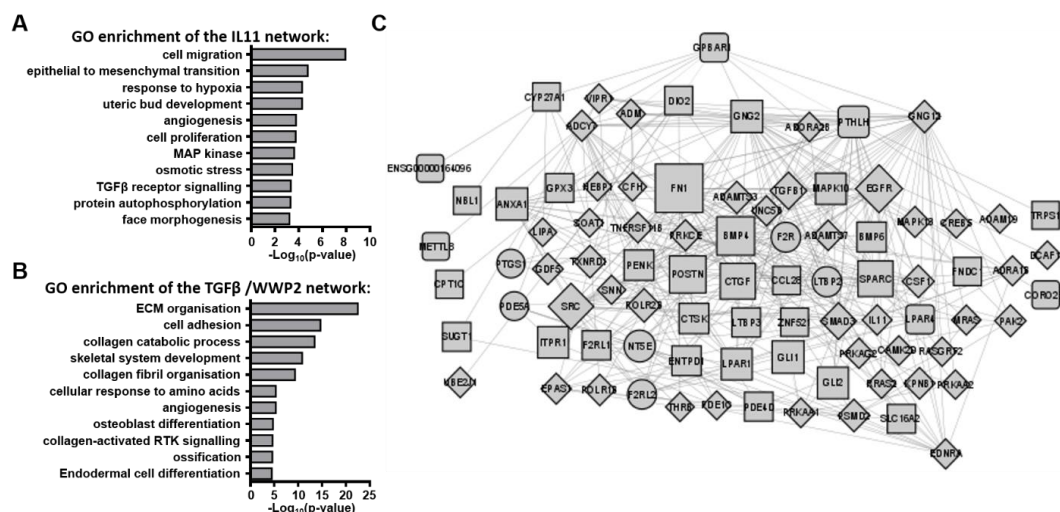


Figure 4.1 Construction and characterization of IL-11 differential co-expression network. **A)** Gene ontology enrichment of IL-11 network. **B)** Gene ontology enrichment of TGF- β / WWP2 network. **C)** A gene expression network constructed from published RNA-seq datasets. Circles represent genes belonging to the IL-11 co-expression network, diamonds represent genes belonging to the WWP2/ TGF- β network, squares represent genes belonging to both pro-fibrotic networks. A slice of the network with genes associated with cardiac fibrosis.

4.2 Application of RNAseq data done in human dilated cardiomyopathy cardiac fibroblasts treated with IL-11 on IL-11 co-expression network

RNAseq performed in human DCM CFs (N = 3) treated or not with IL-11 (5 ng/ μ l) for 24h was suitable in order to test IL-11 co-expression networks [55]. Incubation of cells with IL-11 caused a significant change (p-value < 0.05 or $-\log_{10}(\text{p-value}) > 1.42$) in the expression in 360 genes (Figure 4.2 A). We were aiming to test if IL-11 and TGF β 1/WWP2 co-expression networks were sensitive to gene expression changes caused by IL-11 treatment. By using these networks as a database we conducted enrichment analysis (Figure 4.2 B-D). Both enrichment plots indicate that IL-11 treatment results in significant (FDR < 0.001) enrichment of genes in both networks. It is clearly demonstrated in the bar chart (Figure 4.2 D) on normalized enrichment scores for both networks (IL-11 network = 1.5; TGF β 1 network = 1.6; FDR < 0.001). In other words we confirmed that theoretical model – IL-11 differential co-expression network describes genes modulated by IL-11 treatment, it was visually presented with colors on (Figure 4.2 E). Therefore, we can find a perspective target for IL-11 induced miRNA-27b-5p and miRNA-497-5p.

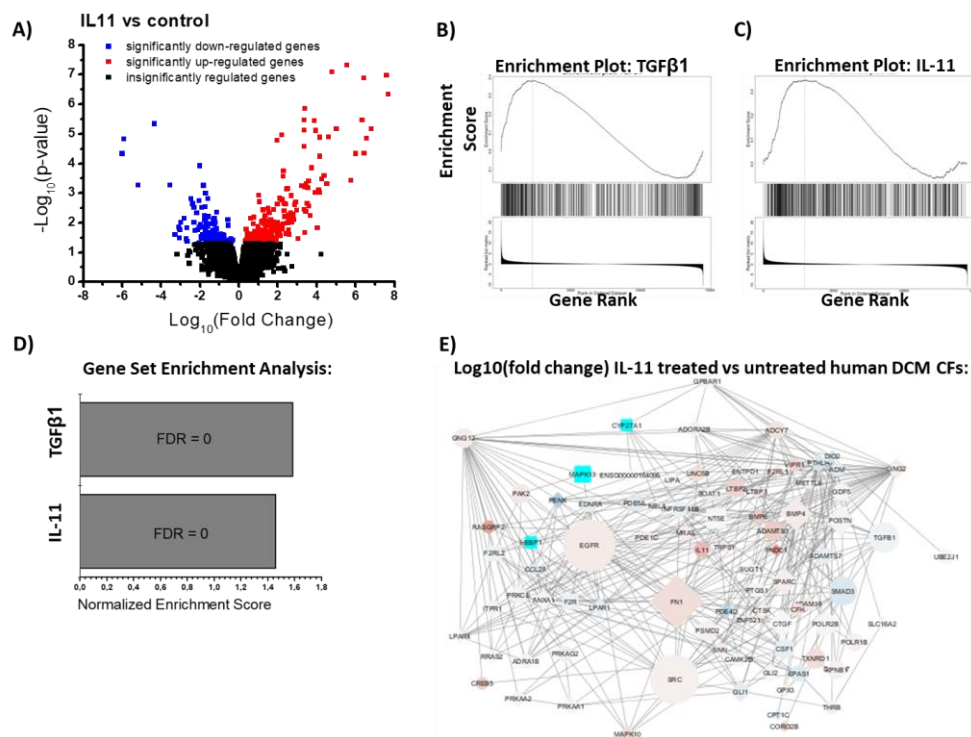


Figure 4.2 Validation of IL-11 differential co-expression network with application of gene expression of IL-11 treated human DCM CFs. A) Volcano plot of differentially expressed genes as determined by RNA-seq. Conditions compared were control (no

treatment) vs 5ng/ml IL-11 stimulated human DCM FB. Significantly upregulated genes are marked in red, significantly down regulated genes are marked in blue. n=3. **B)** Enrichment plot of 683 genes from TGF β 1 co-expression network. Enrichment score = 0.4 FDR < 0.001 **C)** Enrichment plot of 677 genes from IL-11 co-expression network. Enrichment score = 0.4 FDR < 0.001 **D)** Bar chart on normalized enrichment scores for TGF β 1 co-expression network (= 1.6) and IL-11 co-expression network (= 1.5). FDR < 0.001. **E)** A gene expression network constructed from published RNA-seq datasets. Circles represent genes belonging to the IL-11 co-expression network, diamonds represent genes belonging to the WWP2/ TGF- β network, squares represent genes belonging to both pro-fibrotic networks. A slice of the network with genes associated with cardiac fibrosis. Genes are colored according to their expression in human DCM CFs treated with IL-11 (blue color is for -1,5, red color is for 1,5 Gene Rank).

4.3 EGLN1 is down-regulated in vitro by miRNA-27b-5p as a target

For the investigation of miRNA-27b-5p and miRNA-497-5p molecular mechanism we predicted their targets with TargetScan 8.0. We considered only those targets which binding site for miRNA was 1) 3'UTR, 2) was conserved between rat and human, 3) targets should be down-regulated by IL-11 treatment and 4) loss of target function leads to fibrosis. We identified 28 possible targets for miRNA-27b-5p which intersect with IL-11 and TGF β 1 co-expression networks (Figure 4.3 A). Figure 4.3 B was plotted based on the gene ranks (Summary of Gene expression fold change and $-\text{Log}_{10}p\text{-value}$) of RNAseq completed with human dilated cardiomyopathy cardiac fibroblasts treated with IL-11 (5ng/ μ l) [55] and normalized to gene expression of non-treated cells. All the targets were down-regulated by IL-11 treatment. Based on recent results showing that [59] loss of EGLN1 in mice leads to cardiac fibrosis, we proceeded with EGLN1 as a perspective target. Its gene rank was -0.52. Moreover, EGLN1 was significantly down-regulated in IL-11 treated rat CFs and post-MI HF rat CFs in comparison to healthy rat CFs (Figure 4.3 C).

To further validate, EGLN1 targeting by miRNA-27b-5p we conducted a dual luciferase assay (Figure 4.3 D). Inserts presence was validated by gel electrophoresis and sequencing (Figure 4.6). Our results, demonstrated a

significant decrease in relative luminescence when miRNA-27b (miR-27b) was co-transfected with p-MIR luciferase reporter with WT EGLN1 binding site (WT EGLN1) but not in the presence of the mutated binding site (MUT EGLN1). Therefore, miRNA-27b-5p showed an affinity for the EGLN1 binding site, which is conserved in both human and rat.

A) **Gene ranks (Summary of Gene expression fold change and $-\log_{10}$ p-value):**

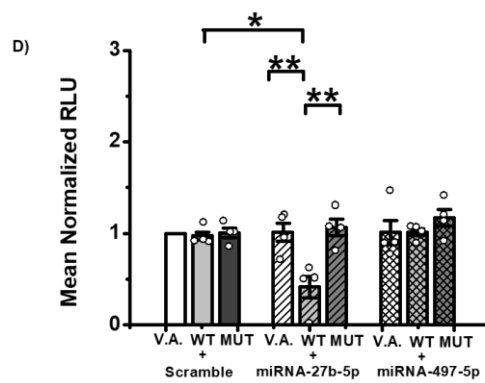
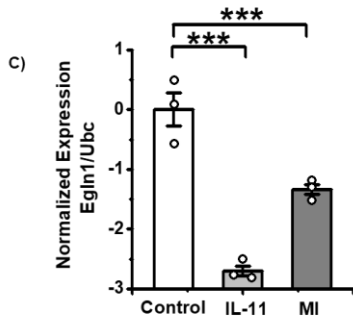
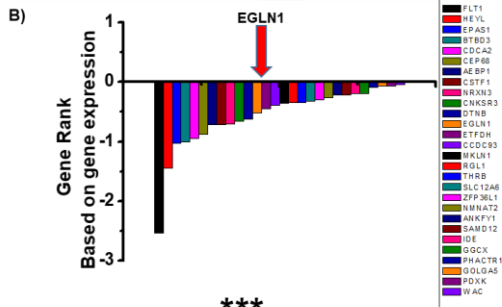
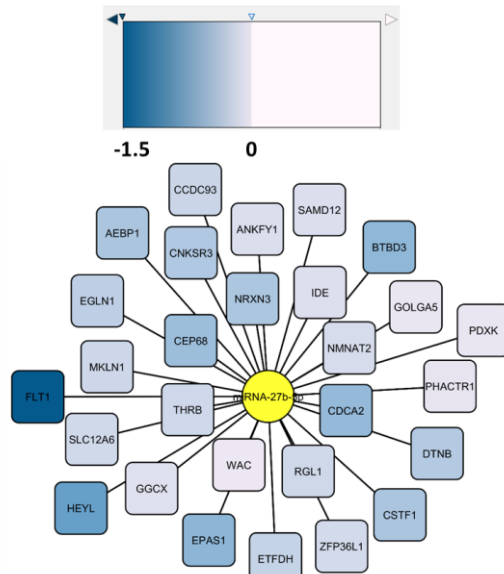


Figure 4.3 Validation of EGLN1 as a target of miR-27b-5p. **A)** List of potential targets of miR-27b-5p (predicted by Targetscan and visualized by Cytoscape 3.8.2 (<https://cytoscape.org/>)). Relative expression of targets in IL-11- treated human cardiac fibroblasts, was determined our published dataset [55]. Continuous color mapping (low gene rank dark blue-> high gene rank- white). **B)** Plot of candidate genes ranked by magnitude of down-regulation. **C)** Modulation of RNA levels of EGLN1 in CFs from healthy rat treated with IL-11 (5ng/ μ l, 24hrs) (light grey) and post-MI HF CFs (grey). **D)** HEK293FT were transfected with vector alone (pLUC) or firefly luciferase constructs that contain either an intact miR-27b-5p binding site (wt), or a mutated miR-27b-5p binding site (mut) for EGLN. Each pLUC plasmid was co-transfected with a plasmid encoding Renilla luciferase along with a plasmid encoding either miR-27b-5p or a scramble sequence (scr) or a miR-497-5p as a negative control. Firefly luciferase luminescence units were normalized against renilla luminescence. All experimental values were compared to the vector-only and scramble vector transfection conditions. N = 3 for RT-qPCR. N = 4 for dual luciferase assay. Data presented as Mean \pm SEM One-way Anova was applied followed by Tukey Mean Comparison test in order to estimate statistical significance *P-value<0.05, **P-value<0.01, ***P-value<0.005.

4.4 TRABD2B is not regulated in vitro as miRNA-497-5p target

For miRNA-497-5p target prediction we used the same approach. We considered only those targets which binding site for miRNA was 1) 3'UTR, 2) was conserved between rat and human, 3) targets should be down-regulated by IL-11 treatment and 4) loss of target function leads to fibrosis. Intersection of possible targets with IL-11 differential co-expression network revealed 14 potential targets (Figure 4.4 A). By analysis of their expression in RNAseq data from IL-11 treated human DCM CFs we found that TRABD2B was the most down-regulated (Figure 4.4 B). Moreover, TRABD2B is naturally a negative regulator of WNT3A and WNT5A which are considered as pro-fibrotic stimulus. However, this data was not confirmed in IL-11 treated rat CFs and CFs from MI rats (Figure 4.4 C). Finally, we performed a dual luciferase assay (Figure 4.4 D) in order to check if WT TRABD2B binding site is targeted by miRNA-497-5p. Unfortunately, we were not able to detect a significant drop in relative luminescence of HEK293FT co-transfected with WT TRABD2B containing plasmid and miRNA-497-5p in

comparison to a mutated (MUT) construct. Overall, we suggested that TRABD2B is not a target of miRNA-497-5p.

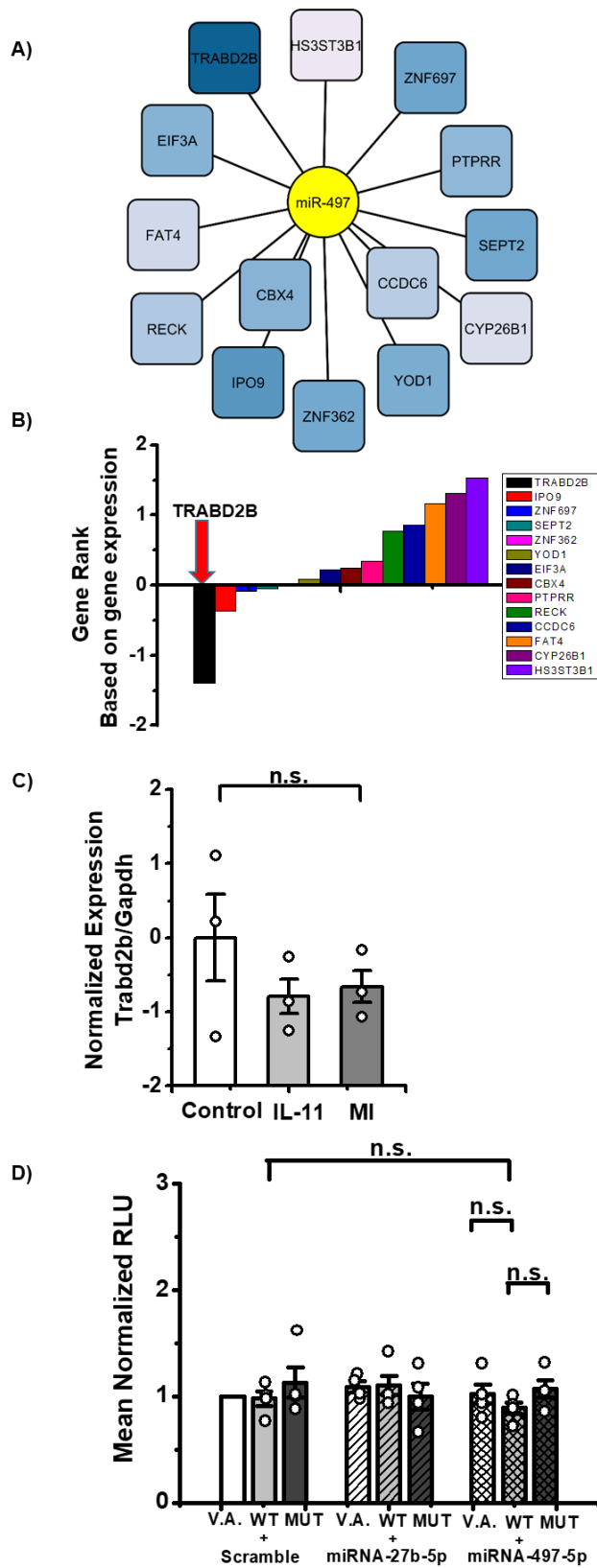
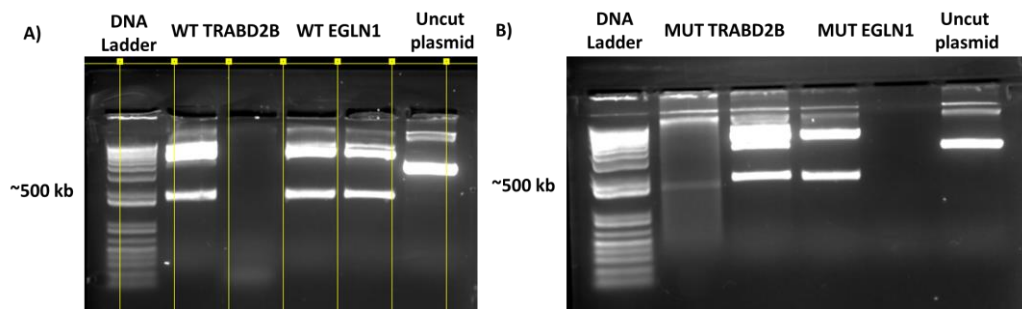


Figure 4.4 Validation of TRABD2B as a target of miR-27b-5p. A) List of potential targets of miR-497-5p (predicted by Targetscan and visualized by Cytoscape 3.8.2

(<https://cytoscape.org/>). Relative expression of targets in IL-11- treated human cardiac fibroblasts, was determined our published dataset [55]. Continuous color mapping (low gene rank dark blue-> high gene rank- white). **B)** Plot of candidate genes ranked by magnitude of regulation. **C)** Modulation of RNA levels of TRABD2B in CFs from healthy rat treated with IL-11 (5ng/μl, 24hrs) (light grey) and post-MI HF CFs (grey). **D)** HEK293FT were transfected with vector alone (pLUC) or firefly luciferase constructs that contain either an intact miR-497-5p binding site (wt), or a mutated miR-497-5p binding site (mut) for TRABD2B. Each pLUC plasmid was co-transfected with a plasmid encoding Renilla luciferase along with a plasmid encoding either miR-27b-5p or a scramble sequence (scr) or a miR-497-5p as a negative control. Firefly luciferase luminescence units were normalized against renilla luminescence. All experimental values were compared to the vector-only and scramble vector transfection conditions. N = 3 for RT-qPCR. N = 4 for dual luciferase assay. Data presented as Mean ± SEM One-way Anova was applied followed by Tukey Mean Comparison test in order to estimate statistical significance n.s. – non significant.

4.5 Validation of the construct presence by gel electrophoresis and DNA-sequencing

For conducting dual luciferase assay we inserted wild type (WT) binding site for miRNA or mutated binding site (MUT) in pMIR-REPORT-Luciferase (pLUC, Ambion), between SpeI and Hind III restriction sites. For this reason, presence of the binding site was confirmed by running a gel electrophoresis. Expected band with an inserted sequence was expected to be around 500kb. Experiment was done in duplicates (Figure 4.5 A, B). Presence of binding sites was confirmed for WT and MUT EGLN1 and TRABD2B. This data was further confirmed by DNA sequencing done by Eurofins Genomics.



4.5 Gel electrophoresis. A) Done for WT TRABD2B and EGLN1 constructs. B) Done for MUT TRABD2B and EGLN1 constructs.

5. DISCUSSION II

It is well-known that miRNAs can interact with multiple targets sometimes within the same biological process or even the same pathway [58, 60-62]. In order to investigate possible targets, we used an IL-11 (677 genes) and TGF β 1 (683 genes) differential co-expression network.

Gene ontology enrichment analysis in genes presented in IL-11 network and TGF β 1 network revealed significant enrichment in similar processes associated with cardiac fibrosis (Figure 4.1 A, B): TGF β 1 signaling. However, most of the processes were different. TGF β 1 network was enriched in processes associated with collagen formation, ECM deposition and focal adhesions (Figure 4.1 B). Every listed process takes its place in cardiac fibrosis [63-65]. IL-11 co-expression network demonstrated to be involved in processes associated with cell migration/proliferation, angiogenesis and response to hypoxia (Figure 4.1 A). These processes are usually activated in fibroblasts during MI or ischemia-reperfusion, when big loss of cells occurs accompanied by insufficient blood flow [66, 67]. Fibroblasts begin proliferate actively and produce ECM matrix in order to maintain heart functions through replacement fibrosis. In Figure 4.1 C we appreciated that both TGF β 1 and IL-11 networks are strongly overlapped, which may indicate a co-dependence of both regulatory networks.

As a next step, we tested our theoretical model of differentially co-expression networks. RNAseq data obtained from Dr. Benedict Reilly 'O Donnell [55] from human DCM CFs treated with IL-11 was analyzed in this thesis. We found that IL-11 stimulation of CFs resulted in significant changes of the gene expression (Figure 4.2 A). We were aiming to test if these changes in gene expression can be reflected in our theoretical model. Separate enrichment tests for IL-11 and TGF β 1 networks revealed that with IL-11 stimulation in significant enrichment of both TGF β 1 co-expression network (Enrichment score = 1.6) and IL-11 co-expression network (Enrichment score = 1.5; FDR < 0.001). (Figure 4.2 B, C, D). We demonstrated these changes visually in the network (Figure 4.2 E).

When we validated relevance of IL-11 and TGF β 1 co-expression networks we intersected it with a full list of possible targets for miRNA-27b-5p and miRNA-497-5p. That intersection together with introduced selection criteria should reduce the number of false positive results from TargetScan [33]. As a result, we found that all 28 ‘successful targets’ (Figure 4.3 A) of miRNA-27b-5p were down-regulated in IL-11 stimulated human DCM CFs (Figure 4.3 B) [55]. EGLN1 was chosen based on the literature search. We found that mice with the Tie2-Cre mediated deletion of EGLN1 exhibit cardiac fibrosis and hypertrophy [59]. At the same time, miRNA-497-5p targets after the intersection had 14 candidates (Figure 4.4 A). Targets expression in human DCM CFs treated with IL-11 demonstrated impressive down-regulation in only one gene, TRABD2B, which is encoding TIKI2 (Figure 4.4 B). It is a metalloprotease that acts as a negative regulator of the Wnt signaling pathway by mediating the cleavage of the 8 N-terminal residues of a subset of Wnt proteins [68]. Following cleavage, Wnt proteins become oxidized and form large disulfide-bond oligomers, leading to their inactivation [69]. Able to cleave WNT3A, WNT5, which are considered to be pro-fibrotic in CFs [70]. Interestingly, that our prediction approach revealed RECK as a possible candidate. As we discussed in section 1.4 miRNA-497-5p inducing fibrosis through RECK inhibition and further ECM reorganization through MMP2/9 in pulmonary [45]. It is possible, that this mechanism remains consistent in CFs as well. However, we decided to proceed with TRABD2B in order to elucidate novel mechanism.

As a next step, we checked EGLN1 expression in RNA from rat CFs treated with IL-11 and MI rat CFs. In both conditions, we observed significant down-regulation of EGLN1 (Figure 4.3 C). Unfortunately, TRABD2B expression was not regulated by IL-11 stimulation or in MI rat CFs.

We designed and conducted dual luciferase assay on miRNA-27b-5p and EGLN1; miRNA-497-5p and TRABD2B (Figure 4.3 D; Figure 4.4 D respectively). By this experiment, we confirmed targeting of EGLN1 by miRNA-27b-5p through its binding site (AAGCTCA). At the same time, drop in luminescence in cells containing plasmid with TRABD2B (TGCTGCTA) and miRNA-497-5p was insignificant. It can be explained by weak interaction between miRNA-497-5 and

TRABD2B or by lacking of specific conditions of this interaction. More likely, that TRABD2B was a false-positive candidate.

6. REFERENCES II

1. Ha M, Pang M, Agarwal V, Chen ZJ. Interspecies regulation of microRNAs and their targets. *Biochim Biophys Acta*. **2008**;1779(11):735-742. doi:10.1016/j.bbagr.2008.03.004
2. Lee Y, Kim M, Han J, et al. MicroRNA genes are transcribed by RNA polymerase II. *EMBO J*. **2004**;23(20):4051-4060. doi:10.1038/sj.emboj.7600385
3. Han J, Lee Y, Yeom KH, Kim YK, Jin H, Kim VN. The Drosha-DGCR8 complex in primary microRNA processing. *Genes Dev*. **2004**;18(24):3016-3027. doi:10.1101/gad.1262504
4. Partin AC, Ngo TD, Herrell E, Jeong BC, Hon G, Nam Y. Heme enables proper positioning of Drosha and DGCR8 on primary microRNAs [published correction appears in Nat Commun. 2018 Sep 18;9(1):3852]. *Nat Commun*. **2017**;8(1):1737. Published 2017 Nov 23. doi:10.1038/s41467-017-01713-y
5. Yi R, Qin Y, Macara IG, Cullen BR. Exportin-5 mediates the nuclear export of pre-microRNAs and short hairpin RNAs. *Genes Dev*. **2003**;17(24):3011-3016. doi:10.1101/gad.1158803
6. Davis BN, Hata A. Regulation of MicroRNA Biogenesis: A miRiad of mechanisms. *Cell Commun Signal*. **2009**;7:18. Published 2009 Aug 10. doi:10.1186/1478-811X-7-18
7. Yoda M, Kawamata T, Paroo Z, et al. ATP-dependent human RISC assembly pathways. *Nat Struct Mol Biol*. **2010**;17(1):17-23. doi:10.1038/nsmb.1733
8. Khvorova A, Reynolds A, Jayasena SD. Functional siRNAs and miRNAs exhibit strand bias [published correction appears in Cell. 2003 Nov 14;115(4):505]. *Cell*. **2003**;115(2):209-216. doi:10.1016/s0092-8674(03)00801-8
9. Ha M, Kim VN. Regulation of microRNA biogenesis. *Nat Rev Mol Cell Biol*. **2014**;15(8):509-524. doi:10.1038/nrm3838

10. Stavast CJ, Erkeland SJ. The Non-Canonical Aspects of MicroRNAs: Many Roads to Gene Regulation. *Cells*. **2019**;8(11):1465. Published 2019 Nov 19. doi:10.3390/cells8111465
11. Ruby JG, Jan CH, Bartel DP. Intronic microRNA precursors that bypass Drosha processing. *Nature*. **2007**;448(7149):83-86. doi:10.1038/nature05983
12. Miyoshi K, Miyoshi T, Siomi H. Many ways to generate microRNA-like small RNAs: non-canonical pathways for microRNA production. *Mol Genet Genomics*. **2010**;284(2):95-103. doi:10.1007/s00438-010-0556-1
13. Yang JS, Maurin T, Robine N, et al. Conserved vertebrate mir-451 provides a platform for Dicer-independent, Ago2-mediated microRNA biogenesis. *Proc Natl Acad Sci U S A*. **2010**;107(34):15163-15168. doi:10.1073/pnas.1006432107
14. Huntzinger E, Izaurralde E. Gene silencing by microRNAs: contributions of translational repression and mRNA decay. *Nat Rev Genet*. **2011**;12(2):99-110. doi:10.1038/nrg2936
15. Ipsaro JJ, Joshua-Tor L. From guide to target: molecular insights into eukaryotic RNA-interference machinery. *Nat Struct Mol Biol*. **2015**;22(1):20-28. doi:10.1038/nsmb.2931
16. Xu W, San Lucas A, Wang Z, Liu Y. Identifying microRNA targets in different gene regions. *BMC Bioinformatics*. **2014**;15 Suppl 7(Suppl 7):S4. doi:10.1186/1471-2105-15-S7-S4
17. Kawamata T, Tomari Y. Making RISC. *Trends Biochem Sci*. **2010**;35(7):368-376. doi:10.1016/j.tibs.2010.03.009
18. Jo MH, Shin S, Jung SR, Kim E, Song JJ, Hohng S. Human Argonaute 2 Has Diverse Reaction Pathways on Target RNAs. *Mol Cell*. **2015**;59(1):117-124. doi:10.1016/j.molcel.2015.04.027
19. Jonas S, Izaurralde E. Towards a molecular understanding of microRNA-mediated gene silencing. *Nat Rev Genet*. **2015**;16(7):421-433. doi:10.1038/nrg3965

20. Nishi K, Nishi A, Nagasawa T, Ui-Tei K. Human TNRC6A is an Argonaute-navigator protein for microRNA-mediated gene silencing in the nucleus. *RNA*. **2013**;19(1):17-35. doi:10.1261/rna.034769.112
21. Alló M, Agirre E, Bessonov S, et al. Argonaute-1 binds transcriptional enhancers and controls constitutive and alternative splicing in human cells. *Proc Natl Acad Sci U S A*. **2014**;111(44):15622-15629. doi:10.1073/pnas.1416858111
22. Truesdell SS, Mortensen RD, Seo M, et al. MicroRNA-mediated mRNA translation activation in quiescent cells and oocytes involves recruitment of a nuclear microRNP. *Sci Rep*. **2012**;2:842. doi:10.1038/srep00842
23. Bukhari SIA, Truesdell SS, Lee S, et al. A Specialized Mechanism of Translation Mediated by FXR1a-Associated MicroRNP in Cellular Quiescence. *Mol Cell*. **2016**;61(5):760-773. doi:10.1016/j.molcel.2016.02.013
24. Ørom UA, Nielsen FC, Lund AH. MicroRNA-10a binds the 5'UTR of ribosomal protein mRNAs and enhances their translation. *Mol Cell*. **2008**;30(4):460-471. doi:10.1016/j.molcel.2008.05.001
25. McGeary SE, Lin KS, Shi CY, Pham TM, Bisaria N, Kelley GM, Bartel DP. The biochemical basis of microRNA targeting efficacy. *Science*. **2019**;366(6472):eaav1741. doi: 10.1126/science.aav1741. Epub 2019 Dec 5. PMID: 31806698; PMCID: PMC7051167.
26. Sticht C, De La Torre C, Parveen A, Gretz N. miRWalk: An online resource for prediction of microRNA binding sites. *PLoS One*. **2018**;13(10):e0206239. doi: 10.1371/journal.pone.0206239. PMID: 30335862; PMCID: PMC6193719.
27. Jeggari A, Marks DS, Larsson E. miRcode: a map of putative microRNA target sites in the long non-coding transcriptome. *Bioinformatics*. **2012**;28(15):2062-3. doi: 10.1093/bioinformatics/bts344. Epub 2012 Jun 19. PMID: 22718787; PMCID: PMC3400968

28. John B, Enright AJ, Aravin A, Tuschl T, Sander C, Marks DS. Human MicroRNA targets [published correction appears in PLoS Biol. 2005 Jul;3(7):e264]. *PLoS Biol.* **2004**;2(11):e363. doi:10.1371/journal.pbio.0020363
29. Liu B, Li J, Cairns MJ. Identifying miRNAs, targets and functions. *Brief Bioinform.* **2014**;15(1):1-19. doi:10.1093/bib/bbs075
30. Mazière P, Enright AJ. Prediction of microRNA targets. *Drug Discov Today.* **2007**;12(11-12):452-458. doi:10.1016/j.drudis.2007.04.002
31. Karlin S, Altschul SF. Methods for assessing the statistical significance of molecular sequence features by using general scoring schemes. *Proc Natl Acad Sci U S A.* **1990**;87(6):2264-2268. doi:10.1073/pnas.87.6.2264
32. Giraldez AJ, Mishima Y, Rihel J, et al. Zebrafish MiR-430 promotes deadenylation and clearance of maternal mRNAs. *Science.* **2006**;312(5770):75-79. doi:10.1126/science.1122689
33. Selbach M, Schwanhäusser B, Thierfelder N, Fang Z, Khanin R, Rajewsky N. Widespread changes in protein synthesis induced by microRNAs. *Nature.* **2008**;455(7209):58-63. doi:10.1038/nature07228
34. Alvarez ML, Khosroheidari M, Eddy E, Done SC. MicroRNA-27a decreases the level and efficiency of the LDL receptor and contributes to the dysregulation of cholesterol homeostasis. *Atherosclerosis.* **2015**;242(2):595-604. doi:10.1016/j.atherosclerosis.2015.08.023
35. Zhang M, Sun W, Zhou M, Tang Y. MicroRNA-27a regulates hepatic lipid metabolism and alleviates NAFLD via repressing FAS and SCD1. *Sci Rep.* **2017**;7(1):14493. Published 2017 Nov 3. doi:10.1038/s41598-017-15141-x
36. Lin Q, Gao Z, Alarcon RM, Ye J, Yun Z. A role of miR-27 in the regulation of adipogenesis. *FEBS J.* **2009**;276(8):2348-2358. doi:10.1111/j.1742-4658.2009.06967.x
37. You L, Pan L, Chen L, Gu W, Chen J. MiR-27a is Essential for the Shift from Osteogenic Differentiation to Adipogenic Differentiation of Mesenchymal

- Stem Cells in Postmenopausal Osteoporosis. *Cell Physiol Biochem.* **2016**;39(1):253-265. doi:10.1159/000445621
38. Lv X, Yan J, Jiang J, Zhou X, Lu Y, Jiang H. MicroRNA-27a-3p suppression of peroxisome proliferator-activated receptor- γ contributes to cognitive impairments resulting from sevoflurane treatment. *J Neurochem.* **2017**;143(3):306-319. doi:10.1111/jnc.14208
39. Murata Y, Yamashiro T, Kessoku T, et al. Up-Regulated MicroRNA-27b Promotes Adipocyte Differentiation via Induction of Acyl-CoA Thioesterase 2 Expression. *Biomed Res Int.* **2019**;2019:2916243. Published 2019 Dec 10. doi:10.1155/2019/2916243
40. Fu Q, Lu Z, Fu X, Ma S, Lu X. MicroRNA 27b promotes cardiac fibrosis by targeting the FBW7/Snail pathway. *Aging (Albany NY).* **2019**;11(24):11865-11879. doi:10.18632/aging.102465
41. Wang, J., Song, Y., Zhang, Y. et al. Cardiomyocyte overexpression of miR-27b induces cardiac hypertrophy and dysfunction in mice. *Cell Res.* 2012 22, 516–527. doi:10.1038/cr.2011.132
42. Veliceasa D, Biyashev D, Qin G, et al. Therapeutic manipulation of angiogenesis with miR-27b. *Vasc Cell.* **2015**;7:6. Published 2015 Jun 24. doi:10.1186/s13221-015-0031-1
43. Itesako T, Seki N, Yoshino H, et al. The microRNA expression signature of bladder cancer by deep sequencing: the functional significance of the miR-195/497 cluster. *PLoS One.* **2014**;9(2):e84311. Published 2014 Feb 10. doi:10.1371/journal.pone.0084311
44. Luo G, He K, Xia Z, Liu S, Liu H, Xiang G. Regulation of microRNA-497 expression in human cancer. *Oncol Lett.* **2021**;21(1):23. doi:10.3892/ol.2020.12284
45. Xiao Y, Zhang X, Fan S, Cui G, Shen Z. MicroRNA-497 Inhibits Cardiac Hypertrophy by Targeting Sirt4. *PLoS One.* **2016**;11(12):e0168078. Published 2016 Dec 16. doi:10.1371/journal.pone.0168078

46. Chen, X., Shi, C., Wang, C. et al. The role of miR-497-5p in myofibroblast differentiation of LR-MSCs and pulmonary fibrogenesis. *Sci Rep.* **2017**;7, 40958 (2017). doi:10.1038/srep40958
47. Schafer S, Viswanathan S, Widjaja AA, et al. IL-11 is a crucial determinant of cardiovascular fibrosis. *Nature.* **2017**;552(7683):110-115. doi:10.1038/nature24676
48. Chen H, Moreno-Moral A, Pesce F, et al. WWP2 regulates pathological cardiac fibrosis by modulating SMAD2 signaling [published correction appears in *Nat Commun.* 2019 Sep 9;10(1):4085]. *Nat Commun.* **2019**;10(1):3616. Published 2019 Aug 9. doi:10.1038/s41467-019-11551-9
49. Robinson MD, McCarthy DJ, Smyth GK. edgeR: a Bioconductor package for differential expression analysis of digital gene expression data. *Bioinformatics.* **2010**;26(1):139-140. doi:10.1093/bioinformatics/btp616
50. Warnes G. (2007). gmodels: Various R Programming Tools for Model Fitting.
51. Sangari S, & Ray H. (2021). Evaluation of imputation techniques with varying percentage of missing data.
52. Mukaka MM. Statistics corner: A guide to appropriate use of correlation coefficient in medical research. *Malawi Med J.* **2012**;24(3):69-71.
53. Huang da W, Sherman BT, Lempicki RA. Bioinformatics enrichment tools: paths toward the comprehensive functional analysis of large gene lists. *Nucleic Acids Res.* **2009**;37(1):1-13. doi:10.1093/nar/gkn923
54. Szklarczyk D, Gable AL, Lyon D, et al. STRING v11: protein-protein association networks with increased coverage, supporting functional discovery in genome-wide experimental datasets. *Nucleic Acids Res.* **2019**;47(D1):D607-D613. doi:10.1093/nar/gky1131
55. Reilly-O'Donnell B, Ferraro E, Tikhomirov R, Nunez-Toldra R, Shchendrygina A, Patel L, Wu Y, Mitchell AL, Endo A, Adorini, L, Chowdhury RA, Srivastava PK, Ng FS, Terracciano CM, Williamson C, Gorelik J. UDCA and INT-777 suppress cardiac fibrosis triggered by IL-11

- through involvement of TGR5. *MedRxiv*, **2022**;2022.05.11.22274945.
<https://doi.org/10.1101/2022.05.11.22274945>
56. Shannon P, Markiel A, Ozier O, et al. Cytoscape: a software environment for integrated models of biomolecular interaction networks. *Genome Res.* **2003**;13(11):2498-2504. doi:10.1101/gr.1239303
57. Assenov Y, Ramírez F, Schelhorn SE, Lengauer T, Albrecht M. Computing topological parameters of biological networks. *Bioinformatics.* **2008**;24(2):282-284. doi:10.1093/bioinformatics/btm554
58. Fasanaro P, D'Alessandra Y, Di Stefano V, et al. MicroRNA-210 modulates endothelial cell response to hypoxia and inhibits the receptor tyrosine kinase ligand Ephrin-A3. *J Biol Chem.* **2008**;283(23):15878-15883. doi:10.1074/jbc.M800731200
59. Dai Z, Cheng J, Liu B, et al. Loss of Endothelial Hypoxia Inducible Factor-Prolyl Hydroxylase 2 Induces Cardiac Hypertrophy and Fibrosis. *J Am Heart Assoc.* **2021**;10(22):e022077. doi:10.1161/JAHA.121.022077
60. Besnier M, Shantikumar S, Anwar M, Dixit P, Chamorro-Jorganes A, Sweaad W, Sala-Newby G, Madeddu P, Thomas AC, Howard L, Mushtaq S, Petretto E, Caporali A, & Emanuelli C. miR-15a/-16 Inhibit Angiogenesis by Targeting the Tie2 Coding Sequence: Therapeutic Potential of a miR-15a/16 Decoy System in Limb Ischemia. *Molecular Therapy - Nucleic Acids*, **2019**;17, 49–62. <https://doi.org/https://doi.org/10.1016/j.omtn.2019.05.002>
61. Pian C, Zhang G, Gao L, Fan X, Li F. miR+Pathway: the integration and visualization of miRNA and KEGG pathways. *Brief Bioinform.* **2020**;21(2):699-708. doi:10.1093/bib/bby128
62. Peng Y, Zhang X, Feng X, Fan X, Jin Z. The crosstalk between microRNAs and the Wnt/ β -catenin signaling pathway in cancer. *Oncotarget.* **2017**;8(8):14089-14106. doi:10.18632/oncotarget.12923

63. Fan D, Takawale A, Lee J, Kassiri Z. Cardiac fibroblasts, fibrosis and extracellular matrix remodeling in heart disease. *Fibrogenesis Tissue Repair*. **2012**;5(1):15. Published 2012 Sep 3. doi:10.1186/1755-1536-5-15
64. Zhang J, Fan G, Zhao H, et al. Targeted inhibition of Focal Adhesion Kinase Attenuates Cardiac Fibrosis and Preserves Heart Function in Adverse Cardiac Remodeling. *Sci Rep*. **2017**;7:43146. Published 2017 Feb 22. doi:10.1038/srep43146
65. Kong P, Christia P, Frangogiannis NG. The pathogenesis of cardiac fibrosis. *Cell Mol Life Sci*. **2014**;71(4):549-574. doi:10.1007/s00018-013-1349-6
66. Le Bras A. Dynamics of fibroblast activation in the infarcted heart. *Nat Rev Cardiol*. **2018**;15(7):379. doi:10.1038/s41569-018-0025-9
67. Shinde AV, Frangogiannis NG. Fibroblasts in myocardial infarction: a role in inflammation and repair. *J Mol Cell Cardiol*. **2014**;70:74-82. doi:10.1016/j.yjmcc.2013.11.015
68. Yuan X, Dong B, Xu Y, et al. TIKI2 is upregulated and plays an oncogenic role in renal cell carcinoma. *Oncotarget*. **2016**;7(13):17212-17219. doi:10.18632/oncotarget.7873
69. Zhang X, Abreu JG, Yokota C, et al. Tiki1 is required for head formation via Wnt cleavage-oxidation and inactivation. *Cell*. **2012**;149(7):1565-1577. doi:10.1016/j.cell.2012.04.039
70. Yousefi F, Shabaninejad Z, Vakili S, et al. TGF- β and WNT signaling pathways in cardiac fibrosis: non-coding RNAs come into focus. *Cell Commun Signal*. **2020**;18(1):87. Published 2020 Jun 9. doi:10.1186/s12964-020-00555-4

CHAPTER III

1. INTRODUCTION III

In the scientific field of cancer biology, it is well-known that miRNAs can be pathology-dependent. In other words, miRNAs can act through different molecular mechanisms in different pathologies.

For this reason, we considered that in different cardiovascular diseases accompanied by cardiac fibrosis miRNA-497-5p and miRNA-27b-5p may contribute to cardiac fibrosis via different mechanisms. In this chapter, we would like to discuss MI, ICM and DCM as our working models.

1.1 Myocardial infarction, ischemic cardiomyopathy: etiology, mechanisms of extracellular matrix remodeling, heart failure progression

1.2 Etiology

According to the WHO (World Health Organization) cardiovascular diseases are taking 17.9 million lives in 1 year. Among different cardiovascular diseases MI is a leading reason of hospital admissions [1]. Myocardial infarction usually caused by a massive cell necrosis due to a long and vast ischemia. Ischemia can be caused by coronary artery occlusion or by coronary artery diseases which implies obstruction to blood flow due to plaques in the coronary arteries [2]. Consequently, risk factors are: smoking, hypertension, alcohol, diabetes mellitus, abdominal obesity etc. [3].

1.3 ECM remodeling in post-myocardial infarction/ischemic cardiomyopathy

When myocardium perfusion decreases for 20-40 minutes, ischemia causes massive cell death. Lack of oxygen leads to the inhibition of oxygen-dependent phosphorylation and decrease in ATP concentration [4]. Cells attempt to compensate lack of ATP with anaerobic glycolysis. However, that attempt leads to the accumulation of the pyruvate and then lactate, with a consequent tissue acidosis [5]. Consequently, cells organelles are getting damaged, that leads to a cell death from necrosis or apoptosis [6].

Massive necrosis is followed by rapid inflammation. In 12-16 h inflammation begins from neutrophils infiltration. Following this, lymphocytes and macrophages are attracted in order to remove consequences of the necrosis [7]. Inflammatory phase can last from 0-4 days (Figure 1.1.1). And the length of inflammatory phase can affect the scar formation process and HF progression after MI [8].

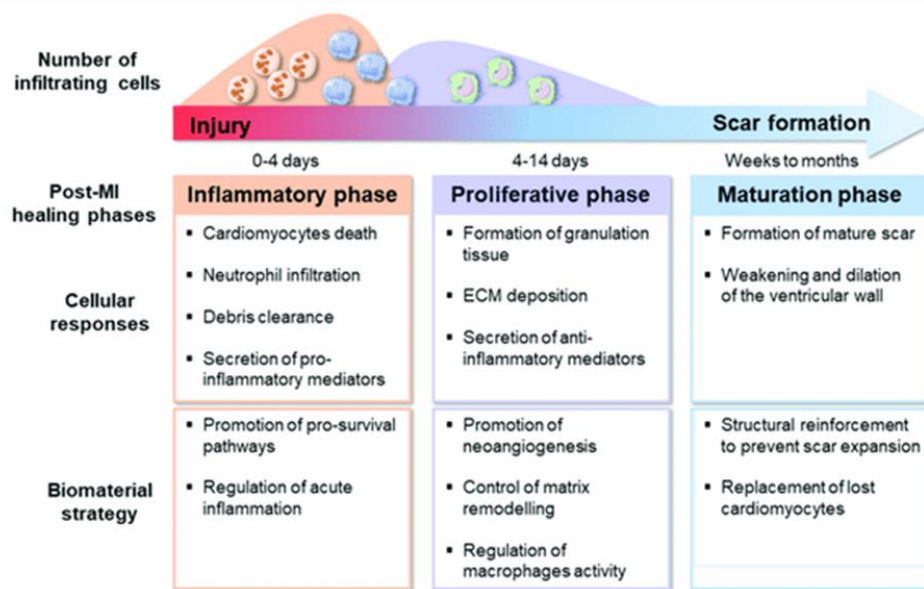


Figure 1.1.1 Phases of cardiac healing after MI [9]

After the inflammatory phase, granulation tissue, which consists from macrophages, blood vessels and myofibroblasts, is formed in the next 2 weeks [9]. Previous structured ECM that maintained cell integrity is destroyed by myofibroblasts-secreted metalloproteases (MMP) like MMP-1 (collagenase) [10]. That helps to release growth factors (like TGF β 1 and CTGF) embedded in the ECM which are promoting myofibroblasts recruitment from fibroblasts [11, 12]. After that, MMPs are inhibited and the collagen deposition begins [13]. Collagen type 1 and 3 are the main source of material for a new ECM [14]. Collagen fibers lose their orientation and become more chaotically-oriented [15]. In addition, myofibroblasts produce α -SMA fibers, which give them ability to contract. This becomes an important feature, due to the low regeneration capacity of the heart. However, contraction by myofibroblasts is insufficient to make ECM contract [16]. Nevertheless, when the scar is formed myofibroblasts can continue

production of more and more ECM proteins what leads to cardiac fibrosis progression and consequent HF [17].

1.4 HF progression after MI or ICM: molecular mechanisms

The development of HF after MI has a significant impact on outcomes, regardless of the HF type. 12 Among patients with a history of MI, HF development increases total mortality risk three-fold and cardiovascular mortality four-fold [18].

After the massive loss of cardiomyocytes, hypertrophy appears as a compensatory mechanism. Tissue remodeling tries to compensate hypertrophy but eventually evolves into maladaptive remodeling, that leads to HF progression [19]. Further pathological remodeling occurs as a consequence of insufficient capillary density that progressively leads to cell death in the infarcted myocardium after the acute event, as well as in the hemodynamically overloaded heart [20].

From a molecular point of view, renin-angiotensin-aldosterone system (RAAS) contributes to further TGF β 1 increased expression [21]. As we discussed, previously TGF β 1 induces following IL-11 autocrine production in CFs [22]. As a result, constantly increasing levels of circulating TGF β 1 and IL-11 promote further fibroblast to myofibroblasts transdifferentiation. In fact, proliferation, hypertrophy, and fibrosis have also been linked to the mitogen-activated protein kinase (MAPK) pathway (particularly, ERK1/2, c-Jun N-terminal kinase (JNK), and p38) [23], which is activated by IL-11 [22] and AT-II/AT-I complexes [23]. Consequently, JNK and p38 induce MMPs and TIMPs [24]. Therefore, unbalanced hypertrophy, increased number of myofibroblasts and hypoxia are leading to an avalanche of cytokines, growth factors that worsen the heart condition through activation of pro-fibrotic and pro-hypertrophic pathways. As a rolling snowball, cells in the heart are leading it to the HF.

1.5 Dilated cardiomyopathy: etiology, mechanisms of extracellular matrix remodeling, heart failure progression

1.6 Etiology

DCM can be described as a dilation of one or both ventricles of the heart which impairs contraction [25]. In some cases, patients affected by DCM may develop HF; the HF is characterized by impaired systolic function [26]. DCM usually presents in patients 20-60 years old. This pathology alone causes 10 000 deaths per year in the USA [27]. Reasons of DCM are usually identifiable. Patients may exhibit genetic predisposition, like Desmin [28], Myosin [29] or Lamin C [30] mutations. Another potential cause is viral infection causing myocarditis [31]. The progressive dilation of the ventricles is leading to significant tricuspid and mitral valve insufficiency. Consequently, ejection fraction of the heart decreases while the mechanical stress on the ventricle wall increases [26]. DCM can be characterized by increased levels of BNP [32], RAAS-system [33] and IL-11 [34]. Interestingly, that cardiac fibrosis in DCM patients is more prevalent for males rather than females [27].

1.7 ECM remodeling in DCM patients

In animal models as well as in DCM patients, scar tissue leads to the ventricle dilation. As a consequence, decrease in the stroke volume and cardiac output, worsen cardiac filling, increase in end-diastolic pressure are present. The prognosis for patients with DCM and fibrosis as a co-morbidity is poor [27].

1.8 ECM remodeling in post-myocardial infarction/ischemic cardiomyopathy

Viral infections and autoimmune diseases cause damage to the myocardium. Necrosis attracts inflammatory cells such as macrophages, mast cells, T helper 2 (T_H2) and TH17 cells [35]. Immune cells are producing cytokines and growth factors like TGF β 1, tumor necrosis factor (TNF), interleukin-1 β , interleukin-33 and interleukin-4. These molecules activate pro-fibrotic pathways in resident CFs, resulting in fibroblast to myofibroblast transdifferentiation and ECM deposition [36]. Further, intervention of collagens into healthy myocardium results in more cardiac damage and immune cells infiltration. Therefore, once a chain of cardiac events began it leads to further inflammation and fibrosis.

2. AIMS OF THE STUDY III

According to the literature miRNA-27b and miRNA-497-5p are known pro-fibrotic miRNAs in settings of pulmonary fibrogenesis. Moreover, data obtained on miRNA-27b-5p and miRNA-497-5p up-regulation in IL-11 treated CFs and pathological CFs from MI rats may indicate miRNAs role in induction of fibroblasts to myofibroblasts transition or in suppression of CFs anti-fibrotic mechanisms. For this we wanted:

- 1) To elucidate the effect of miRNA-27b-5p and miRNA-497-5p on gene expression and phenotype in CFs. For this to overexpress/inhibit each miRNA separately in healthy rat/human CFs and CFs from a pathological condition (MI rat, human DCM, human ICM).**

- 2) To validate relevance of EGLN1 repression by miRNA-27b-5p in cardiac pathologies like: MI, DCM and ICM**

3. METHODS III

3.1 Animal models and cell culture

All animal models were established and used in the United Kingdom (UK) with established standards for the care of animal subjects written by the UK Home Office (ASPA1986 Amendments Regulations 2012) incorporating the EU directive 2010/63/EU. Ethics was approved by committee of Imperial College London.

Age-matched male Sprague-Dawley rats were used as a control group to rat with MI. In order to induce MI in rat's coronary artery ligation was performed. After 16 weeks, animals were sacrificed when end stage heart failure (HF) develops [37]. These animal experiments were approved by the Animal Welfare and Ethical Review Board (AWERB) of Imperial College London, UK and carried out in accordance with the UK Animals (Scientific Procedures) Act 1986, incorporating the European Union Directive 2010/63/EU.

CFs were isolated after Langendorff perfusion with enzymatic digestion of rats LV [38]. Following this, cells were centrifuged in order to remove cardiomyocytes (CMs). After that, CFs were pelleted and plated in high-glucose (4500 mg/l) Dulbecco's Modified Eagle Medium supplemented with 10% Fetal Bovine Serum and 1% of penicillin/streptomycin. Cells were cultured 20 day's maximum after fixation or lysis at 37 °C and 5% CO₂. Confluent T-25 flask of CFs was treated with IL11 (5 ng/ul) or TGFβ1 (100 ng/ul). After 24 hours, first treatments cells were washed with 2.5 ml of PBS and used for further experiments.

3.2 Cultivation of human cardiac fibroblasts

Human cardiac fibroblasts from healthy donor (N = 1, biological replicates = 4), DCM (N = 4, biological replicates = 2) and ICM (N = 4, biological replicates = 2) patients were obtained from LV organotypic culture [39]. LV pieces were fixed in the 6-well plate covered with fibronectin. Cardiac fibroblasts were growing from pieces for 2-3 weeks in 20% Fetal Bovine Serum and 1% of penicillin/streptomycin at 37 °C and 5% CO₂. Following this, cells were seeded

equally in 12-well plate for further experiments. Ethics was approved by the NHS committee (REC reference 19/SC/0257; IRAS project ID:264059).

3.3 miRNA-27b-5p and miRNA-497-5p gain/loss of functions in rat cardiac fibroblasts

Rat CFs (N = 3) from un-operated Sprague-Dawley rats and MI-induced rats were plated in 12-well plate in duplicates (10⁶ cells/well) for 24 h at 37 °C 5% CO₂. As a next step, cells were transfected with scramble nucleotides (scr) (Horizon Discovery D-001810-10-20), or with mirVana mimics/inhibitors: mmu-miR-497a-5p mimic (mim) (Cat. Number MC11293), mmu-miR-497a-5p inhibitor (inh) (Cat. Number MH11293), rno-miR-27b-5p mimic (Cat. Number MC20018) and rno-miR-27b-5p inhibitor (Cat. Number MH20018). mirVana mimics for miRNA-497-5p were designed to work in both rat (rno-) and mouse (mmu-) model. Oligonucleotides used for this study were utilized at concentration equals 5nM.

3.4 miRNA-27b-5p gain/loss of functions in human cardiac fibroblasts from donor, DCM and ICM patients

In this study we focused only on miRNA-27b-5p since the number of cells was limited and we were aiming to check EGLN1 regulation via miRNA-27b-5p in human CFs.

Human donor (N = 1, n = 3), DCM (N ≥ 3, n = 2) and ICM (N ≥ 3, n = 2) CFs were plated in 12-well plate in duplicates (10⁶ cells/well) for 24 h at 37 °C 5% CO₂. On the next day, cells were transfected with scramble nucleotides (scr) (Horizon Discovery D-001810-10-20), or mirVana mimics and inhibitors: hsa-miR-27b-5p (Cat. Number MC12831, miRVana) and hsa-miR-27b-5p (Cat. Number MH12831, miRVana) respectively. Oligonucleotides used for this study were utilized at concentration equals 15nM, since we expected from human cells a longer response to a transfection due to the different metabolism in comparison with rat CFs.

Transfection of cardiac fibroblasts with oligonucleotides and Lipofectamine 3000

At the start of the transfection protocol, two separate tubes were prepared:

1) 1 μ l LipofectamineTM 3000 Reagent was diluted within 25 μ l of Opti-MEMTM medium, and

2) Oligonucleotides and 2 μ l P3000TM Reagent (2 μ l/1 μ g DNA) diluted within 25 μ l of Opti-MEM medium

Both tubes were vortexed briefly and incubated at room temperature for 3-5 mins. After this, samples were mixed together and left to incubate for another 10-15 mins at room temperature. CFs were washed 3 consecutive times with 1 ml of Opti-MEMTM medium, prior to 50 μ l of oligonucleotides mixture was added to CFs and were then left for an incubation period at 37°C and 5% CO₂ for 1 hr. For the final step, residual oligonucleotides-lipid complex was removed, before 2 ml of DMEM (1X) with 15% (v/v) fetal bovine serum (FBS) were added to each culture and left overnight.

3.5 Immunostaining against Vimentin and α -SMA

CFs were fixed with 4% paraformaldehyde with further permeabilization with 0.05% TritonX-100 diluted in PBS. Any non-specific binding was prevented by blocking of fixed cells with 5% (w/v) BSA for 1 hour at room temperature. After that, cells were stained with primary antibodies overnight at 4°C: α -SMA mouse monoclonal DAKO antibody (M0851) and vimentin chicken polyclonal antibody from Invitrogen (PA1-16759). On the next day, coverslips were washed three times with PBS and incubated for three hours at room temperature in a dark place with secondary antibodies: anti-mouse donkey polyclonal AlexaFluor-488 from Invitrogen (A21202) and anti-chicken goat polyclonal AlexaFluor-546 from Invitrogen (A11040). After that, coverslips were washed in PBS three times and mounted onto the labelled slides, using hard-set mountant medium (ProlongTM Gold Antifade reagent with DAPI) [40]. Slides were then stored under aluminium foil at 4°C until imaging.

3.6 Image acquisition and analysis for immunostaining in cell culture

CFs and MI CFs that were stained according to 3.2 were analyzed with the optical system [Nikon Eclipse Ti with pE-4000 light source (Cool LED) and ORCA-Flash 4 camera (Hamamatsu)]. With 20x magnification we collected 5-7 images for one coverslip with ~10 cells per image. Images processing was done in Fiji

(ImageJ). In order to distinguish α -smooth muscle actin positive cells (α -SMA) from healthy CFs images were thresholded to control condition. Raw images in DAPI and vimentin channels were uploaded in ImageJ and turned to 16-bit images where cells were manually highlighted and mean fluorescence for each cell was detected in α -SMA channel with help of ROI Manager. After that, mean fluorescence from each cell was used for distribution analysis, where 90th percentile was chosen as a threshold value for all conditions. Fibers morphology was also considered as important criteria for α -SMA positive cell detection [41].

3.7 RNA isolation and reverse transcription polymerase chain reaction on transfected cardiac fibroblasts

RNA was collected and converted to cDNA as it is described in chapter I 3.5. Designed primers in order to detect genes of interest are present in table 3.7.

Table 3.7 List of primers

Gene name	Species	Forward primer sequence 5'->3'	Reverse primer sequence 5'->3'
α -SMA	rat	ACCATCGGGAATGAACGCTT	CTGTCAGCAATGCCTGGGTA
Col1a1	rat	CCCAGCCGCAAAGAGTCTAC	CAGGTTTCCACGTCTCACCA
Egln1	rat	GAGACCATCGGCCTGTCAT	CGACCATGGCTTTCGTTCCGG
Gapdh	rat	TGATTCTACCCACGGCAAGTT	TGATGGGTTTCCCATTGATGA
CTGF	human	GTTTGGCCAGACCCAATA	GGCTCTGCTTCTAGCCTG
EGLN1	human	GGCAAAGCCAGTTTGCTGAC	TTAGCTCGTGCTCTCATCTGC
α -SMA	human	ATGCTCCCAGGGCTGTTTTCCAT	GTGGTGCCAGATCTTTTCCATGTGC
HIF1 α	human	GTGAAGACATCGCGGGGACC	GTGGAAGTGCAACTGATGAGC
HIF2 α	human	CACCTCGGACCTTACCAC	CCGGGACTTCTCCTTCTCC
GAPDH	human	GGTCACTGGTCTGCCAAAT	TGACAACGAGTGGGGATACA

3.8 Validation of transfection with RT-qPCR on miRNA-27b-5p and miRNA-497-5p in cardiac fibroblasts

RT-qPCR was performed in the way it is described in chapter I 3.5. A list of analyzed miRNAs can be observed in table 3.8.

Table 3.8 List of analyzed miRNAs

miRNA	Mature miRNA sequence	Species	Assay ID
rno-miR-27b-5p	AGAGCUUAGCUGAUUGGUGAACAG	rat	4440886
rno-miR-497-5p	CAGCAGCACACUGUGGUUUGUA	mouse, rat	001346
hsa-miRNA-27b-5p	AGAGCUUAGCUGAUUGGUGAAC	mouse, human	002174
hsa-miRNA-497-5p	CAGCAGCACACUGUGGUUUGU	human	001043
U6		mouse, rat, human	001973

3.9 Statistics

Statistical analysis was performed with Origin 8 Pro. The tests performed were indicated in the figure legends. Normal distribution of the data was checked with Shapiro-Wilk test. For two groups comparison Student's t-test was applied. For multiple experimental group comparison One-Way Anova with following Tukey's multiple comparison was used. N= number of patients/ animals, n= number of technical repeats. Data were presented as Mean \pm SEM. P values <0.05 were considered statistically significant.

4. RESULTS III

4.1 In vitro modulation of miRNA-27b-5p and miRNA-497-5p in rat cardiac fibroblasts.

In order to evaluate the functional role and significance of miRNA-27b-5p and miRNA-497-5p in CFs, we overexpressed or inhibited them separately in rat CFs. Modulation of miRNA-27b-5p and miRNA-497-5p expression by mimics or inhibitors was firstly confirmed by RT-qPCR in rat CFs and MI rat CFs (Figure 4.1). As it is demonstrated, 24 hr after the transfection with oligonucleotides we were able to detect significant increase/decrease in miRNA-27b-5p and miRNA-497-5p levels in both healthy (Figure 4.1 A, B) and pathological CFs derived from rats with MI (Figure 4.1 C, D).

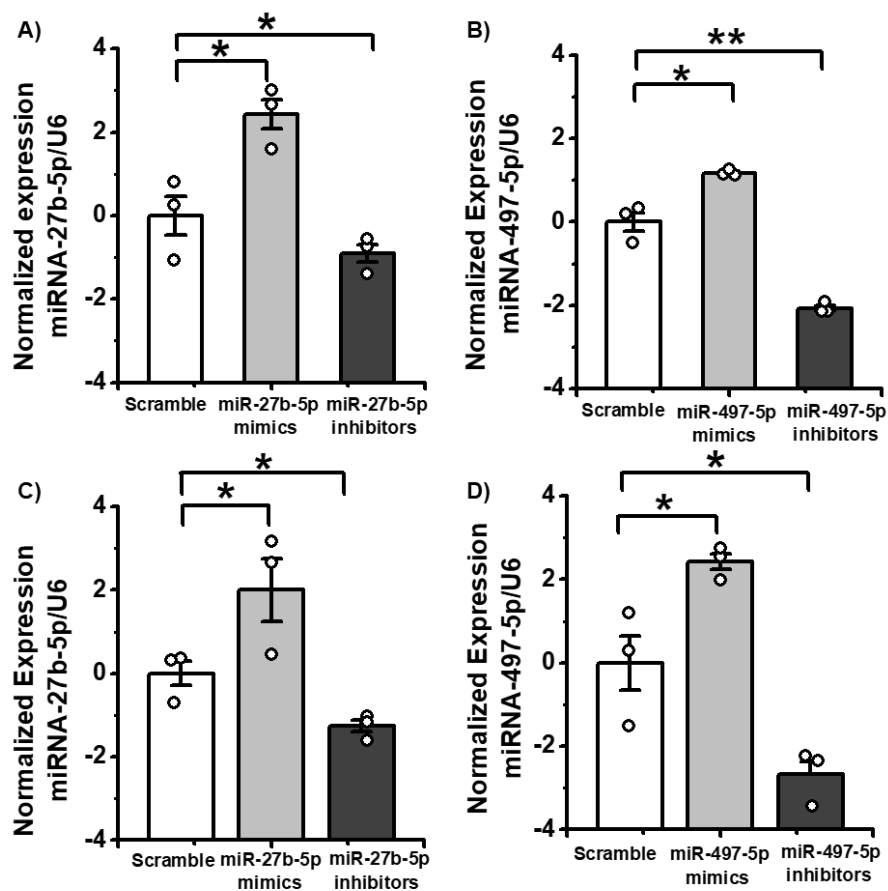


Figure 4.1 In vitro modulation of miRNA-27b-5p and miRNA-497-5p in rat cardiac fibroblasts. A)-D) Transfection of CFs with scramble nucleotides (white

bar), miRNA-27b-5p or -497 mimics (light grey) and inhibitors (dark grey) at 5nM concentration. miRNA of interest expression was normalized to U6 and further referred to a scramble condition. **A)** miRNA-27b-5p expression in healthy rat CFs. **B)** miRNA-497-5p expression in healthy rat CFs. **C)** miRNA-27b-5p expression in MI rat CFs **D)** miRNA-497-5p expression MI rat CFs. Values presented as Mean \pm SEM, N = 3 isolations, n = 3 replicates. One-way Anova was applied with following Tukey's Mean Comparison was performed in order to estimate statistical significance *p-value<0.05, **p-value<0.01

4.2 miRNA-27b-5p and miRNA-497-5p overexpression leads a significant increase in the number of α -SMA and Vimentin positive cells in rat cardiac fibroblasts

Overexpression of both miRNAs led to an increased percentage of α -SMA and vimentin positive cells in CFs transfected with miRNA-27b-5p and miRNA-497-5p mimics (Figure 4.2 A, B, D), while miRNA inhibition had no effect. (Figure 4.2 C, E). Quantification on all collected images (Figure 4F-G) revealed significant (p-value<0.05) increase of α -SMA positive cells in rat CFs transfected with miRNA-27b-5p (α -SMA cells (%) = 78.3 \pm 5.0) and miRNA-497-5p (α -SMA cells (%) = 79.1 \pm 8.9) mimics.

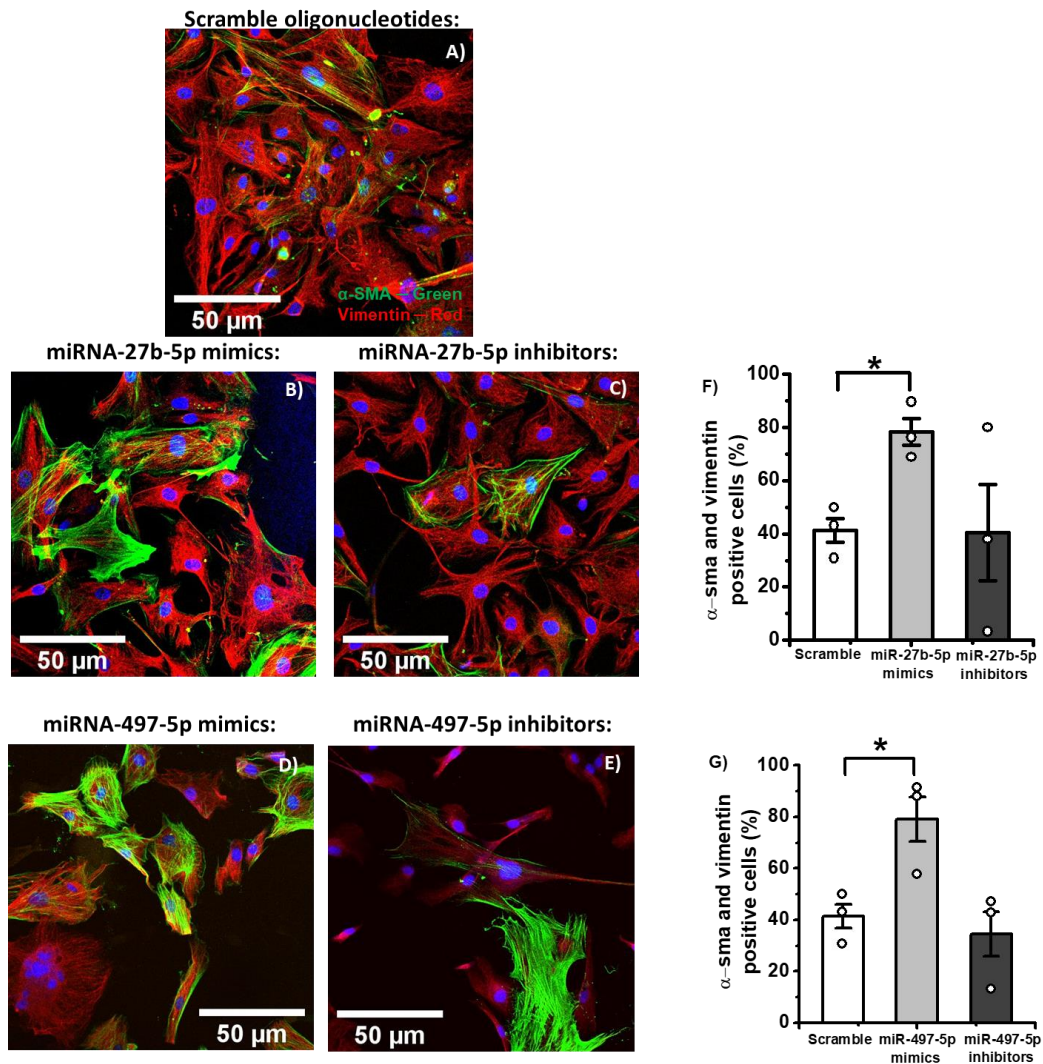


Figure 4.2 miRNA27b-5p and miRNA-497-5p modulation regulates the number of α -SMA positive cells in rat CFs. A)-E) panels show representative images of rat CFs transfected with 5nM scramble, mimics or inhibitors of miRNA-27b-5p or miRNA-497-5p and stained after 24h with vimentin (PA1-16759, red) and α -SMA (M0851, green) and DAPI (blue). F)-G) Bar charts of the percentage of α -SMA positive cells in rat CFs transfected with 5nM scramble (white bar) miRNA mimics (light grey) or miRNA inhibitors (dark grey). Values are represented as Mean \pm SEM, N = 3, n = 2. One-way Anova was applied followed by Tukey's Mean Comparison test was performed in order to estimate statistical significance *P-value<0.05.

4.3 miRNA-27b-5p and miRNA-497-5p gain and loss of functions causing gene expression changes in myofibroblasts associated markers in rat cardiac fibroblasts

We observed significant up-regulation of α -SMA expression (Figure 4.3 A, B) when miRNA-27b-5p or miRNA-497-5p was overexpressed by mimics. At the same time, only miRNA-497-5p inhibitors down-modulated α -SMA expression. We also checked expression of Coll1a1 in rat CFs transfected with miRNA-27-5p mimics (Figure 4.3 C). Interestingly, that miRNA-497-5p gain of functions was also leading to increased expression of Coll1a1 while loss of function decreased the expression (Figure 4.3 D). As we expected, miRNA-27b-5p inhibition significantly (p -value <0.05) increased EGLN1 expression ($-\Delta\Delta CT = 1.6\pm 0.2$) in healthy rat CFs (Figure 4.3 E).

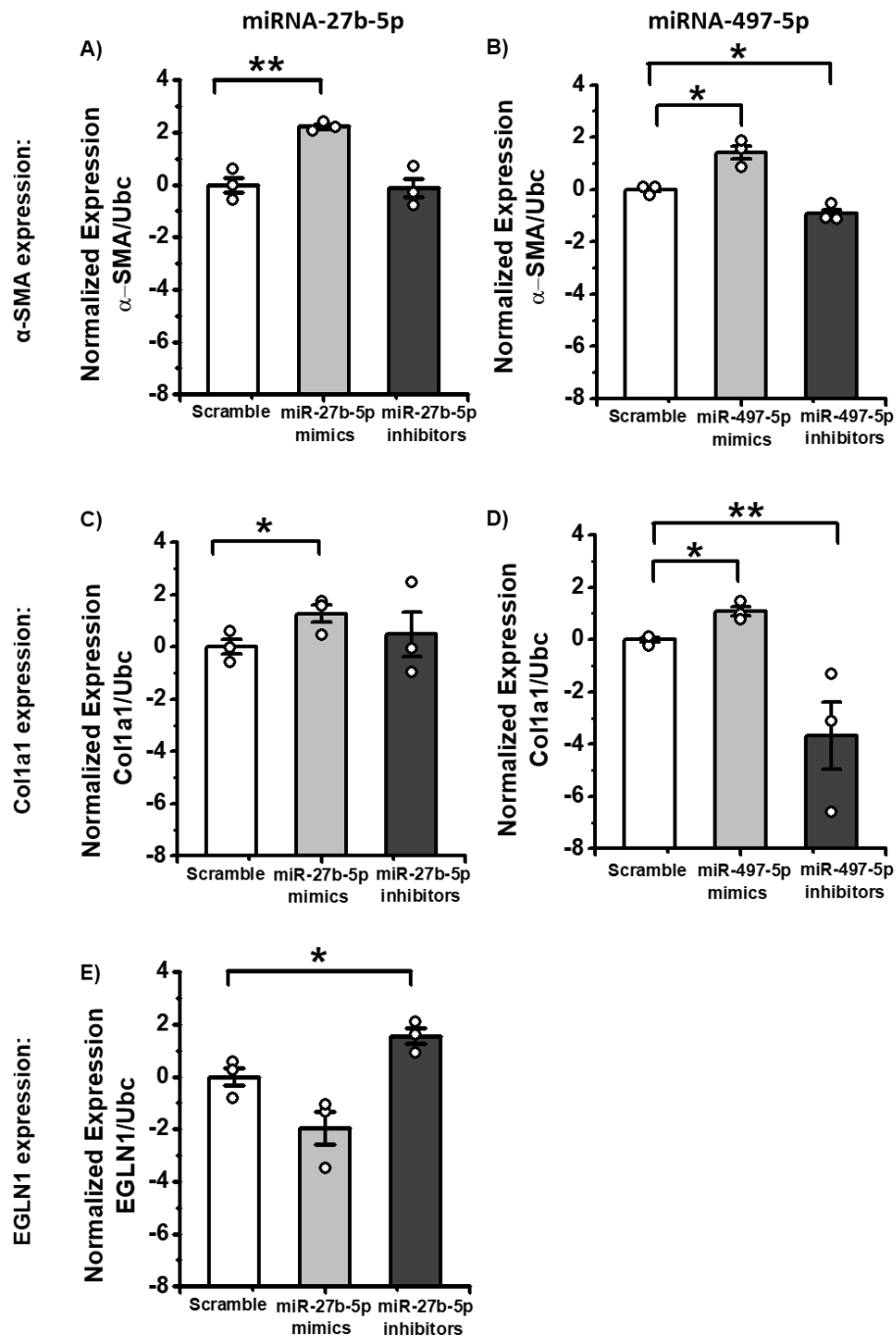


Figure 4.3 miRNA27b-5p and miRNA-497-5p modulation regulates the expression of pro-fibrotic genes in rat cardiac fibroblasts. A) – B) Modulation of RNA levels of α -SMA in rat CFs transfected with 5nM scramble (white bar), miR-27b-5p or miRNA-497-5p mimic (light grey) or inhibitor (dark grey) for 24h. C) – D) Modulation of RNA levels of Col1a1 in rat CFs transfected with 5nM scramble (white bar), miRNA-27b-5p or miR-497-5p mimic (light grey) or inhibitor (dark grey) for 24h. E) Modulation of RNA levels of EGLN1 in rat CFs transfected with 5nM scramble (white bar), miRNA-27b-5p

mimic (light grey) or inhibitor (dark grey) for 24h. Values are represented as Mean \pm SEM, N = 3, n = 3. One-way Anova was applied followed by Tukey's Mean Comparison test was performed in order to estimate statistical significance *P-value<0.05, **p<0.01.

4.4 miRNA-27b-5p and miRNA-497-5p overexpression leads a significant increase in the number of α -SMA and Vimentin positive cells in MI rat cardiac fibroblasts

We also were interested in testing miRNAs regulation and function in cardiac fibroblasts originated from pathological condition like MI. Therefore, we evaluated an increased number of α -SMA positive cells in MI rat CFs transfected with miRNA-27b-5p (α -SMA cells (%) = 88.8 ± 1.7 , p-value<0.05) and miRNA-497-5p mimics (α -SMA cells (%) = 89.4 ± 1.0 , p-value<0.05) (Figure 4.4A-G). Again, transfection with miRNA inhibitors did not affect the number of α -SMA and Vimentin positive cells. It is possible that loss of miRNA-27b-5p or miRNA-497-5p functions cannot reverse myofibroblasts phenotype. Number of myofibroblasts treated with (scr) equals 82% what is comparable with our previous findings demonstrated in the Figure 4.2 E in chapter one.

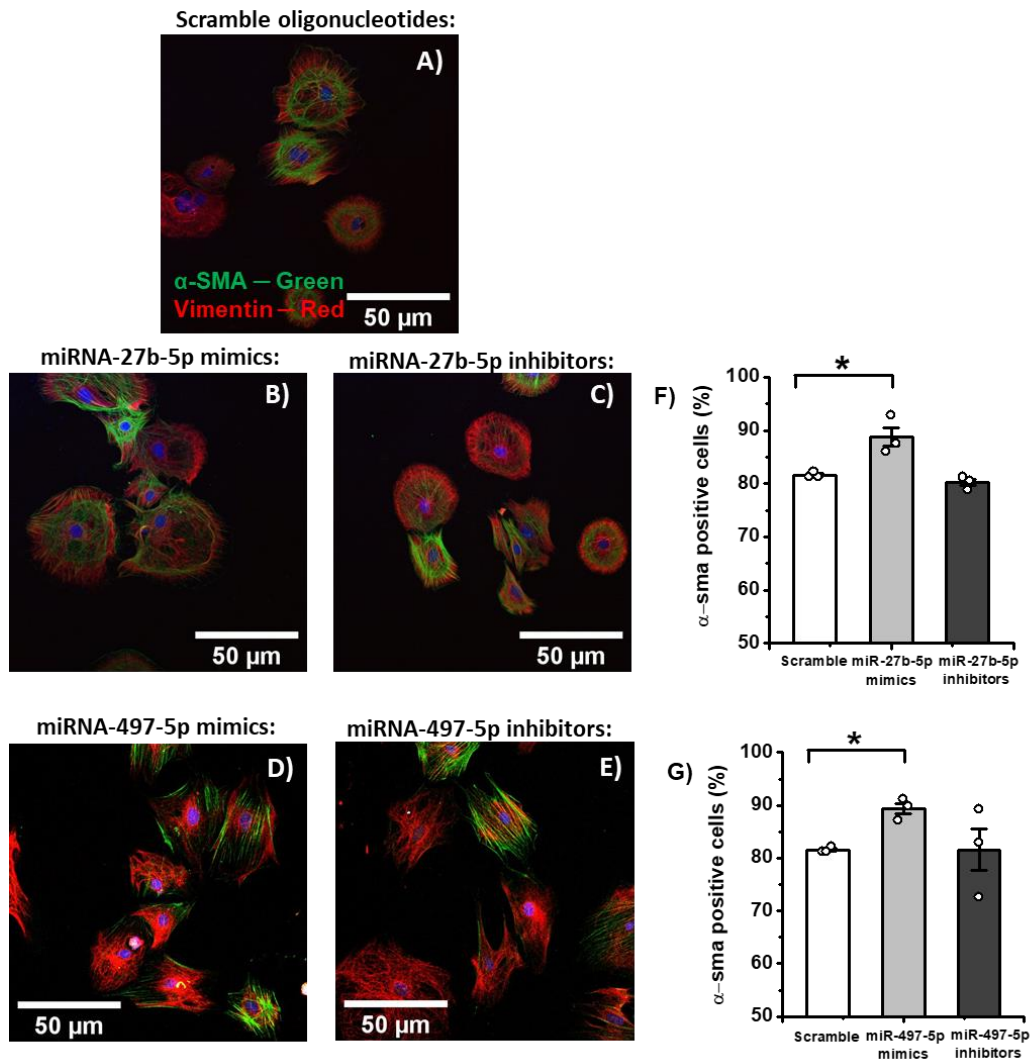


Figure 4.4 miRNA27b-5p and miRNA-497-5p modulation regulates the number of α -SMA positive cells in MI rat CFs. A)-E) panels show representative images of MI rat CFs transfected with 5nM scramble, mimics or inhibitors of miRNA-27b-5p or miRNA-497-5p and stained after 24h with vimentin (PA1-16759, red) and α -SMA (M0851, green) and DAPI (blue). F)-G) Bar charts of the percentage of α -SMA positive cells in MI rat CFs transfected with 5nM scramble (white bar) miRNA mimics (light grey) or miRNA inhibitors (dark grey). Values are represented as Mean \pm SEM, N = 3, n = 2. One-way Anova was applied followed by Tukey's Mean Comparison test was performed in order to estimate statistical significance *P-value<0.05.

4.5 miRNA-27b-5p and miRNA-497-5p gain and loss of functions causing gene expression changes in myofibroblasts associated markers in MI rat cardiac fibroblasts

In this experiment we studied how miRNA-27b-5p or miRNA-497-5p gain and loss of functions affects gene expression of myofibroblasts associated markers in CFs from pathological model – MI. Our results repeat data collected for healthy rat CFs. For example, miRNA-27b-5p gain of functions was leading to significantly (p -value <0.05) increased expression of α -SMA ($-\Delta\Delta CT = 1.7\pm 0.1$) and Col1a1 ($-\Delta\Delta CT = 2.3\pm 0.1$). On the other hand, miRNA-27b-5p loss of functions significantly decreased α -SMA expression ($-\Delta\Delta CT = -1.7\pm 0.2$). At the same time, miRNA-497-5p mimics only were causing changes in α -SMA ($-\Delta\Delta CT = 2.3\pm 0.2$) and Col1a1 ($-\Delta\Delta CT = 2.7\pm 0.4$) but not miRNA-497-5p inhibitors. Moreover, miRNA-27b-5p overexpression leads to a significant decrease of EGLN1 ($-\Delta\Delta CT = -0.5\pm 0.1$) while its inhibition results in EGLN1 increase ($-\Delta\Delta CT = 0.8\pm 0.2$) (Figure 5E).

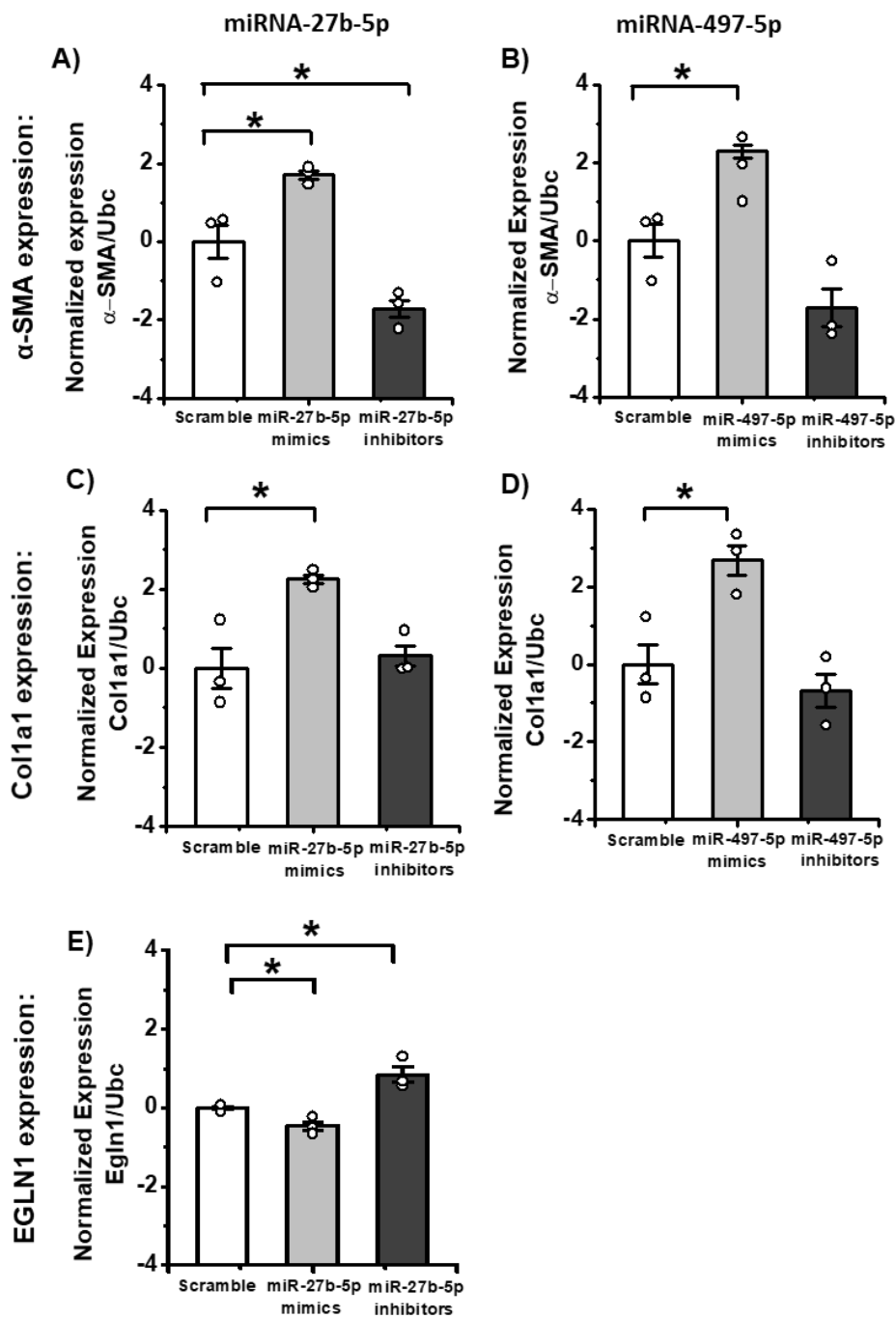


Figure 4.5 miRNA27b-5p and miRNA-497-5p modulation regulates the expression of pro-fibrotic genes in MI rat cardiac fibroblasts. A) – B) Modulation of RNA levels of α -SMA in MI rat CFs transfected with 5nM scramble (white bar), miR-27b-5p or miRNA-497-5p mimic (light grey) or inhibitor (dark grey) for 24h. C) – D) Modulation of RNA levels of Col1a1 in MI rat CFs transfected with 5nM scramble (white bar), miRNA-27b-5p or miRNA-497-5p mimic (light grey) or inhibitor (dark grey) for 24h. E) Modulation of RNA levels of EGLN1 in MI rat CFs transfected with 5nM scramble

(white bar), miRNA-27b-5p mimic (light grey) or inhibitor (dark grey) for 24h. Values are represented as Mean \pm SEM, N = 3, n = 3. One-way Anova was applied followed by Tukey's Mean Comparison test was performed in order to estimate statistical significance *P-value<0.05, **p<0.01.

4.6 In vitro modulation of miRNA-27b-5p in human cardiac fibroblasts.

In this study we focused only on miRNA-27b-5p since the number of cells was limited and we were aiming to check EGLN1 regulation via miRNA-27b-5p in human CFs from donors and pathological conditions accompanied by cardiac fibrosis like DCM and ICM.

In order to evaluate the functional role and significance of miRNA-27b-5p in CFs from donors and patients, we overexpressed or inhibited with mimics (mim) and inhibitors (inh) respectively. Modulation of miRNA-27b-5p expression by mimics or inhibitors was firstly confirmed by RT-qPCR in human CFs (Figure 4.6). As it is demonstrated, 24 hr after transfection with oligonucleotides we were able to detect significant increase/decrease in miRNA-27b-5p transfected healthy (Figure 4.6 A) and pathological CFs derived from patients with ICM and DCM (Figure 4.1 B, C). Unfortunately, transfection of DCM CFs with miRNA-27b-5p was unsuccessful.

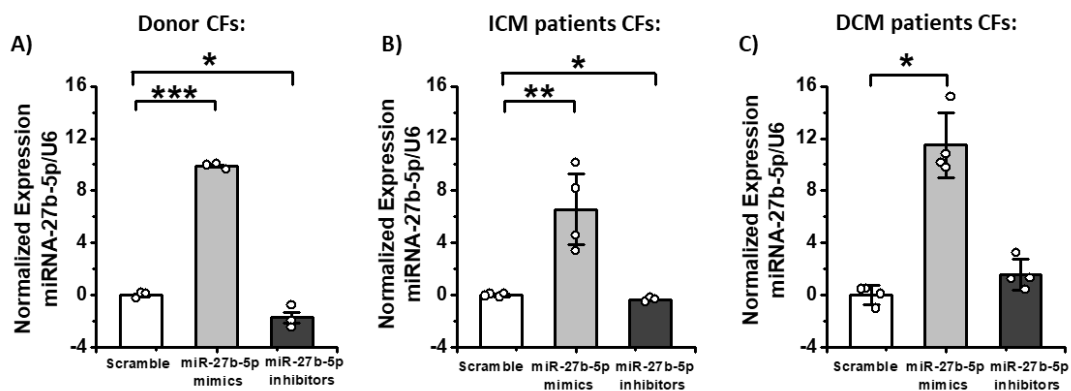


Figure 4.6 In vitro modulation of miRNA-27b-5p in human cardiac fibroblasts. A)- C) Transfection of human CFs with scramble nucleotides (white bar), miRNA-27b-5p mimics (light grey) and inhibitors (dark grey) at 15nM concentration. miRNA of interest expression was normalized to U6 and further referred to a scramble condition. A) miRNA-27b-5p expression in human donor CFs (N = 1, n =4). B) miRNA-27b-5p expression in human ICM CFs (N = 4, n = 2) C) miRNA-27b-5p expression human DCM

CFs (N = 4, n =2). One-way Anova was applied with following Tukeys Mean Comparison was performed in order to estimate statistical significance *p-value<0.05, **p-value<0.01

4.7 miRNA-27b-5p function in human donor cardiac fibroblasts.

In this experiment we were aiming to demonstrate a functional role of miRNA-27b-5p in the fibrogenic processes in human CFs. Our previous findings, section 4.2 chapter III, indicate a pro-fibrotic role of miRNA-27b-5p with a consequent repression of EGLN1 in rat CFs.

First of all, we investigated effect of miRNA-27b-5p gain and loss of functions on the phenotype of CFs from human donor.

Overexpression of miRNA-27b-5p led to an increased percentage of α -SMA and vimentin positive cells in CFs transfected with miRNA-27b-5p mimics (from 21.6% to 56.3 α -SMA and vimentin positive cells) (Figure 4.7). These data indicate a pro-fibrotic role of miRNA-27b-5p in human CFs.

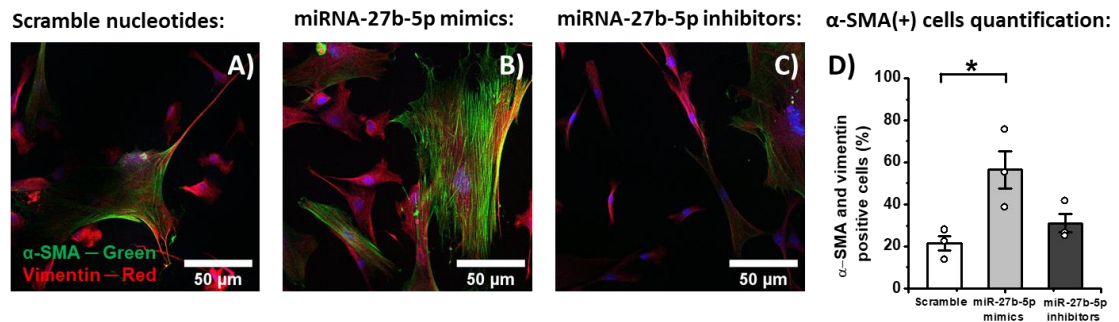


Figure 4.7 miRNA27b-5p modulation regulates the number of α -SMA positive cells in human donor CFs. A)-C) panels show representative images of human donor CFs transfected with 15nM scramble, mimics or inhibitors of miRNA-27b-5p and stained after 24h with vimentin (PA1-16759, red) and α -SMA (M0851, green) and DAPI (blue). D) Bar charts of the percentage of α -SMA positive cells in human donor CFs transfected with 15nM scramble (white bar) miRNA mimics (light grey) or miRNA inhibitors (dark grey). Values are represented as Mean \pm SEM, N = 1, n = 3. One-way Anova was applied followed by Tukey's Mean Comparison test was performed in order to estimate statistical significance *P-value<0.05.

4.8 miRNA-27b-5p gain and loss of functions causing gene expression changes in myofibroblasts and hypoxia associated markers in human donor cardiac fibroblasts.

In this experiment we investigated effect of miRNA-27b-5p overexpression/inhibition on the human donor CFs genotype. We were interested in the analysis of myofibroblasts associated markers (α -SMA). Moreover, we analyzed expression of hypoxia inducible factors 1 α and 2 α (HIF1 α , HIF2 α) – subsequent targets of protein (PHD2), encoded by EGLN1. Both hypoxia inducible factors are known contributors to the fibrosis.

We demonstrated significant (p-value<0.05) down-regulation of α -SMA expression in CFs treated with miRNA-27b-5p inhibitors and insignificant trend for the up-regulation in CFs treated with miRNA-27b-5p mimics (Figure 4.8 A). EGLN1 expression exhibited significant decrease (p-value<0.05) in human donor CFs transfected with miRNA-27b-5p mimics ($-\Delta\Delta\text{CT} = -0.32$) in comparison to CFs transfected with scramble nucleotides (Figure 4.8 B). This drop of EGLN1 expression was accompanied by an increased HIF2 α expression ($-\Delta\Delta\text{CT} = 1.0$) but not HIF1 α when CFs were transfected with miRNA-27b-5p mimics (Figure 4.8 C, D). These data may suggest that miRNA-27b-5p provoke pro-fibrotic response in healthy human CFs through facilitation of hypoxia signaling via down-regulation of EGLN1 and up-regulation of HIF2 α .

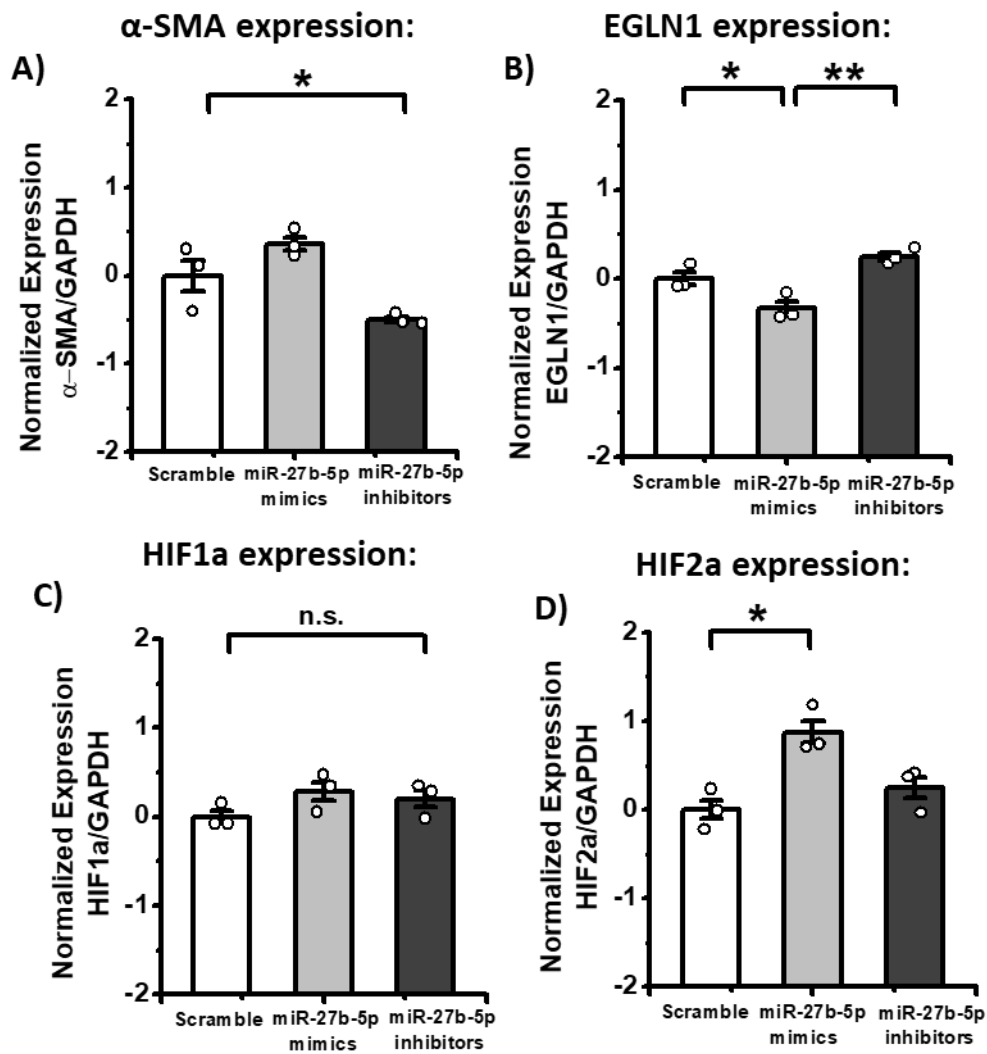


Figure 4.8 miRNA27b-5p modulation regulates the expression of pro-fibrotic and hypoxia related genes in human donor cardiac fibroblasts. Modulation of RNA levels in human donor CFs transfected with 15nM scramble (white bar), miR-27b-5p mimic (light grey) or inhibitor (dark grey) for 24h. **A)** Modulation of RNA levels of α -SMA **B)** Modulation of RNA levels of EGLN1. **C)** Modulation of RNA levels of HIF1 α . **D)** Modulation of RNA levels of HIF2 α . Values are represented as Mean \pm SEM, N = 1, n = 3. One-way Anova was applied followed by Tukey's Mean Comparison test was performed in order to estimate statistical significance *P-value<0.05, **p<0.01.

4.9 miRNA-27b-5p effect on the phenotype of cardiac fibroblasts from ICM patients.

Previously studied ICM CFs did not show any significant changes in miRNA-27b-5p levels in comparison to human donor CFs (Chapter I section 4.7).

However, we were interested in studying of miRNA-27b-5p functions and molecular mechanism in the pathological models accompanied by cardiac fibrosis. We investigated effect of miRNA-27b-5p gain and loss of functions on the phenotype of CFs from ICM patients. As in previous experiments (Sections 4.2; 4.4; 4.7), we observed a significant increase in the number (from 31.5% up to 50%) of α -SMA and vimentin positive cells in CFs transfected with miRNA-27b-5p mimics.

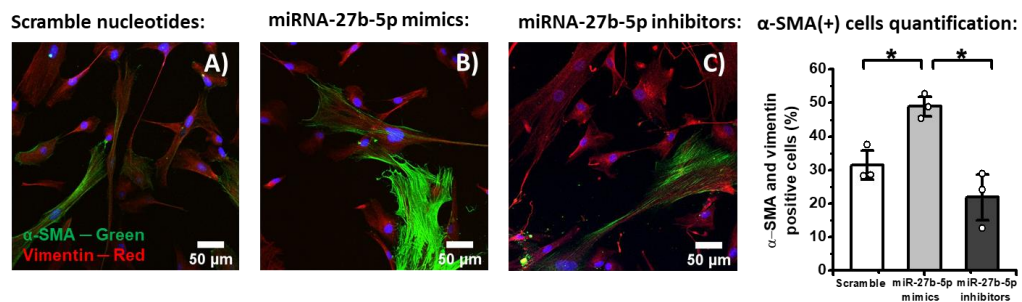


Figure 4.9 miRNA-27b-5p modulation regulates the number of α -SMA positive cells in ICM patients CFs. A)-C) panels show representative images of patients ICM CFs transfected with 15nM scramble, mimics or inhibitors of miRNA-27b-5p and stained after 24h with vimentin (PA1-16759, red) and α -SMA (M0851, green) and DAPI (blue). D) Bar charts of the percentage of α -SMA positive cells in patients ICM CFs transfected with 15nM scramble (white bar) miRNA mimics (light grey) or miRNA inhibitors (dark grey). Values are represented as Mean \pm SEM, N = 3, n = 2. One-way Anova was applied followed by Tukey's Mean Comparison test was performed in order to estimate statistical significance *P-value<0.05.

4.10 miRNA-27b-5p gain and loss of functions causing gene expression changes in myofibroblasts but not hypoxia associated markers in cardiac fibroblasts from ICM patients.

In this experiment we investigated effect of miRNA-27b-5p overexpression/inhibition on the genotype of CFs from ICM patients. We observed significant up-regulation of α -SMA expression ($-\Delta\Delta\text{CT} = 5.1$) in CFs from ICM patients transfected with miRNA-27b-5p mimics (Figure 4.10 A). These data are supported by our findings in the previous experiment where we demonstrated a significant increase in the number of myofibroblasts. However, we did not observe any significant correlations in ICM patients CFs in terms of

EGLN1 expression. It can be explained by a high biological variability which is present as standard error (Figure 4.10 B). Despite this limitation, it is possible that miRNA-27b-5p provokes pro-fibrotic response in ICM CFs through another mechanism. HIF2 α expression was increased significantly ($-\Delta\Delta\text{CT} = 1.32$) in CFs transfected with mimics but not HIF1 α .

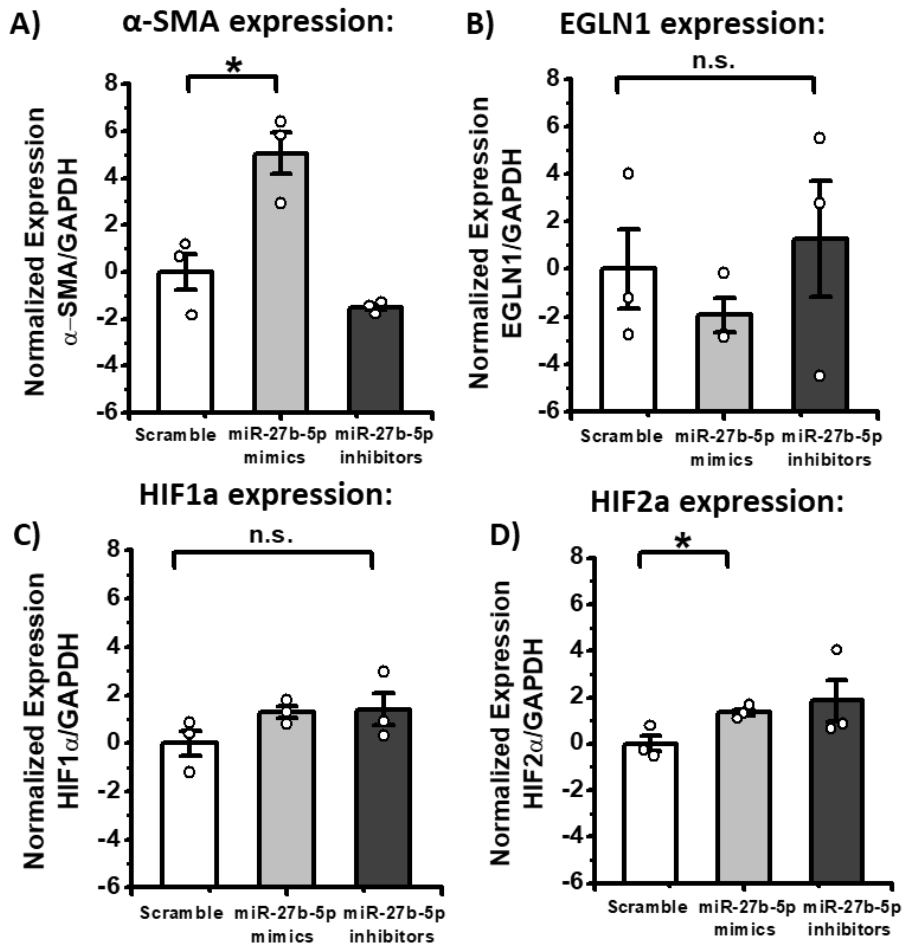


Figure 4.10 miRNA-27b-5p modulation regulates the expression of pro-fibrotic but not hypoxia related genes in cardiac fibroblasts from ICM patients. Modulation of RNA levels in CFs from ICM patients transfected with 15nM scramble (white bar), miR-27b-5p mimic (light grey) or inhibitor (dark grey) for 24h. **A)** Modulation of RNA levels of α -SMA **B)** Modulation of RNA levels of EGLN1. **C)** Modulation of RNA levels of HIF1 α . **D)** Modulation of RNA levels of HIF2 α . Values are represented as Mean \pm SEM, N = 3, n = 3. One-way Anova was applied followed by Tukey's Mean Comparison test was performed in order to estimate statistical significance *P-value<0.05, n.s. – non-significant.

4.11 miRNA-27b-5p effect on the phenotype of cardiac fibroblasts from DCM patients.

Previously studied DCM CFs as well as ICM CFs did not show any significant changes in miRNA-27b-5p levels in comparison to human donor CFs (Chapter I section 4.7). However, in section 4.9-4.10 we observed a pro-fibrotic role of miRNA-27b-5p in pathological ICM CFs. Therefore, we were aiming to test miRNA-27b-5p functional role in the pathological DCM CFs.

We investigated effect of miRNA-27b-5p gain and loss of functions on the phenotype of CFs from ICM patients. As in previous experiments (Sections 4.2; 4.4; 4.7; 4.9), we observed a significant increase in the number (from 22.7% up to 34.2%) of α -SMA and vimentin positive cells in CFs transfected with miRNA-27b-5p mimics.

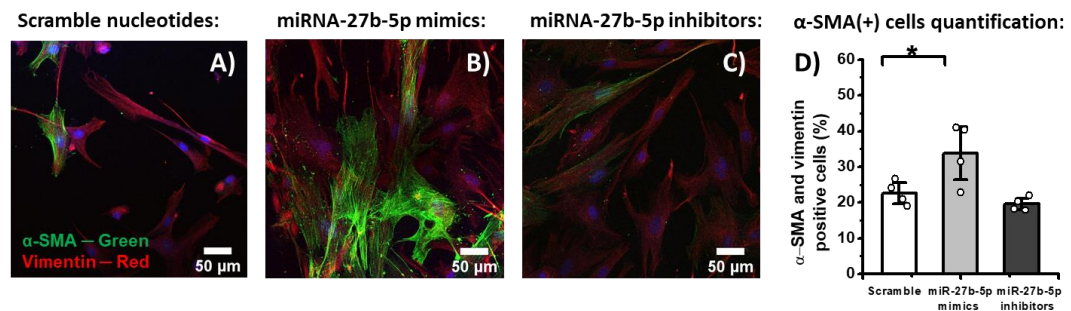


Figure 4.11 miRNA-27b-5p modulation regulates the number of α -SMA positive cells in DCM patients CFs. A)-C) panels show representative images of patients DCM CFs transfected with 15nM scramble, mimics or inhibitors of miRNA-27b-5p and stained after 24h with vimentin (PA1-16759, red) and α -SMA (M0851, green) and DAPI (blue). D) Bar charts of the percentage of α -SMA positive cells in patients DCM CFs transfected with 15nM scramble (white bar) miRNA mimics (light grey) or miRNA inhibitors (dark grey). Values are represented as Mean \pm SEM, N = 4, n = 2. One-way Anova was applied followed by Tukey's Mean Comparison test was performed in order to estimate statistical significance *P-value<0.05.

4.12 miRNA-27b-5p gain and loss of functions does not cause any changes in gene expression of myofibroblasts and hypoxia related markers in cardiac fibroblasts from DCM patients

In this experiment we investigated effect of miRNA-27b-5p overexpression/inhibition on the genotype of CFs from DCM patients. We did not observe any significant changes in gene expression associated with myofibroblasts and hypoxia (Figure 4.12). As we discussed previously in chapter I section 4.7, genetic factor can be a strong obstacle in gene expression interpretation data. Another limitation, was that we did not the exact location of the heart from which biopsy was collected. Overall, we demonstrated significant changes in DCM CFs phenotype but not on the genotypical level.

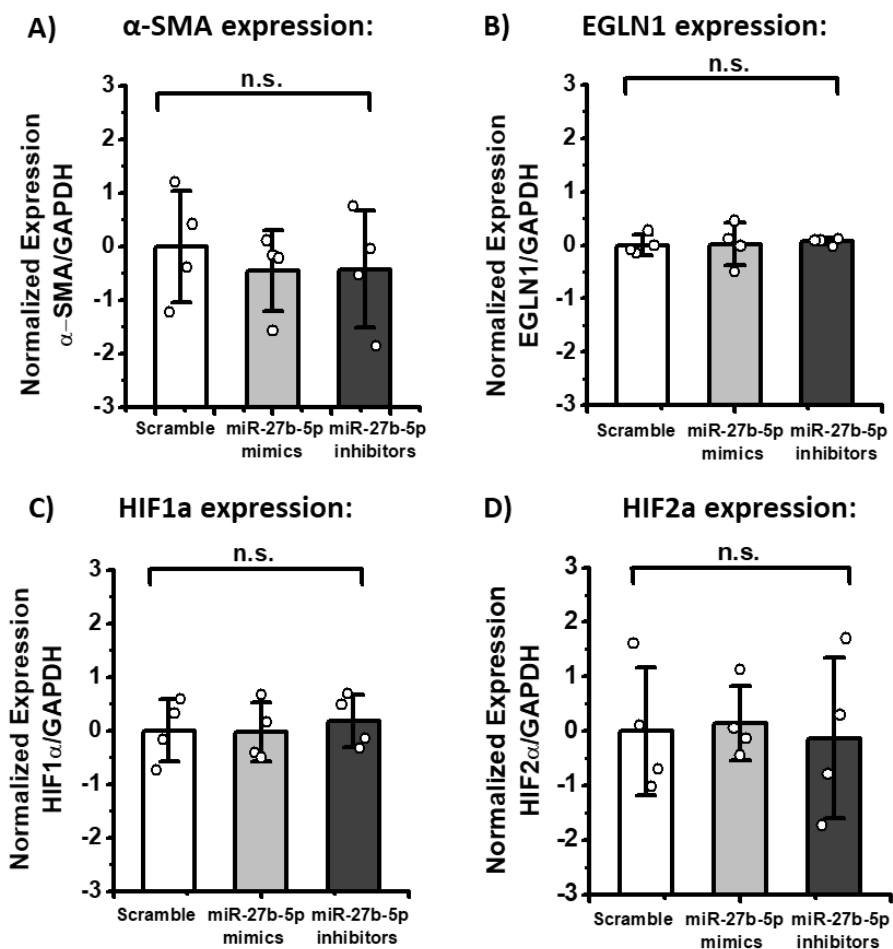


Figure 4.12 miRNA-27b-5p modulation does not regulate the expression of pro-fibrotic and hypoxia related genes in cardiac fibroblasts from DCM patients. Modulation of RNA levels in CFs from DCM patients transfected with 15nM scramble (white bar), miR-27b-5p mimic (light grey) or inhibitor (dark grey) for 24h. **A)** Modulation of RNA levels of α -SMA **B)** Modulation of RNA levels of EGLN1. **C)** Modulation of RNA levels of HIF1 α . **D)** Modulation of RNA levels of HIF2 α . Values are

represented as Mean \pm SEM, N = 4, n = 3. One-way Anova was applied followed by Tukey's Mean Comparison test was performed in order to estimate statistical significance
n.s. – non-significant.

5. DISCUSSION III

In this chapter we investigated functional role of miRNA-27b-5p in healthy and MI rat CFs. miRNA-497-5p functional role was studied only in healthy and MI rat CFs. After successful transfection of all *in vitro* models with miRNAs mimics and inhibitors (Figure 4.1 and Figure 4.6) we characterized cells with immunostaining against α -SMA and RT-qPCR on Colla1 and α -SMA.

Studies on miRNA-27b-5p role in healthy and MI rat CFs revealed its pro-fibrotic role (Figure 4.2-4.5). In both healthy and pathological cells miRNA-27b-5p gain of function was accompanied by increased number of myofibroblasts in cell culture (Figure 4.2 B, C, F, Figure 4.4 B, C, F). Beside, phenotypical changes we demonstrated miRNA-27b-5p effect on gene expression of healthy and pathological CFs. Overexpression of the miRNA leads to a significant increase in α -SMA expression and colla1 expression in healthy rat (Figure 4.3 A, C) and in MI rat CFs (Figure 4.5 A,C). Interestingly, that inhibitors of miRNA-27b-5p successfully transfected in rat CFs did not change neither gene expression of myofibroblasts markers neither the number of myofibroblasts. However, EGLN1 in healthy rat CFs was significantly up-regulated in cells with inhibited miRNA-27b-5p (Figure 4.3 E). This data was reproduced for inhibitors in MI rat CFs, while miRNA-27b-5p gain of functions suppresses EGLN1 expression (Figure 4.5 E). Therefore, we concluded that the mechanism of EGLN1 down-regulation by miRNA-27b-5p remains in both healthy and pathological rat CFs. Such mechanism make sense in resident CFs from MI: long ischemia leads to an activation of hypoxia signaling through hypoxia inducible transcription factors (HIFs) in all cell types [42]. In normoxia condition PHD2 (protein encoded by EGLN1) is marking HIFs for the ubiquitin-proteasome degradation pathway [43]. Consequently, down-regulation of EGLN1 will lead to accumulation of HIFs, which are causing expression of ECM proteins [44,45]. In chapter II section 3.1 we also demonstrated that IL-11 network of genes was enriched in genes associated with a response to hypoxia.

Investigation on miRNA-497-5p role in healthy rat CFs and pathological MI CFs also indicated its pro-fibrotic role. *In vitro* overexpression of miRNA-497-5p was leading to a significant increase in the number of myofibroblasts in healthy cells (Figure 4.2 D, E, G) and pathological cells (Figure 4.4 D, E, G). These changes were accompanied by increased expression of α -SMA (Figure 4.3 B) and *coll1a1* (Figure 4.3 D). Alternatively, loss of miRNA-497-5p functions leads to an attenuation of both markers expression (Figure 4.3 B, D). While miRNA gain of functions in MI CFs up-regulated gene expression of α -SMA and *coll1a1*, miRNA-497-5p loss of functions did not change gene expression of measured markers (Figure 4.5 B, D). Unfortunately, we did not have a validated target for miRNA-497-5p to measure it in described *in vitro* models. However, we can assume that pro-fibrotic role of miRNA is implemented through RECK [46] or Smad 7 [47] gene regulation.

We investigated miRNA-27b-5p/EGLN1/HIFs axis in donor CFs and CFs from patients with ICM and DCM. Our findings, indicate a pro-fibrotic role of miRNA-27b-5p in human donor CFs described by an increase of myofibroblasts in cell culture during miRNA overexpression (Figure 4.7 A-D). These morphological changes supported by a significant increase in α -SMA gene expression (Figure 4.8 A). In the same graph (Figure 4.8 B) we demonstrated significant down-modulation of EGLN1 by miRNA-27b-5p gain of functions. To our surprise, we also detected that miRNA overexpression is followed by a significant increase in HIF2 α expression (Figure 4.8 D) but not HIF1 α . In the work of Dai *et al.* [48] HIF2 α was proved to be a critical mediator of signaling related to cardiac hypertrophy and fibrosis. Its pharmacological inhibition attenuated fibrosis and hypertrophy.

Analysis of CFs from ICM patients revealed that miRNA-27b-5p keeps its pro-fibrotic functions in this pathology. Again, miRNA-27b-5p overexpression was leading to a significant increase in the number of myofibroblasts (Figure 4.9) and α -SMA expression (Figure 4.10 A). Inhibition of miRNA-27b-5p did not affect cells morphology and gene expression. In ICM model we were not able to demonstrate EGLN1 repression by miRNA-27b-5p during overexpression (Figure

4.10 B), due to the high biological variability. Unfortunately, we do not have information on the biopsy location from which CFs were grown. However, trends for EGLN1 gene regulation during miRNA-27b-5p overexpression/inhibition were correct. In addition, HIF2 α overexpression was detected in miRNA-27b-5p gain of functions group. We demonstrated similar results obtained in ICM patients and MI rats.

Study on miRNA-27b-5p gains and loss of functions in DCM CFs resulted in the unclear role of the studied miRNA. On the one hand, miRNA-27b-5p mimics were increasing the number of myofibroblasts *in vitro* (Figure 4.11). On the other hand, we did not observe any significant changes in gene expression of α -SMA and hypoxia related genes (Figure 4.12). It is likely, that miRNA-27b-5p in DCM model acts via different molecular mechanism. Worth to check molecular mechanisms are miRNA-27b-5p regulation through FBW7/Snail [49] or through gremlin 1 [50].

6. REFERENCES III

1. Asaria P, Elliott P, Douglass M, et al. Acute myocardial infarction hospital admissions and deaths in England: a national follow-back and follow-forward record-linkage study. *Lancet Public Health*. **2017**;2(4):e191-e201. doi:10.1016/S2468-2667(17)30032-4
2. Ojha N, Dhamoon AS. Myocardial Infarction. **2022** In: StatPearls [Internet]. Treasure Island (FL): StatPearls Publishing; 2022 Jan-.
3. Anand SS, Islam S, Rosengren A, et al. Risk factors for myocardial infarction in women and men: insights from the INTERHEART study. *Eur Heart J*. **2008**;29(7):932-940. doi:10.1093/eurheartj/ehn018
4. Kalogeris T, Baines CP, Krenz M, Korthuis RJ. Cell biology of ischemia/reperfusion injury. *Int Rev Cell Mol Biol*. **2012**;298:229-317. doi:10.1016/B978-0-12-394309-5.00006-7
5. Zhou L, Huang H, McElfresh TA, Prosdocimo DA, Stanley WC. Impact of anaerobic glycolysis and oxidative substrate selection on contractile function and mechanical efficiency during moderate severity ischemia. *Am J Physiol Heart Circ Physiol*. **2008**;295(3):H939-H945. doi:10.1152/ajpheart.00561.2008
6. Teringova E, Tousek P. Apoptosis in ischemic heart disease. *J Transl Med*. **2017**;15(1):87. Published 2017 May 1. doi:10.1186/s12967-017-1191-y
7. Frangogiannis NG, Smith CW, Entman ML. The inflammatory response in myocardial infarction. *Cardiovasc Res*. **2002**;53(1):31-47. doi:10.1016/s0008-6363(01)00434-5
8. Ong SB, Hernández-Reséndiz S, Crespo-Avilan GE, et al. Inflammation following acute myocardial infarction: Multiple players, dynamic roles, and novel therapeutic opportunities. *Pharmacol Ther*. **2018**;186:73-87. doi:10.1016/j.pharmthera.2018.01.001

9. Ferrini A, Stevens MM, Sattler S, Rosenthal N. Toward Regeneration of the Heart: Bioengineering Strategies for Immunomodulation. *Front Cardiovasc Med.* **2019**;6:26. Published 2019 Mar 21. doi:10.3389/fcvm.2019.00026
10. DeLeon-Pennell KY, Meschiari CA, Jung M, Lindsey ML. Matrix Metalloproteinases in Myocardial Infarction and Heart Failure. *Prog Mol Biol Transl Sci.* **2017**;147:75-100. doi:10.1016/bs.pmbts.2017.02.001
11. Tatti O, Vehviläinen P, Lehti K, Keski-Oja J. MT1-MMP releases latent TGF-beta1 from endothelial cell extracellular matrix via proteolytic processing of LTBP-1. *Exp Cell Res.* **2008**;314(13):2501-2514. doi:10.1016/j.yexcr.2008.05.018
12. Lipson KE, Wong C, Teng Y, Spong S. CTGF is a central mediator of tissue remodeling and fibrosis and its inhibition can reverse the process of fibrosis. *Fibrogenesis Tissue Repair.* **2012**;5(Suppl 1):S24. Published 2012 Jun 6. doi:10.1186/1755-1536-5-S1-S24
13. Lindsey ML. MMP induction and inhibition in myocardial infarction. *Heart Fail Rev.* **2004**;9(1):7-19. doi:10.1023/B:HREV.0000011390.44039.b7
14. Yue B. Biology of the extracellular matrix: an overview. *J Glaucoma.* **2014**;23(8 Suppl 1):S20-S23. doi:10.1097/IJG.0000000000000108
15. Brazile BL, Butler JR, Patnaik SS, et al. Biomechanical properties of acellular scar ECM during the acute to chronic stages of myocardial infarction. *J Mech Behav Biomed Mater.* **2021**;116:104342. doi:10.1016/j.jmbbm.2021.104342
16. Shinde AV, Humeres C, Frangogiannis NG. The role of α -smooth muscle actin in fibroblast-mediated matrix contraction and remodeling. *Biochim Biophys Acta Mol Basis Dis.* **2017**;1863(1):298-309. doi:10.1016/j.bbdis.2016.11.006
17. Porter KE, Turner NA. Cardiac fibroblasts: at the heart of myocardial remodeling. *Pharmacol Ther.* **2009**;123(2):255-278. doi:10.1016/j.pharmthera.2009.05.002

18. Gerber Y, Weston SA, Enriquez-Sarano M, et al. Mortality Associated With Heart Failure After Myocardial Infarction: A Contemporary Community Perspective. *Circ Heart Fail.* **2016**;9(1):e002460. doi:10.1161/CIRCHEARTFAILURE.115.002460
19. Harvey PA, Leinwand LA. The cell biology of disease: cellular mechanisms of cardiomyopathy. *J Cell Biol.* **2011**;194(3):355-365. doi:10.1083/jcb.201101100
20. Shiojima I, Sato K, Izumiya Y, et al. Disruption of coordinated cardiac hypertrophy and angiogenesis contributes to the transition to heart failure. *J Clin Invest.* **2005**;115(8):2108-2118. doi:10.1172/JCI24682
21. Sciarretta S, Paneni F, Palano F, et al. Role of the renin-angiotensin-aldosterone system and inflammatory processes in the development and progression of diastolic dysfunction. *Clin Sci (Lond).* **2009**;116(6):467-477. doi:10.1042/CS20080390
22. Schafer S, Viswanathan S, Widjaja AA, et al. IL-11 is a crucial determinant of cardiovascular fibrosis. *Nature.* **2017**;552(7683):110-115. doi:10.1038/nature24676
23. Mehta PK, Griendling KK. Angiotensin II cell signaling: physiological and pathological effects in the cardiovascular system. *Am J Physiol Cell Physiol.* **2007**;292(1):C82-C97. doi:10.1152/ajpcell.00287.2006
24. Deschamps AM, Spinale FG. Pathways of matrix metalloproteinase induction in heart failure: bioactive molecules and transcriptional regulation. *Cardiovasc Res.* **2006**;69(3):666-676. doi:10.1016/j.cardiores.2005.10.004
25. Eijgenraam TR, Silljé HHW, de Boer RA. Current understanding of fibrosis in genetic cardiomyopathies. *Trends Cardiovasc Med.* **2020**;30(6):353-361. doi:10.1016/j.tcm.2019.09.003
26. Mandawat A, Chattranukulchai P, Mandawat A, et al. Progression of Myocardial Fibrosis in Nonischemic DCM and Association With Mortality

- and Heart Failure Outcomes. *JACC Cardiovasc Imaging*. **2021**;14(7):1338-1350. doi:10.1016/j.jcmg.2020.11.006
27. Schultheiss HP, Fairweather D, Caforio ALP, et al. Dilated cardiomyopathy. *Nat Rev Dis Primers*. **2019**;5(1):32. Published 2019 May 9. doi:10.1038/s41572-019-0084-1
28. Taylor MR, Slavov D, Ku L, et al. Prevalence of desmin mutations in dilated cardiomyopathy. *Circulation*. **2007**;115(10):1244-1251. doi:10.1161/CIRCULATIONAHA.106.646778
29. Ujfalusi Z, Vera CD, Mijailovich SM, et al. Dilated cardiomyopathy myosin mutants have reduced force-generating capacity. *J Biol Chem*. **2018**;293(23):9017-9029. doi:10.1074/jbc.RA118.001938
30. Tesson F, Saj M, Uvaize MM, Nicolas H, Płoski R, Bilińska Z. Lamin A/C mutations in dilated cardiomyopathy. *Cardiol J*. **2014**;21(4):331-342. doi:10.5603/CJ.a2014.0037
31. Imanaka-Yoshida K. Inflammation in myocardial disease: From myocarditis to dilated cardiomyopathy. *Pathol Int*. **2020**;70(1):1-11. doi:10.1111/pin.12868
32. Schade van Westrum S, Dekker L, de Haan R, et al. Brain natriuretic peptide is not predictive of dilated cardiomyopathy in Becker and Duchenne muscular dystrophy patients and carriers. *BMC Neurol*. **2013**;13:88. Published 2013 Jul 16. doi:10.1186/1471-2377-13-88
33. Sullivan RD, Mehta RM, Tripathi R, Reed GL, Gladysheva IP. Renin Activity in Heart Failure with Reduced Systolic Function-New Insights. *Int J Mol Sci*. **2019**;20(13):3182. Published 2019 Jun 28. doi:10.3390/ijms20133182
34. 11 Levels Are Correlated with Cardiac Events in Patients with Chronic Heart Failure. *Mediators Inflamm*. **2019**;2019:1575410. Published 2019 Jan 8. doi:10.1155/2019/1575410
35. Noutsias M, Rohde M, Göldner K, et al. Expression of functional T-cell markers and T-cell receptor Vbeta repertoire in endomyocardial biopsies from

- patients presenting with acute myocarditis and dilated cardiomyopathy. *Eur J Heart Fail.* **2011**;13(6):611-618.
36. Wynn TA. Cellular and molecular mechanisms of fibrosis. *J Pathol.* **2008**;214(2):199-210. doi:10.1002/path.2277
37. Liu YH, Yang XP, Nass O, Sabbah HN, Peterson E, Carretero OA. Chronic heart failure induced by coronary artery ligation in Lewis inbred rats. *Am J Physiol.* **1997**;272(2 Pt 2):H722-7. doi: 10.1152/ajpheart.1997.272.2.H722. PMID: 9124430.
38. Watanabe M, Okada T. Langendorff Perfusion Method as an Ex Vivo Model to Evaluate Heart Function in Rats. *Methods Mol Biol.* **2018**;1816:107-116. doi: 10.1007/978-1-4939-8597-5_8. PMID: 29987814.
39. Brandenburger M, Wenzel J, Bogdan R, Richardt D, Nguemo F, Reppel M, Hescheler J, Terlau H, Dendorfer A. Organotypic slice culture from human adult ventricular myocardium. *Cardiovasc Res.* **2012**;93(1):50-9. doi: 10.1093/cvr/cvr259. Epub 2011 Oct 4. PMID: 21972180.
40. Schultz F, Hasan A, Alvarez-Laviada A, Miragoli M, Bhogal N, Wells S, Poulet C, Chambers J, Williamson C, Gorelik J. The protective effect of ursodeoxycholic acid in an in vitro model of the human fetal heart occurs via targeting cardiac fibroblasts. *Prog Biophys Mol Biol.* **2016**;120(1-3):149-63. doi: 10.1016/j.pbiomolbio.2016.01.003. Epub 2016 Jan 8. PMID: 26777584.
41. Fu X, Liu Q, Li C, Li Y, & Wang L. Cardiac Fibrosis and Cardiac Fibroblast Lineage-Tracing: *Recent Advances In Frontiers in Physiology*, **2020**; 11. <https://www.frontiersin.org/article/10.3389/fphys.2020.00416>
42. Wang JH, Zhao L, Pan X, et al. Hypoxia-stimulated cardiac fibroblast production of IL-6 promotes myocardial fibrosis via the TGF- β 1 signaling pathway [published correction appears in *Lab Invest.* 2016 Sep;96(9):1035]. *Lab Invest.* **2016**;96(8):839-852. doi:10.1038/labinvest.2016.65
43. Fong GH, Takeda K. Role and regulation of prolyl hydroxylase domain proteins. *Cell Death Differ.* **2008**;15(4):635-641. doi:10.1038/cdd.2008.10

44. Gilkes DM, Bajpai S, Chaturvedi P, Wirtz D, Semenza GL. Hypoxia-inducible factor 1 (HIF-1) promotes extracellular matrix remodeling under hypoxic conditions by inducing P4HA1, P4HA2, and PLOD2 expression in fibroblasts. *J Biol Chem.* **2013**;288(15):10819-10829. doi:10.1074/jbc.M112.442939
45. Xiong A, Liu Y. Targeting Hypoxia Inducible Factors-1 α As a Novel Therapy in Fibrosis. *Front Pharmacol.* **2017**;8:326. Published 2017 May 30. doi:10.3389/fphar.2017.00326
46. Chen X, Shi C, Wang C, et al. The role of miR-497-5p in myofibroblast differentiation of LR-MSCs and pulmonary fibrogenesis. *Sci Rep.* **2017**;7:40958. Published 2017 Jan 18. doi:10.1038/srep40958
47. Li Z, Wang P, Zhang J, Zhao D. MicroRNA-497-5p downregulation inhibits cell viability, reduces extracellular matrix deposition and induces apoptosis in human hyperplastic scar fibroblasts by regulating Smad7. *Exp Ther Med.* **2021**;21(4):384. doi:10.3892/etm.2021.9815
48. Dai Z, Cheng J, Liu B, et al. Loss of Endothelial Hypoxia Inducible Factor-Prolyl Hydroxylase 2 Induces Cardiac Hypertrophy and Fibrosis. *J Am Heart Assoc.* **2021**;10(22):e022077. doi:10.1161/JAHA.121.022077
49. Fu Q, Lu Z, Fu X, Ma S, Lu X. MicroRNA 27b promotes cardiac fibrosis by targeting the FBW7/Snail pathway. *Aging (Albany NY).* **2019**;11(24):11865-11879. doi:10.18632/aging.102465
50. Graham JR, Williams CM, Yang Z. MicroRNA-27b targets gremlin 1 to modulate fibrotic responses in pulmonary cells. *J Cell Biochem.* **2014**;115(9):1539-1548. doi:10.1002/jcb.24809

CHAPTER IV

1. INTRODUCTION IV

1.1 Aortic valve: biomechanics, functions and composition

AV in heart lets blood flow unidirectionally when pressure in LV is bigger than blood pressure in aorta during systole. Conversely, at diastole, when LV blood pressure drops behind the aortic pressure, AV is closed. The major goal of AV, which is consisted of three leaflets, is to prevent blood flow back to LV in order to prevent its volume overload during diastole [1]. At that time, 1 mm AV leaflets withstand pressure equals to 80 mmHg [2]. It has a unique biomechanical structure that is specially designed to work under mechanical exhaustion. Valve which consist from various ECM proteins perform its functions about 3×10^9 times over life span [3]. In order to bear with such crucial conditions leaflet consists mainly from collagens: collagen type I (74 %), type II (24%), type V (2%), which form first layer of AV – fibrosa [3]. Collagen fibers are oriented circumferentially and perform supportive, protective and scaffolding function. On the other side of a collagen coat, LV oriented elastin enriched layer helps the valve to close rapidly. This layer is called ventricularis. Middle layer, which is called spongiosa, acts as amortization system. It extinguishes and scatters mechanical force with by its structure, which is full of proteoglycans and glycosamino-(GAG)-elements [4].

The functionality of AV decreases with age. However, there are also other risk factors, such as: congenital heart disease, diabetes and chronic kidney disease [5]. Due to the age and constant mechanical fatigue stiffness of AV is growing and is correlating with a ECM contain, basically collagens [6]. Changes in ECM composition leads to unequal force distribution all other AV. Valve cells which are sensitive to mechanical perturbations, VICs, go through myofibroblasts transdifferentiation [7]. Therefore, this process leads to an increased expression of α -SMA and disorganized collagens. For this reason, stiffness and thickness of AV is growing. Moreover, stress fibers of α -SMA and collagens can contract, what brings tension and alterations in the normal work of AV [8]. Interestingly, that VICs located in the left side of AV have an increased stiffness if we compare

them with VICs residing in the right-sided AV [9]. VECs, VICs and myofibroblasts are considered to be main resident cell types in AV [10] (Figure 1). Unlike VECs, VICs are resident within all three layers in subpopulations. They act as a main source of ECM proteins, which are crucial for scaffold, elasticity and ability to maintain the valve functional under high pressures [11]. The last dominant cell type in AV is myofibroblasts, which usually constitute 5% of VICs population. Nevertheless, in the pathological condition of AVS their population grows up to 30% [12,13]. Such a dramatic change leads to loss of AV integrity. Myofibroblasts influence immune cell chemotaxis, migration, retention, and apoptosis, thereby acting as key effector cells in the persistence of inflammation [14]. Increased population of myofibroblasts results in ECM remodeling, intensive collagen and α -SMA fibers accumulation. Moreover, myofibroblasts produce MMPs which disrupt important and organized ECM. In parallel, ECM embedded growth factors and cytokines are released in extracellular space, where they can promote further transdifferentiation and EMT [14].

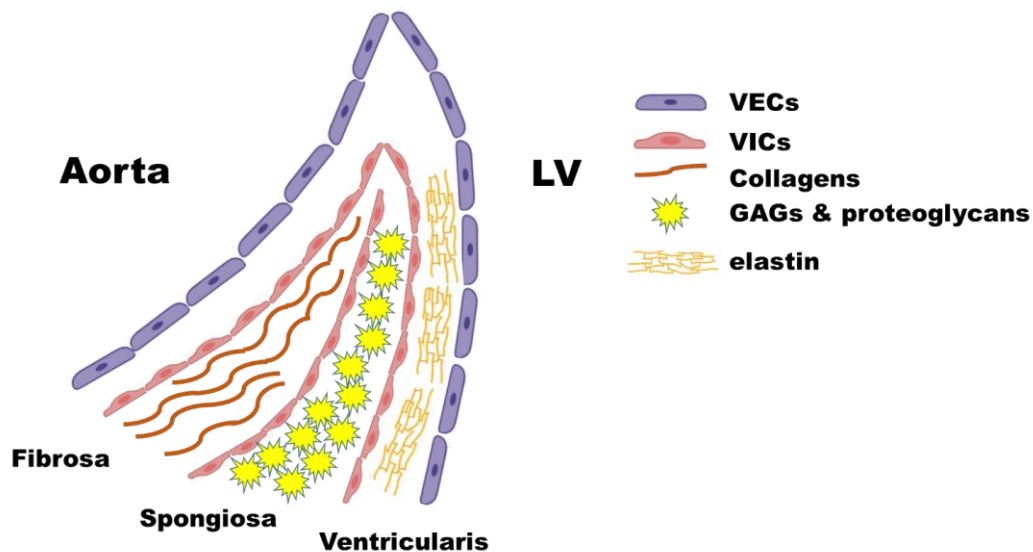


Figure 1.1 AV architecture: cellular compartment

1.2 Aortic valve stenosis

AVS is the most frequent heart valve disease in the western world [15,16]. More than 2% of patients above 60 years are suffering from its conditions. Unfortunately, statistics is that 2-year mortality rates of severe AVS equals 50%

[15]. As we already mentioned, this pathology is connected with loss of AV structural integrity, what leads to reverse blood flow during diastole. That leads to LV overload, hypertrophy, remodeling and consequent HF.

Typical symptoms which evidence irreversible pathological changes in AV are classic symptoms of HF and dyspnea. Physical finding that can be used for diagnosis is usually a harsh, crescendo-decrescendo systolic murmur that is loudest over the second right intercostal space and radiates to the carotid arteries. This may be accompanied by a slow and delayed carotid upstroke, a sustained apical impulse, and an absent or diminished aortic second sound [17].

Interestingly, that AVS has sex differences. Currently, it is known that at the same severity of AVS men have more extreme LV remodeling with larger indexed volumes, mass, mass/volume, lower ejection fraction, and more focal fibrosis. At the same time, women have concentric remodeling with higher ejection fraction and wall thickness. Moreover, processes of fibrosis are predominant in females AV, while males have more calcification processes in AV [18].

What is about prognosis of patients with severe AVS? In the recent work of Yukihiro *et al.* 2021 [19] it was demonstrated that 30-day mortality increases in elderly patients (N = 143, ≥ 85 years old) in comparison to younger patients (N = 290, < 85 years old) (3.5% vs 0.7%, $p=0.042$). Nevertheless, mortality is not dramatic when patients received aortic valve replacement (AVR) or transcatheter aortic valve replacement (TAVR) on time [20]. However, asymptomatic patients survival rates through 5 years time drops dramatically (from 74% in patients who received their AVR on time to 39% in patients who did not have AVR) [21]. For this reason, development of diagnostic tools is extremely important.

1.3 Current diagnostic tools used for aortic valve stenosis detection

Cardiac imaging

Cardiac imaging is considered to be a main direction for the diagnosis of AVS. However, it requires sufficient reproducibility and robustness to detect small changes in disease severity with high accuracy [22]. In the work of Doris *et al.* current heart imaging techniques with their benefits and drawback are summarized in Figure 1.3 [22]. From all techniques, echocardiography and

cardiac magnetic resonance (CMR) are widely used. With echocardiography main clinical parameters which are changing during AVS progression (peak velocity, mean gradient, and aortic valve area) can be identified. Also echocardiography can provide LV mass and ejection fraction what is crucial in identification of HF [24-25]. However, these measurements display considerable variability, potentially leading to inaccuracies when estimating disease progression [25]. On the other hand, (CMR) is able to provide precise information on the remodeling and hypertrophy occurring during the disease progression [26]. Unfortunately, CMR is an expensive procedure which is not always. For this reason, search on biomarkers which are describing AVS progression remains an important issue.

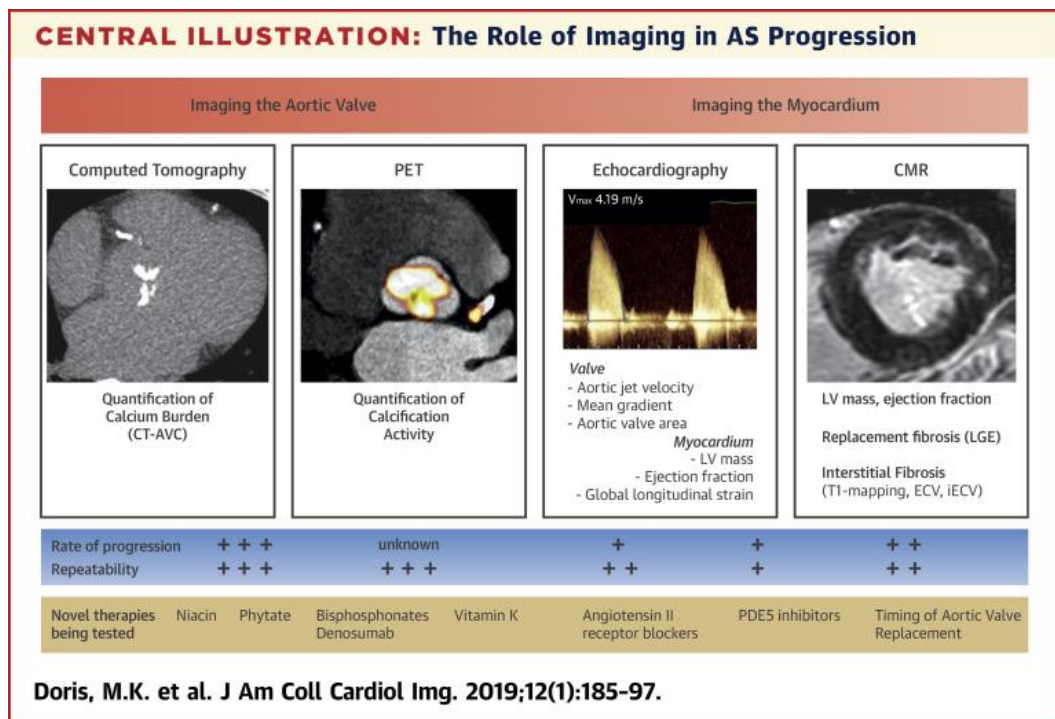


Figure 1.3 The role of imaging techniques in administration of aortic stenosis progression

BNP as a biomarker in AVS patients

Currently, in asymptomatic severe AVS, baseline B-type natriuretic peptide (BNP) levels are predictive of an abnormal blood pressure response to exercise, earlier symptom onset, and increased risk of re-hospitalization due to HF, need for AVR, and mortality [27,28]. Despite the fact, that BNP is the only biomarker that

is acknowledged by current guidelines to have an established prognostic value [29] its release mechanism is incompletely understood.

LV remodeling biomarkers in AVS patients

Maladaptive response of the LV in AVS characterized with increased numbers of myofibroblasts, extensive ECM proteins production and collagens deposition. Biomarkers, responsible for triggering molecular mechanisms underlie fibroblasts to myofibroblasts transdifferentiation, like TGF β 1 [30], matrix metalloproteinases (MMPs), and tissue inhibitors of MMPs (TIMP) [31] correlated with ECM remodeling.

miRNAs as a promising class of biomarkers in AVS patients

By the ability to regulate gene expression through mRNA cleavage or through translational repression miRNAs function as regulators of cellular processes [32]. Circulating miRNA may be involved in critical biological processes underlying cardiovascular disorders and are currently being investigated as biomarkers in cardiovascular disease [33]. For example, miRNA-133a was shown to be a potential biomarker of LV hypertrophy regression [34]. miRNA-21-5p was reported to be a potential biomarkers of LV fibrosis [35] in AVS patients.

Extracellular vesicles as biomarkers in AVS patients

The adult human heart is made up of billions of cells, approximately a third of these (by number) are cardiomyocytes whilst the remaining 60-70% are endothelial cells, fibroblasts, neural cells and other vascular cell types [36]. The orchestrated function of different cardiac cell populations and patrolling immune cell subsets provide a complex network of intercellular circuits of communication, which are essential to cardiac homeostasis and repair [37,38]. In this context, extracellular vesicle (EVs) play fundamental roles. The term EVs denotes a highly diverse family of membrane vesicles of different biogenesis and sizes: apoptotic bodies (500 nm -2 μ m in diameter), microvesicles (100 nm–1 μ m) and exosomes (circa 30–150 nm) [39]. EVs can transfer proteins, lipids, non-codingRNAs (miRNAs, lncRNAs, circRNAs) from cell to cell [40]. Recently, in the work of

Wang *et al.* (2018) demonstrated that reduced expression of miRNA-425 and miRNA-744 in the peripheral blood plasma EVs was correlating with overexpression of collagen 1 and α -SMA in HF patients [41].

Clinically relevant, we were thinking that IL-11 induced miRNAs can be regulated in patients with AVS and preserved ejection fraction characterized by extensive ECM remodeling. Since IL-11 was shown to be regulated mice models of arterial pressure loading [42].

2. AIMS OF THE STUDY IV

Aims of chapter IV:

We aimed at studying the potential of utilizing miRNA-27b-5p and miRNA-497-5p as circulating biomarkers of cardiac fibrosis in AVS patients with preserved ejection fraction. For this we wanted to achieve several aims:

- 1). Characterize clinical parameters of patients from aortic valve stenosis and control group.**
- 2). Characterize left ventricle remodeling in aortic valve stenosis patients.**
- 3). Measure miRNA-27b-5p, miRNA-497-5p and EGLN1 expression in left ventricle of aortic valve stenosis patients.**
- 4). Measure miRNA-27b-5p and miRNA-497-5p levels in peripheral blood plasma of aortic valve stenosis patients.**
- 5). Characterize extracellular vesicles from peripheral blood of aortic valve stenosis patients and measure miRNA-27b-5p and miRNA-497-5p expression in extracellular vesicles.**
- 6). Plot receiver operating characteristics curves for miRNA-27b-5p and miRNA-497-5p expression in peripheral blood of aortic valve stenosis patients.**
- 7). Study correlations of miRNA-27b-5p and miRNA-497-5p expression with left ventricle remodeling and other clinical parameters.**

3. METHODS IV

3.1 Patient populations

Table 3.1.1 summarizes the characteristics of volunteers contributing to this study: 1) patients with severe high gradient aortic valve stenosis (AVS) undergoing elective surgical aortic valve replacement (AVR) (n=30) (who donated blood and heart tissues); 2) healthy volunteers (n = 10) who donated blood (controls). Moreover, control healthy tissue samples were obtained from unused transplantation donor hearts (n=25). The AVS were prospectively recruited (2018 to 2021) at the Policlinico G.B. Rossi, Verona (n=30). The patients selected for the present study had symptomatic severe, high-gradient aortic stenosis confirmed on echocardiogram mean gradient ≥ 40 mmHg, peak velocity ≥ 4.0 m/s and valve area ≤ 1.0 cm² (or ≤ 0.6 cm²/m²), trileaflet aortic valve and preserved left ventricular ejection fraction (LVEF) ≥ 50 %. Exclusion criteria were: (1) bicuspid anatomy, (2) low flow-low gradient aortic stenosis (3) history of coronary artery disease or significant coronary artery disease with indication to surgical revascularization concomitant to AVR, (4) impaired left ventricular function, (5) history of arrhythmia. Patients with significantly hypertrophic septum underwent concomitant septal myectomy. Blood plasma and left ventricle (LV) samples (frozen, formalin fixed) were collected when it was not threatening patient's health. Detailed characteristics and comorbidities of the AVS patients are presented in Table 3.1.2. Control blood donors were recruited at IRCCS Policlinico San Donato, Milan Donor hearts were provided by the Department of Heart Failure and Transplantology, Cardinal Stefan Wyszyński Institute of Cardiology, Warszawa, Poland. The human studies and use of human samples complied the principles outlined in the Helsinki Declaration and to the Italian and Polish laws and guidelines, and was authorized by local Ethics Committee (from Italy: protocol #2438, 27/01/2009 and CE#85/int/2016 9/6/2016; from Poland protocol # IK-NPIA-0021-14/1426/18).

Table 3.1.1 Patients Baseline Characteristics

Patient Characteristic	Severe Aortic Valve Stenosis (SAVS)	Healthy Donors (Control)	p-value (Mann-Whitney test)
n	30	35	
Age (y)	72.2 ± 1.5	48.1 ± 3.2	<0.0001
Sex (M/F)	15/15	23/12	0.22
BMI	28.4 ± 0.9		
Hypertension n, (%)	23, (76.7%)	6, (17.1%)	<0.0001
Dyslipidaemia n, (%)	14, (46.7%)	3, (8.6%)	0.0006
Smoking history n, (%)	4, (13.3%)	2, (5.7%)	0.22
Diabetes n, (%)	10, (30.0%)	3, (8.6%)	0.05
Creatinine levels (mmol/L)	81.9 ± 4.2	105.7 ± 19.6	0.82
Coronary artery disease n, (%)	1, (3.3%)	0, (0%)	>0.99
History of arrhythmia n, (%)	0, (0%)	0, (0%)	>0.99
LVEF (%)	57.6 ± 1.9	57.7 ± 0.9	0.46

Table 3.1.2 AVS Patients characteristics

Patient Characteristic	Aortic Valve Stenosis (AVS)
Aortic Valve MG (mmHg)	52.9 ± 3.2
Aortic Valve PG (mmHg)	87.7 ± 6.5
Aortic Area (cm ²)	0.73 ± 0.04
IVS (mm)	14.3 ± 0.5
EDVi (ml/m ²)	54.5 ± 4.9

3.2 Histology and morphometric analysis

Formalin-fixed paraffin-embedded sections of 18 AVS samples and 10 donors samples from patients died of non-cardiovascular disease reasons were dewaxed, hydrated through graded decrease alcohol series and stained for histological analysis.

For the quantification of ECM deposition, sections were stained with Picro Sirius Red stain Kit, according to manufacturer's protocol. Images were collected by a Zeiss AxioLab-A1 microscopy (Zeiss, Oberkochen, Germany) equipped with a True Chrome HD II S camera (Tiesse Lab, Cassano d'Adda (MI), Italy) in the brightfield with 2.5x objective at a resolution equals to 3264x1836 pixels. The quantification of the areas of ECM deposition in the whole sections was performed with Fiji ImageJ software.

For immunofluorescence staining of LV biopsies from patients, the following antibodies were used: anti-collagen 1 (ab34710 Abcam Cambridge, UK) and anti-alpha sarcomeric actin clone 5C5 (#2172, Sigma-Aldrich, Merck Darmstadt, Germany). Images were taken by a DeltaVision Ultra high resolution microscope. The analysis of collagen I positive areas (expressed as percentage of the total area of the section) was carried out by Fiji ImageJ software. For the quantification of Collagen I area in LV biopsies of patients, images were obtained using high-resolution microscope DeltaVision Ultra (Cytiva, a Danaher Corporation Life Sciences company) with a 20X/0.75 objective by automatic stitching and a z-stack step of 2.5 μm . Images were acquired and analyzed by DeltaVision Ultra advanced software.

3.3 miRNA isolation from patient's blood plasma with Nucleospin^R miRNA Plasma kit

Blood plasma (BP) from patients was stored -80°C . In the day of isolation BP was thawed on ice. RNA isolation was performed by using Nucleospin^R miRNA. Wash buffers and rDNase were prepared according to manufacturer's protocol. 300 μl of blood plasma or EVs from blood plasma was transferred to a new 2 ml tube. Then, it was centrifuged at 4°C for 10 minutes at 300 x g. Following this step, blood plasma was centrifuged again at 16 000 x g for 5 minutes at 4°C in order to remove residual cells, cell debris, and particulate matter. Remaining supernatant was mixed with 90 μl MLP Buffer (Table 3.3) and 5 μl of cel-miR-39 spike in (5 fmol/ μl) (Thermofisher). Mixture was vortexed for 5 seconds and left for 3 minutes incubation at room temperature. When lysis completed we move to protein precipitation. By addition of 30 μl of MPP Buffer (Protein Precipitation Buffer, Table 3.3) we were aiming to remove proteins from our preparations. Mixture was vortexed for 5 seconds and incubated 1 minute at RT. After that, we centrifuged solution for 3 minutes at 11 000 x g to pellet the protein. Clear supernatant was transferred to a new tube where it was immediately mixed with 400 μl of isopropanol.

As a next step, we used NucleoSpin[®] miRNA Column to bind nucleic acids to silica membrane. Column was placed into 2ml Collection Tube and sample was

applied on the column. We incubated mixture for 2 minutes at RT. Then, it was centrifuged for 30 seconds at 11 000 x g at RT. Flow-through was discarded.

After that, DNA digestion step was performed. 700 µl of Buffer MW2 (Table 3.3) was applied to the column with following centrifugation at 11 000 x g for 30 seconds at room temperature. Flow-through was discarded. Then, 250 µl of Buffer MW2 was added to the column. It was centrifuged at 11 000 x g for 2 minutes at RT. At the end of this step, we applied 50 µl of rDNase directly to silica membrane of the column. Lid was closed and column was left to incubate 15 minutes at RT.

When incubation was finished, 100 µl of Buffer MW1 was added to NucleoSpin® miRNA Column. Membrane was washed by centrifugation at 11 000 x g for 30 seconds at RT. Flow-through was discarded. Second wash was done by addition of 700 µl Buffer MW2 and following centrifugation at the same conditions. Flow-through was discarded. Finally, membrane was dried by application of 250 µl of MW2 buffer to the column and centrifugation at 11 000 x g for 2 min at RT.

NucleoSpin® miRNA Column was placed to a 1.5 ml tube. 30 µl of RNase free water was applied to silica membrane. After 1 min of incubation at RT RNA was eluted by centrifugation at 11 000 x g for 1 min at RT.

RNA was immediately used for cDNA preparation or was stored at -80 °C for future applications. Added cel-miR-39 was measured with RT-qPCR and used for data normalization and estimation of quality of isolation.

Table 3.3 Products/reagents used during miRNA isolation from blood plasma with NucleospinR miRNA Plasma kit

Product/reagent name	Description	Volume (µl)
MLP Buffer	Lysis buffer	90
MPP Buffer	Protein Precipitation Buffer	30
cel-miR-39	spike-in	5
Isopropanol	RNA/DNA precipitation and binding to silica membrane	400

NucleoSpin® miRNA Column	silica membrane column for rna isolation	
MW1 Buffer	Washing Buffer 1	100
MW2 Buffer	Washing Buffer 2	700/250
rDNase	DNA digestion	50

3.4 Extracellular vesicles isolation from patient's blood plasma with Exo-spin blood kit

Blood plasma was thawed on ice one hour before isolation. For this research we used blood plasma from 24 AVS patients and 10 Control patients. 1 sample from AVS patient was excluded since EVs isolation for this sample constantly fails. 300 µl of blood plasma centrifuged at 300 x g for 10 minutes at 4 °C in order to remove any remaining cells. Samples were next centrifuged at 16 000 x g for 30 minutes at 4 °C in order to remove cell debris. Remaining supernatant was transferred to new tubes and was mixed with Exo-Spin Buffer in a 1:2 ratios. The mixture was inverted several times and left overnight at 4 °C. Next the mixture was centrifuged at 16 000 x g for 1 hour at 4 °C. At the end of centrifugation, a beige extracellular vesicles containing pellet can be observed at the bottom of a tube. The supernatant was carefully removed and the pellet was resuspended in 100 µl of PBS. The 100 µl of unpurified EVs were applied to the column and incubated for 5 minutes at room temperature. The column was centrifuged again at 50x g for 60 seconds. 300 µl PBS was immediately added to the column and incubated for 5 minutes and then centrifuged at the same speed for 60 seconds. EVs were stored at -80 °C, before TEM or RNA isolation.

3.5 Transmission electron microscopy for validation of extracellular vesicles preparation

EVs preparations validated by using transmission electron microscopy (TEM) with 2% uranyl acetate staining (transmission electron microscope TALOS L120C ThermoScientific at 120 kv).

3.6 RNA isolation and reverse transcription polymerase chain reaction in left ventricle biopsies

RNA isolation from LV (N = 30; 15/15 AVS patients vs Control group) biopsies was performed by Trizol (ThermoFisher Scientific) following the manufacturer's protocol. GoScript Reverse Transcriptase (Promega) was used to generate cDNA. Genes analyzed in this study are indicated in table 3.6.

Gene expression was detected by StepOnePlus™ Real-Time PCR System with by mixing prepared cDNA with the Universal SYBR Green Supermix (dilution factor 1:20). Forward and reverse primers were pre-mixed together and diluted 1:20.

Reaction was performed in two stages: hold stage at 95 °C for 10 minutes and PCR stage (95 °C for 15 seconds; 60 °C for 1 minute). Data was analyzed with $-\Delta\Delta C_t$ method [43]. Gene of interest expression was normalized to the expression of endogenous housekeeper gene (UBC). After that, $-\Delta C_t$ for control group was calculated as average and all samples were normalized to this $-\Delta C_t$, what gives us a $-\Delta\Delta C_t$ for each sample.

Table 3.6 List of primers

Gene name	Species	Forward primer sequence 5'->3'	Reverse primer sequence 5'->3'
CTGF	human	GTTTGGCCCGACCCAACTA	GGCTCTGCTTCTAGCCTG
EGLN1	human	GGCAAAGCCAGTTTGCTGAC	TTAGCTCGTGCTCTCATCTGC
UBC	rat, human	GATGGCTGTGATCGTCACTTGACAA	AGTCAGACAGGGTGCGCCCA

3.7 Reverse transcription polymerase chain reaction on miRNAs

MicroRNAs and U6 small nuclear RNA (Table 3.7) were polyadenylated and converted into cDNA by using TaqMan™ MicroRNA Reverse Transcription (RT) kit (Thermo Fisher Scientific). Briefly, 3.4 ng of total RNA was mixed with 1.06 µl of Nuclease-free water, 0.5 µl of 10X RT Buffer, 0.05 µl of dNTP mix w/dTTP (100M Total), 0.06 µl of RNase inhibitor (20U/µL), and 0.33 µl of MultiScribe™ RT enzyme (50U/µL). Finally, 3 µl of RT primer was added, in a total volume of 15 µl. Reverse transcription was then performed on a Thermal Cycler according to the manufacturer's instruction. and expression of miRNAs and U6 was then quantified by using StepOnePlus™ Real-Time PCR System and

TaqMan™ Fast Universal PCR Master Mix (2X) kit. The reaction was performed in the final volume of 20 µl, containing 4 µl of cDNA, 15 µl TaqMan™ PCR master mix, and 1 µl of TaqMan primers.

Data was analyzed by the $-\Delta\Delta C_t$ method [43], and gene expression was normalized to the expression of endogenous housekeeper gene (UBC for gene expression and U6 or cel-miR-39 for miRNA expression).

Table 3.7 Analyzed miRNAs

miRNA	Species	Assay ID
hsa-miRNA-27b-5p	mouse, human	002174
hsa-miRNA-497-5p	human	001043
U6	mouse, rat, human	001973
cel-miR-39-5p		000200

3.8 Statistics

Statistical analysis was performed with Origin 8 Pro. The tests performed were indicated in the figure legends. Normal distribution of the data was checked with Shapiro-Wilk test. For two groups comparison Student's t-test was applied. Correlations with miRNA-27b-5p, miRNA-497-5p and EGLN1 expression levels were quantified with Pearson's correlation test. Receiver operative characteristics (ROC) curves were used to assess the diagnostic accuracy of miRNAs in distinguish healthy donors of BP and AVS patients. N= number of patients, n= number of technical repeats. Data were presented as Mean \pm SEM. P values <0.05 were considered statistically significant.

4. RESULTS IV

4.1 Patients baseline characteristics

AVS and control groups and their baseline clinical characteristics are summarized in table 3.1.1. Aortic stenosis patients were significantly older compared to the control group (72.2 ± 1.5 years vs 48.1 ± 3.2 years, $p < 0.0001$). Both control and aortic stenosis group have mixed sex and males to female ratio was not significantly different. Hypertension and dyslipidaemia were significantly more present in the aortic stenosis group (76.7% vs 17.1%, $p\text{-value} < 0.0001$ and 46.7% vs 8.6%, $p\text{-value} 0.0006$). There was no difference in number of patients with smoking history: aortic stenosis group has (13.3%) and control group has (5.7%). Patients with aortic stenosis has (30%) of diabetic patients while control group has (8.6%), $p\text{-value}$ equals 0.05. There was no significant difference in the creatinine levels between the two group. As it was discussed in methods section, patients were included in the study if they have no previous coronary artery diseases or arrhythmias. Only one patient in the AVS group had a moderate coronary disease and the surgeon decided to proceed to surgical revascularization. No difference was observed in the LV function in both groups. The existing differences in patients age, presence of hypertension and dyslipidaemia, were considered them for further normalization.

Severe aortic valve mean gradient (MG 57.6 ± 1.9 mmHg) and peak gradient (87.7 ± 6.5 mmHg), Area (0.73 ± 0.04 cm²) with IVS (14.3 ± 0.5 mm) and end diastolic volume index (54.5 ± 4.9 ml/m²) (Table 3.1.2). Parameters were measured by the echocardiography only for aortic stenosis group. EDVi which is slightly below the normal range (58 ml/m²). Following this, we found that IVS was also slightly enlarged in these patients in comparison to normal meaning (11.2 mm).

4.2 Left ventricle biopsies were characterized with increased collagens area and CTGF expression

The LV samples which underwent histological analysis were collected from patients undergoing concomitant septal myectomy during surgical AVR (N = 18). In these samples there was extensive replacement and interstitial fibrosis when compared to control group (N = 10) (Figure 4.2 A). Quantification of collagen area (Figure 4.2 B) demonstrated increase of ECM area in AVS patients. This data was supported by immunostaining against Collagen I (the main Collagen type in the ECM) (Figure 4.2 C). Quantification on Collagen I area in analyzed biopsies revealed a significant increase in AVS patients (Figure 4.2 D). In addition, we measured CTGF expression in (N = 15) snap frozen LV biopsies and (N = 15) control group patients. CTGF is a matricellular protein which is actively produced in injured cardiomyocytes and cardiac fibroblasts [30]. We demonstrated significant up-regulation of CTGF expression in LV of AVS patients (Figure 4.2 E).

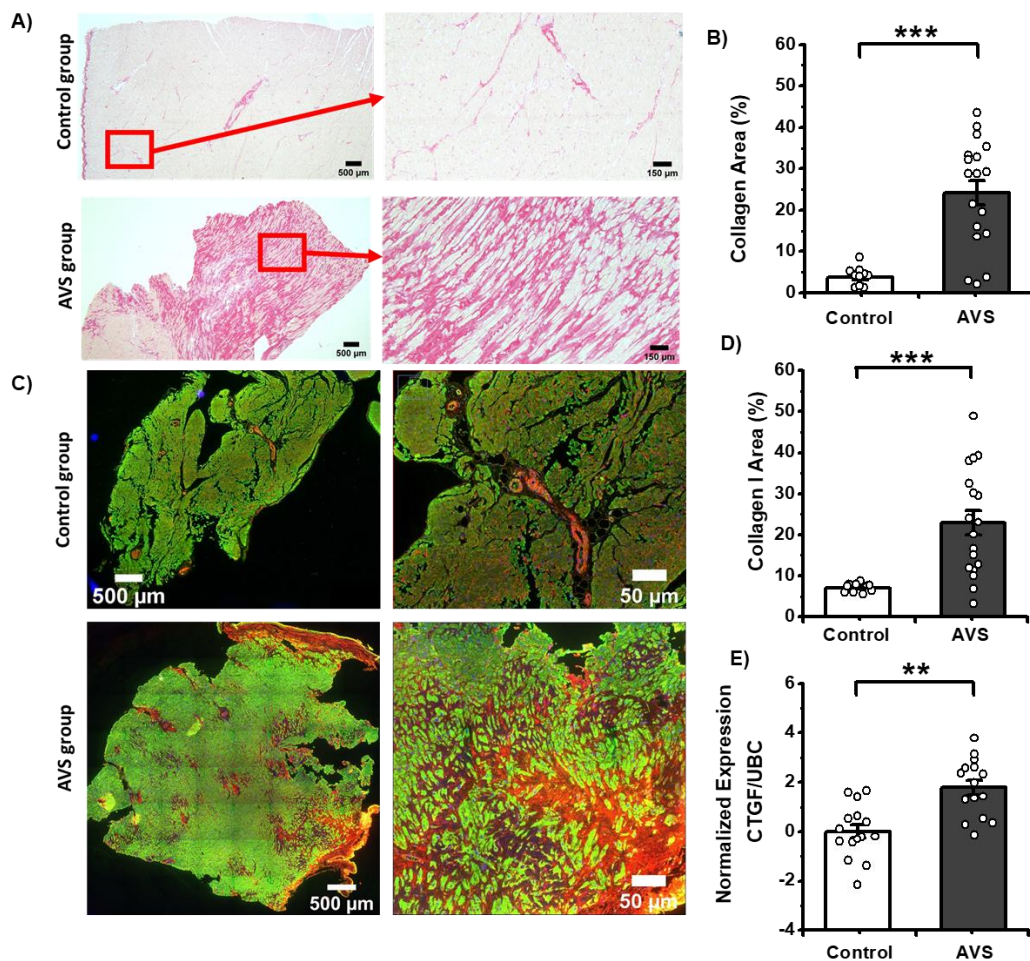


Figure 4.2 Characterization of extracellular matrix remodeling in aortic valve

stenosis patients. A) Representative images of LV biopsies from control group and AVS patients. Biopsies were stained with sirius red to reveal collagen: red color indicates areas of collagen accumulation while the myocardium is of beige color. **B)** Quantification on collagens area (%) in LV biopsies stained with sirius red in control (white bar) and AVS group (dark grey). **C)** Representative images on LV biopsies from patients in control group and AVS patients. Biopsies were stained with against collagen I (red), α -SRC (green) and DAPI (blue). **D)** Quantification on collagen I area in stained LV biopsies. **E)** Mean normalised expression of CTGF normalized to UBC expression in LV of AVS group (dark grey) and referred to a control group (white bar). Values presented as mean \pm SEM. Student's t-test was performed in order to estimate statistical significance**p-value<0.01.***p-value<0.005.

4.3 miRNA-497-5p, miRNA-27b-5p and its target EGLN1 expression in left ventricle of aortic valve stenosis patients

We measured miRNA-27b-5p target EGLN1 expression (Figure 4.2 A). We observed a significant decrease of EGLN1 expression ($-\Delta\Delta\text{CT} = -0.5\pm 0.1$) in LV of AVS patients. This data corresponds to the up-regulation of miRNA-27b-5p ($-\Delta\Delta\text{CT} = 1.9\pm 0.4$) in the same biopsies (Figure 4.2 B), which was accompanied by miRNA-497-5p overexpression in LV biopsies of AVS patients ($-\Delta\Delta\text{CT} = 1.4\pm 0.3$) (Figure 4.2 C). In other words, miRNA-27b-5p and miRNA-497-5p are significantly up-regulated in LV of AVS patients characterized with increased collagens deposition.

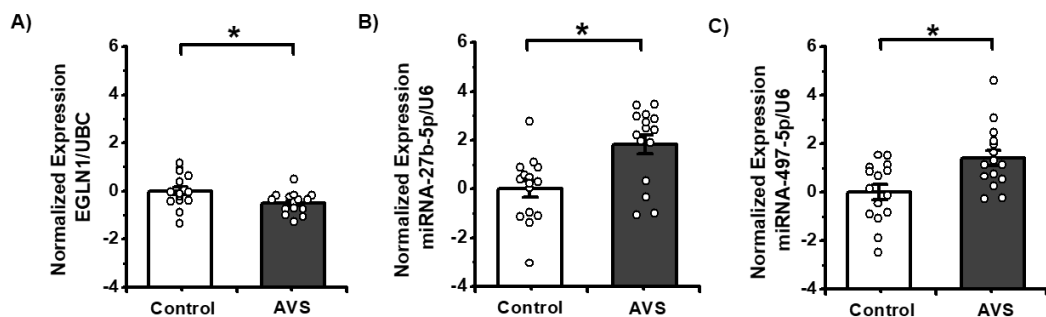


Figure 4.3 miRNA-27b-5p and miRNA-497-5p are up-regulated in LV of AVS patients characterized with increased Collagen deposition. A) Mean Normalized Expression of EGLN1 normalized to UBC expression in LV of AVS group (dark grey) and referred to a control group (white bar). **B)** Mean Normalized Expression of miRNA-27b-5p normalized to U6 expression in LV of AVS group (dark grey) and referred to a

control group (white bar). C) Mean Normalized Expression of miRNA-497-5p normalized to U6 expression in LV of AVS group (dark grey) and referred to a control group (white bar). Values presented as Mean \pm SEM. Student's t-test was performed in order to estimate statistical significance*P-value<0.05.

4.4 miRNA-497-5p and miRNA-27b-5p expression in peripheral blood plasma of aortic valve stenosis patients

As a next step, we managed both miRNAs expression in blood plasma of AVS patients (N = 25) and compared its expression with (N = 10) sex/age matched healthy donors of blood plasma. Interestingly, that both miRNA-27b-5p and miRNA-497-5p (Figure 4.4 A, B) were up-modulated in blood plasma of AVS patients ($-\Delta\Delta\text{CT} = 3.7\pm 0.4$) and ($-\Delta\Delta\text{CT} = 2.0\pm 0.4$).

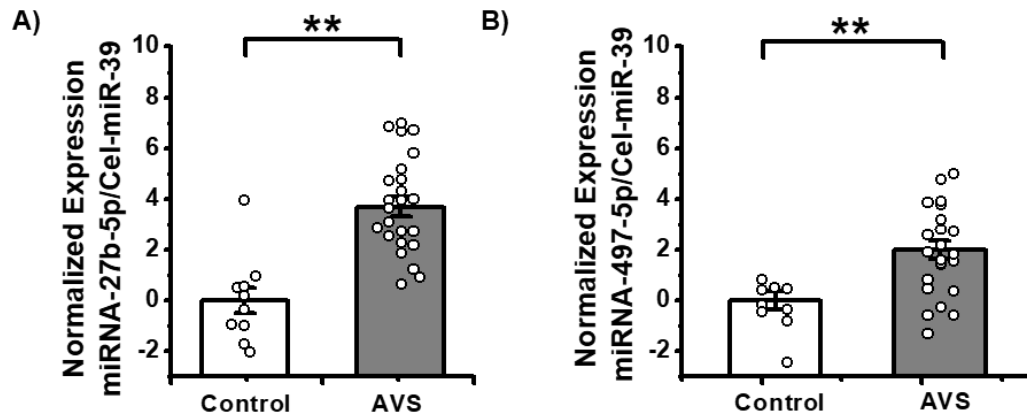
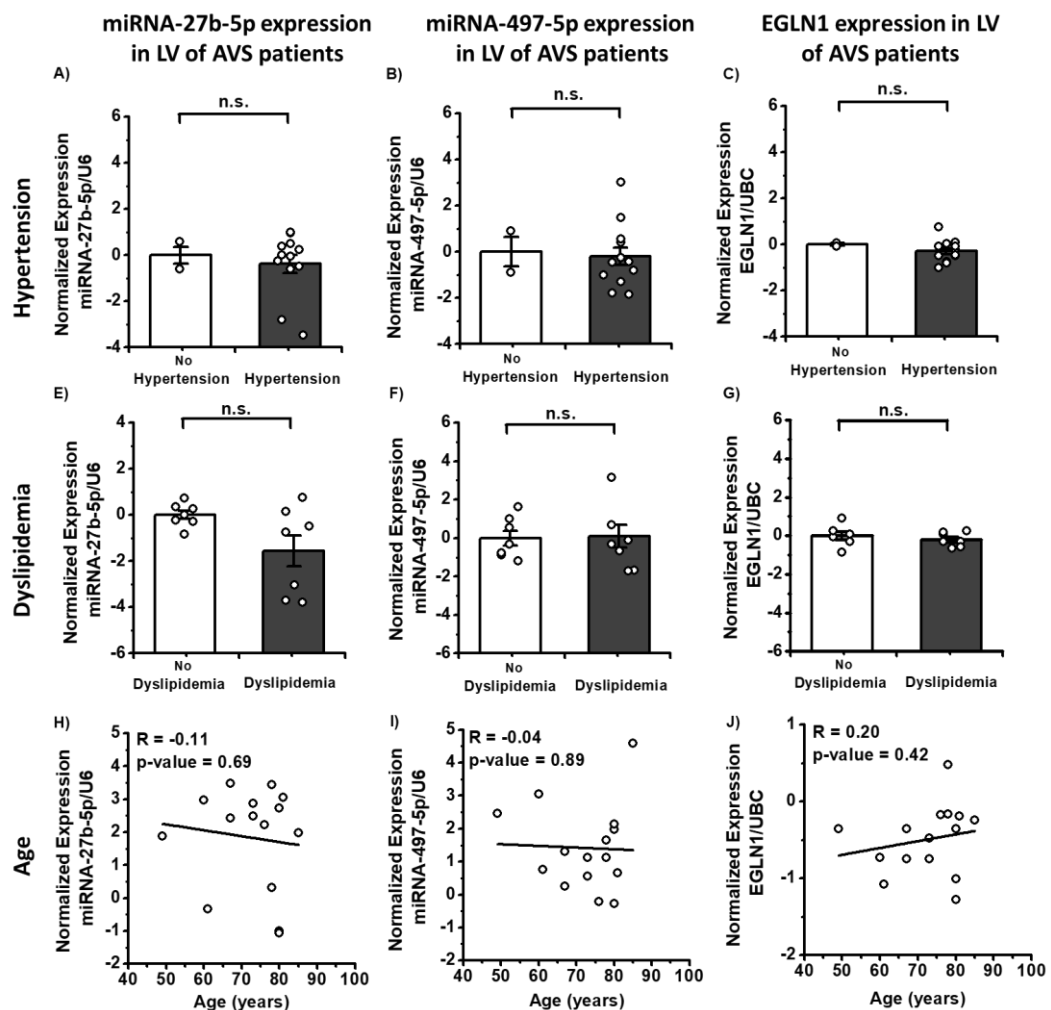


Figure 4.4 miRNA-27b-5p and miRNA-497-5p are up-regulated in BP of AVS patients characterized with increased collagen deposition. A) Mean normalized expression of miRNA-27b-5p normalized to U6 expression in BP of AVS group (grey) and referred to a control group (white bar). B) Mean normalized expression of miRNA-497-5p normalized to U6 expression in BP of AVS group (grey) and referred to a control group (white bar). Values presented as mean \pm SEM. Student's t-test was performed in order to estimate statistical significance. **p-value<0.01.

4.5 Co-morbidities effect on miRNA-27b-5p, miRNA-497-5p and EGLN1 expression in left ventricle biopsies from aortic valve stenosis patients

As we already mentioned in sections 4.1 and 3.1 of chapter IV, there are significant differences in the AVS and control groups in terms of age, presence of hypertension and dyslipidemia. For this reason, we performed a sub-analysis on

miRNA-27b-5p, miRNA-497-5p and EGLN1 expression in LV of AVS patients with hypertension or dyslipidemia (Figure 4.5). We demonstrated that our measured values are not different in terms of expression between AVS patients with or without hypertension (Figure 4.5 A-C). There was no significant regulation of miRNAs and EGLN1 expression observed in settings of dyslipidemia (Figure 4.5 D-F). In addition, miRNA-27b-5p, miRNA-497-5p and EGLN1 expression in LV of AVS patients did not demonstrate any significant correlation with patients age (Figure 4.5 H-J).



Supplementary Figure 5. miRNA-27b-5p, miRNA-497-5p and EGLN1 expression in LV of AVS patients with Hypertension, Dyslipidemia and in old patients. A)-J) RNA was isolated with Trizol from (N = 15) LV from AVS patients and (N = 15) controls that died from nonCVD reasons. **A)-B), E)-F), H)-I)** RT-qPCR on miRNAs. **C), G), J)** RT-qPCR on EGLN1. **A)-C)** miRNA-27b-5p, miRNA-497-5p and EGLN1

expression in LV of AVS patients with hypertension (N = 12) compared with AVS patients without hypertension (N = 2). **D)-F)** miRNA-27b-5p, miRNA-497-5p and EGLN1 expression in LV of AVS patients with dyslipidemia (N = 7) compared with AVS patients without dyslipidemia (N = 7). **H)-J)** Pearson correlation of miRNA-27b-5p, miRNA-497-5p and EGLN1 expression in LV of AVS with age (N = 15). **A)-G)** Values presented as Mean \pm SEM. Mann-Whitney was performed in order to estimate statistical significance, n.s. — non-significant. **H)-J)** Pearson correlation between expression and patients age.

4.6 miRNA-27b-5p and miRNA-497-5p are transferred via extracellular vesicles and can be potentially utilized as circulating biomarkers of cardiac fibrosis in aortic valve stenosis patients

miRNAs can circulate in blood encapsulated in extracellular vesicles (EVs) [31,32]. We isolated EVs from BP of AVS patients (N = 24) and (N = 10) healthy donors. EVs were characterized by transmission electron microscope with negative uranyl acetate staining (Figure 4.6 A). As was observed in EVs derived from blood plasma, miRNA-27b-5 (Figure 4.6 B) and miRNA-497-5p (Figure 4.6 C) expression in EVs was significantly higher in AVS patients. In addition, miRNAs levels in EVs derived from BP were correlating significantly (p-value<0.05) with miRNAs expression in BP itself (Figure 4.6 D, E).

As a next step we plotted ROC Curves based on miRNAs levels in EVs isolated from BP (Figure 4.6 F). Both miRNA-27b-5p and miRNA-497-5p were sensitive and specific biomarkers of AVS, as suggested by significantly high area under the curve (AUC) for each miRNA. This data demonstrated that both EVs encapsulated miRNA-27b-5p and miRNA-497-5p are sensitive and specific biomarkers when we are trying to distinguish patients AVS and healthy donors with preserved ejection fraction.

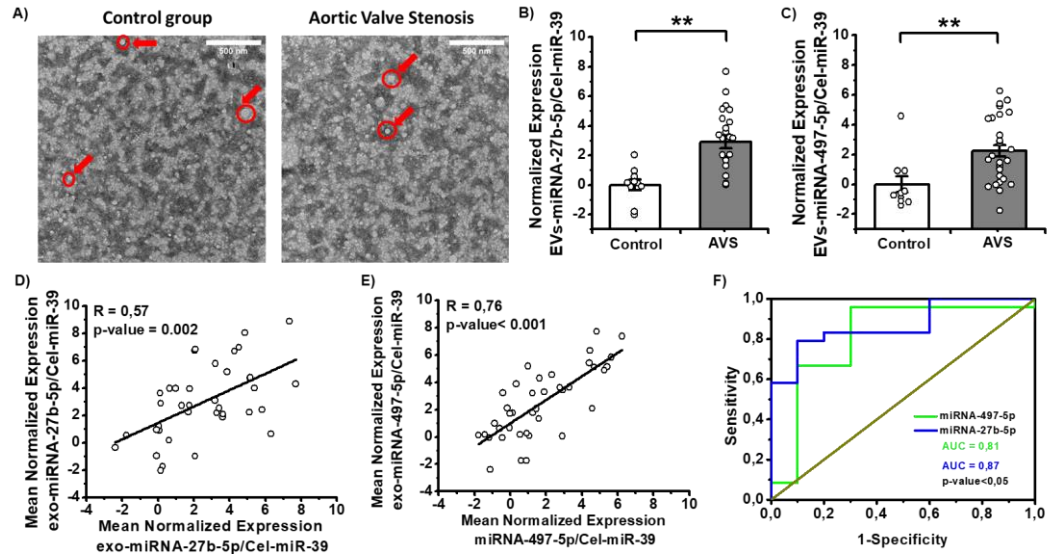


Figure 4.6 miRNA-27b-5p and miRNA-497-5p expression in EVs from peripheral blood and correlations with miRNAs levels in blood plasma. **A)** Representative images of EVs isolated from blood plasma. With red arrows and circles we highlighted single EVs. **B)** miRNA-27b-5p levels in EVs from BP (N = 24) (N = 10). Statistical significance was evaluated with Student's t-test **p-value<0.01. **C)** miRNA-497-5p expression in EVs from BP of AVS patients (N = 24) and healthy donors (N = 10). Statistical significance was evaluated with Student's t-test **p-value<0.01. **D)** Pearson correlation (N = 34) between mean normalized expression of exo-miRNA-27b-5p and miRNA-27b-5p expression in blood plasma. **E)** Pearson correlation (N = 34) between mean normalized expression of exo-miRNA-497-5p and miRNA-497-5p expression in blood plasma. **F)** ROC curve analysis based on expression of miRNA-497-5p (green), miRNA-27b-5p (blue) in EVs from BP of AVS (N = 24) and healthy donors (N = 10). All three options revealed significant AUC with p-value estimated by 2-tailed test of significance.

4.7 miRNA-27b-5p, miRNA-497-5p and EGLN1 correlations with extracellular remodeling characterized by histology, RT-qPCR and echo

We tested Pearson correlations between miRNA expression in LV, BP and EVs from BP with histology data, CTGF expression and clinical parameters in patients. As a result, we observed that miRNA-497-5p expression in LV positively correlates with collagen area (%) (Figure 4.7 A), CTGF expression (Figure 4.7 B) and with miRNA-27b-5p expression in LV (Figure 4.7 C). At the

same time, miRNA-27b-5p expression in LV of AVS patients was positively correlated with IVS thickness (Figure 4.7 D). Moreover, miRNA-27b-5p target, EGLN1, was negatively correlated with collagen area (%) (Figure 4.7 E) and CTGF expression (Figure 4.7 F). Surprisingly, miRNA expression in blood plasma did not show any correlation with clinical parameters. Interestingly, miRNA-27b-5p and miRNA-497-5p levels in EVs derived from BP of AVS patients was positively correlated with aortic peak gradient in AVS patients (Figure 4.7 G,H).

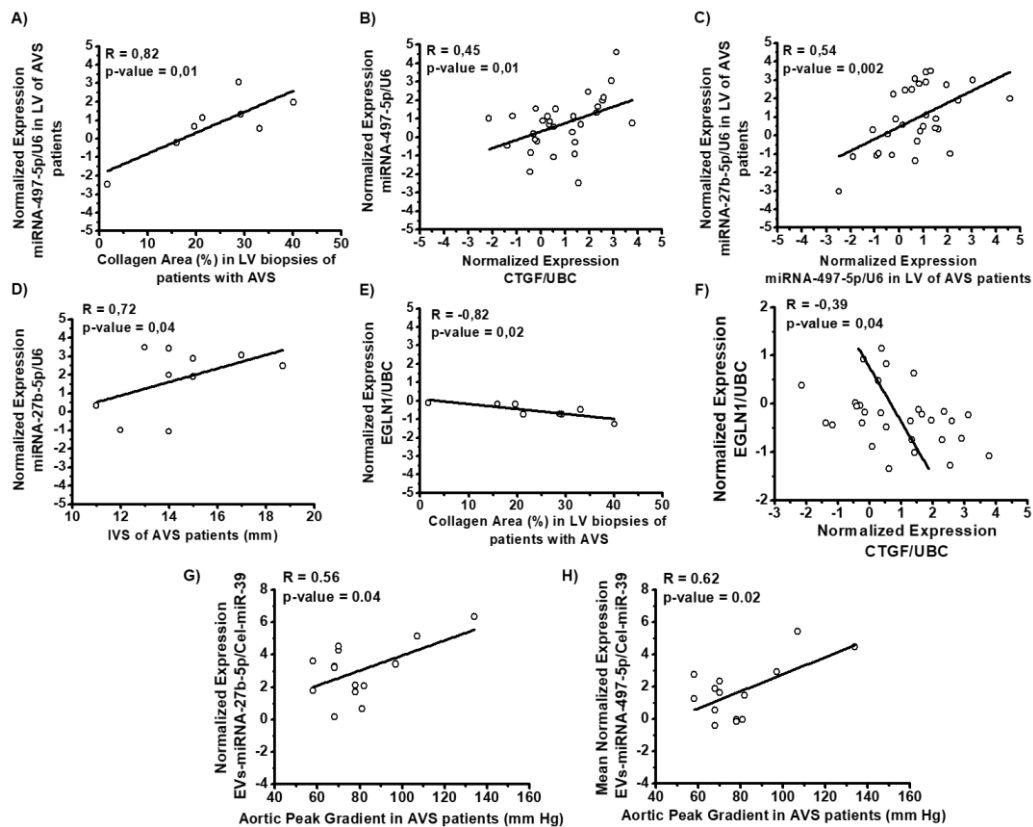


Figure 4.7 miRNA-27b-5p and miRNA-497-5p expression in EVs from peripheral blood and correlations with expression of fibrotic markers. **A)** Pearson correlation ($N = 8$) between mean normalized expression of miRNA-497-5p in LV of AVS patients with collagens area (%) measured in LV biopsies of AVS patients stained with sirius red. **B)** Pearson correlation ($N = 30$) between mean normalized expression of miRNA-497-5p in LV with mean normalized expression with CTGF in LV. **C)** Pearson correlation ($N = 30$) between mean normalized expression of miRNA-27b-5p in LV with mean normalized expression of miRNA-497-5p in LV. **D)** Pearson correlation ($N = 10$) between mean normalized expression of miRNA-27b-5p in LV of AVS patients with IVS (mm) in LV of AVS patients. **E)** Pearson correlation ($N = 8$) between Mean Normalized Expression of

EGLN1 in LV of AVS patients with collagens area (%) measured in LV biopsies of AVS patients stained with Sirius Red. **F)** Pearson correlation (N = 30) between mean normalized expression of EGLN1 in LV of AVS patients with mean normalized expression with CTGF in LV of AVS patients. **G)** Pearson correlation (N = 14) between mean normalized expression of miRNA-497-5p in EVs from BP of AVS patients with patients aortic peak gradient (mmHg). **H)** Pearson correlation (N = 14) between mean normalized expression of miRNA-27b-5p in EVs from BP of AVS patients with patients aortic peak gradient (mmHg).

4.8 Co-morbidities effect on miRNA-27b-5p and miRNA-497-5p expression in peripheral blood plasma from patients with aortic valve stenosis

As we already mentioned in sections 4.1 and 3.1 of chapter IV, there are significant differences in the AVS and control groups in terms of age, presence of hypertension and dyslipidemia. For this reason, we performed a sub-analysis on miRNA-27b-5p, miRNA-497-5p expression in peripheral PB and EVs derived from peripheral BP. We found that these co-morbidities did not affect miRNAs expression (Figure 4.8.1 and Figure 4.8.2). However, miRNA-497-5p expression in EVs derived from BP demonstrated a dependence on patient age (Figure 4.8.2 F).

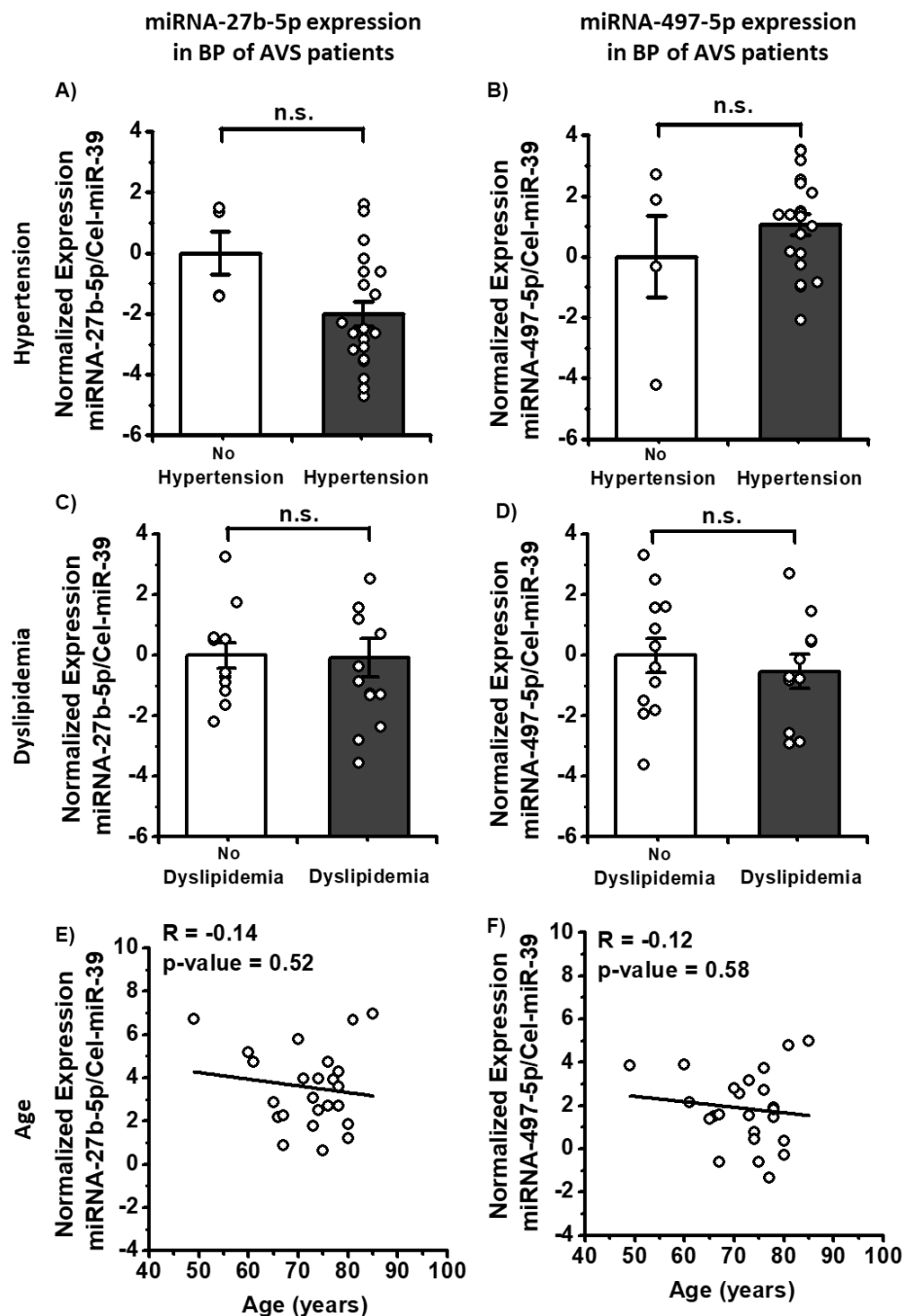
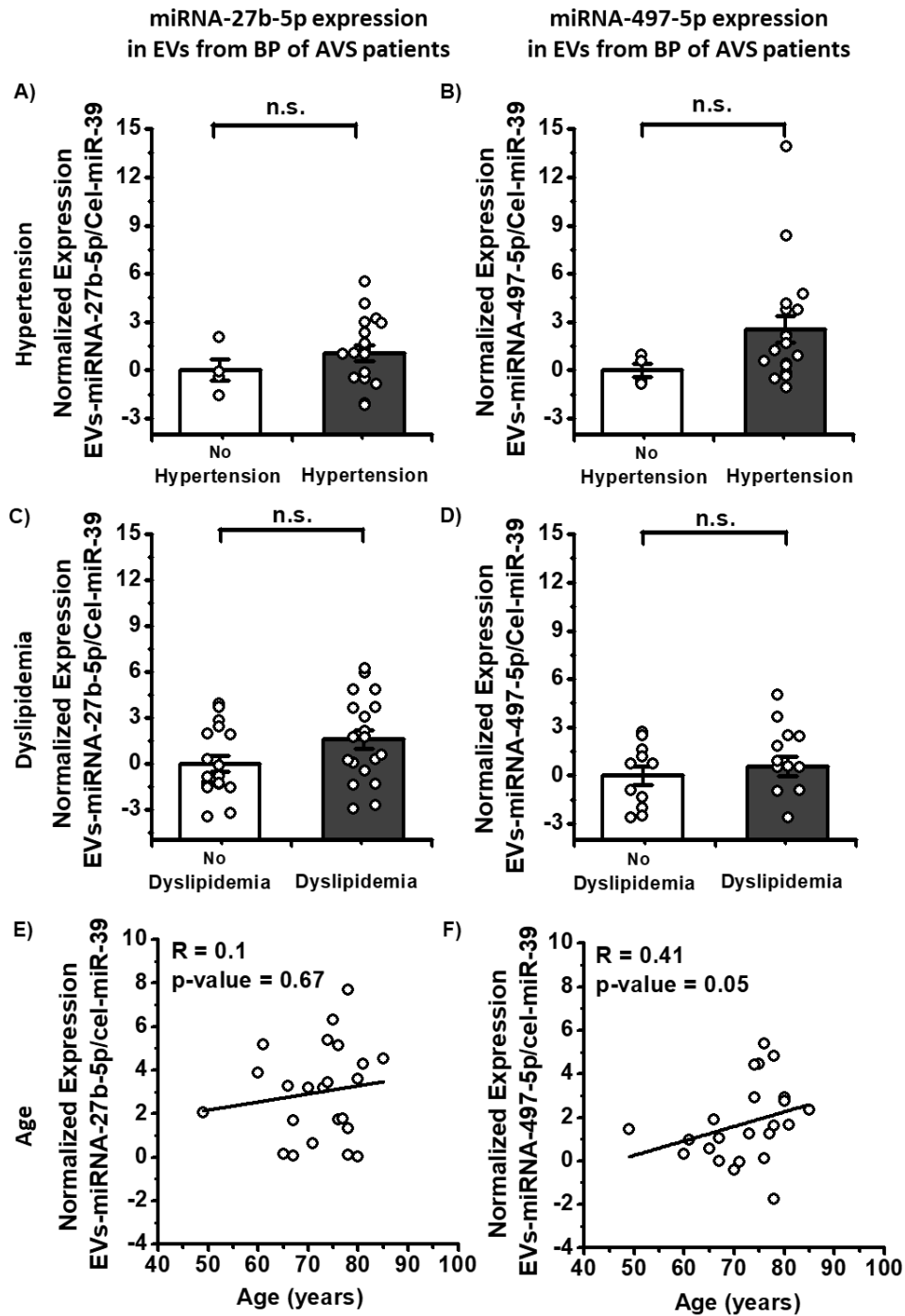


Figure 4.8.1 miRNA-27b-5p, miRNA-497-5p expression in peripheral blood from AVS patients with Hypertension, Dyslipidemia and in old patients. A) – F) miRNA from (N = 25) from BP of AVS patients and compared with miRNA isolated from (N = 10) healthy donors. miRNA of interest expression was normalized to cel-miR-39 and further referred to a Control group. **A)** miRNA-27b-5p in BP, **B)** miRNA-497-5p expression in AVS patients with Hypertension (N = 20) and compared with AVS patients without Hypertension (N = 4). **C)** miRNA-27b-5p in BP, **D)** miRNA-497-5p expression in AVS patients with Dyslipidemia (N = 12) and compared with AVS patients without

Dyslipidemia (N = 12). Pearson correlation between AVS patients age and **E**) miRNA-27b-5p in BP, **F**) miRNA-497-5p in BP. Values presented as Mean \pm SEM. Mann-Whitney was performed in order to estimate statistical significance, n.s. — non-significant.



Figure

4.8.2 miRNA-27b-5p, miRNA-497-5p expression in EVs from peripheral blood of AVS patients with Hypertension, Dyslipidemia and in old patients. A) – F) miRNA

from (N = 24) EVs from BP of AVS patients and compared with miRNA isolated from (N = 10) healthy donors. miRNA of interest expression was normalized to cel-miR-39 and further referred to a Control group. **A)** miRNA-27b-5p in EVs from BP, **B)** miRNA-497-5p in EVs from BP expression in AVS patients with Hypertension (N = 20) and compared with AVS patients without Hypertension (N = 4). **C)** miRNA-27b-5p in EVs from BP, **D)** miRNA-497-5p EVs from BP expression in AVS patients with Dyslipidemia (N = 12) and compared with AVS patients without Dyslipidemia (N = 12). Pearson correlation between AVS patients age and **E)** miRNA-27b-5p in EVs from BP, **F)** miRNA-497-5p in EVs from BP. Values presented as Mean \pm SEM. Mann-Whitney was performed in order to estimate statistical significance, n.s. — non-significant.

5. DISCUSSION IV

In order to identify if these miRNAs we characterized represent potential biomarker status, we observed their expression in patients with AVS with preserved ejection fraction. Current guidelines recommend that treatment of this patient group begin when patients begin to experience symptoms [29]. However, symptoms are difficult to assess in clinical practice in elderly comorbid patient and survival rates decrease dramatically after the onset of symptoms [44]. In asymptomatic patients, treatment is recommended for those with preserved LV function and critical AVS ($V_{max} > 5.5$ m/s) or rapid progressing AVS (> 0.3 m/s/year) or when LV function is impaired (LVEF $< 55\%$) without another cause. However, the latter condition is associated with an ongoing LV damage already established and the most recent guidelines have moved the threshold for considering LV dysfunction from $< 50\%$ [45] to $< 55\%$, highlighting the importance of early recognition of myocardial damage. Fibrosis represents a key feature of myocardial damage induced by the aortic stenosis which is interstitial at the early stages and later becomes replacement fibrosis, which is irreversible [46]. Therefore, timing for aortic valve replacement performed either by surgery or transcatheter (TAVI) is crucial to improve left ventricular remodeling and prognosis [47,48]. For this reason, identifying reliable blood biomarkers of cardiac fibrosis in these patients is extremely important. IL-11 was shown to be up-regulated in two mice models of arterial pressure loading and was playing a crucial role in aortic inflammation and fibrosis [42]. Therefore, we were aiming to check if IL-11 induced miRNA-27b-5p and miRNA-497-5p can be utilized as potential biomarkers of cardiac fibrosis within AVS patients with preserved ejection fraction. Group of AVS patients that we observed can be classified as severe AVS patients that require AVR or TAVR (table 3.1.2). In this study we demonstrated that both miRNA-27b-5p and miRNA-497-5p are up-regulated in the myocardium (Figure 4.2), blood plasma (Figure 4.3) and EVs derived from BP of AVS patients (Figure 4.6) characterized with intensive ECM accumulation (Figure 4.2). Interestingly, EGLN1, a target of miRNA-27b-5p, is down-regulated in the myocardium (Figure 4.3 A) of these patients and is negatively correlated with CTGF expression and collagen area in histology slides (Figure 4.7 E, F).

Plotted correlations indicated strong correlation of miRNA-497-5p levels in LV with CTGF expression and collagen area in histology slides (Figure 4.7 A, B), while miRNA-27b-5p was positively correlated with size of IVS (Figure 4.7 D). We were able to detect an up-regulation in levels of miRNA-27b-5p and miRNA-497-5p in EVs from peripheral BP (Figure 4.6 B, C). Interestingly, that plotted correlations between miRNAs levels in BP and in EVs from BP (Figure 4.6 D, E) may indicate that miRNAs are transferred with a blood flow encapsulated in vesicles. At the same time, we showed that miRNAs levels in EVs from blood plasma can be potentially used in order to distinguish healthy patients from AVS patients with preserved ejection fraction (Figure 4.6 F). Finally, miRNAs levels in EVs from peripheral BP of AVS patients was correlating with aortic PG, which is measured by echo and considered to be a reliable value that represents severity of AVS [49]. Using this data, we report miRNA-27b-5p and miRNA-497-5p as potential biomarkers of cardiac fibrosis in AVS patients with preserved ejection fraction.

6. REFERENCES IV

1. Brazile B, Wang B, Wang G, et al. On the bending properties of porcine mitral, tricuspid, aortic, and pulmonary valve leaflets. *Journal of Long-term Effects of Medical Implants*. **2015**;25(1-2):41-53. DOI: 10.1615/jlongtermeffmedimplants.2015011741. PMID: 25955006; PMCID: PMC6721960.
2. Schoen FJ. Evolving concepts of cardiac valve dynamics: the continuum of development, functional structure, pathobiology, and tissue engineering. *Circulation*. **2008**;118(18):1864-1880. doi:10.1161/CIRCULATIONAHA.108.805911
3. Taylor PM. Biological matrices and bionanotechnology. *Philos Trans R Soc Lond B Biol Sci*. **2007**;362(1484):1313-1320. doi:10.1098/rstb.2007.2117
4. Büttner P, Feistner L, Lurz P, Thiele H, Hutcheson JD, Schlotter F. Dissecting Calcific Aortic Valve Disease-The Role, Etiology, and Drivers of Valvular Fibrosis. *Front Cardiovasc Med*. **2021**;8:660797. Published 2021 May 10. doi:10.3389/fcvm.2021.660797
5. Faggiano P, Antonini-Canterin F, Baldessin F, Lorusso R, D'Aloia A, Cas LD. Epidemiology and cardiovascular risk factors of aortic stenosis. *Cardiovasc Ultrasound*. **2006**;4:27. Published 2006 Jul 1. doi:10.1186/1476-7120-4-27
6. van Geemen D, Soares AL, Oomen PJ, Driessen-Mol A, Janssen-van den Broek MW, van den Bogaardt AJ, Bogers AJ, Goumans MJ, Baaijens FP, Bouten CV. Age-Dependent Changes in Geometry, Tissue Composition and Mechanical Properties of Fetal to Adult Cryopreserved Human Heart Valves. *PLoS One*. **2016**;11(2):e0149020. doi: 10.1371/journal.pone.0149020. PMID: 26867221; PMCID: PMC4750936.
7. Otto CM, Kuusisto J, Reichenbach DD, Gown AM, O'Brien KD. Characterization of the early lesion of 'degenerative' valvular aortic

- stenosis. Histological and immunohistochemical studies. *Circulation*. **1994**;90(2):844-853. doi:10.1161/01.cir.90.2.844
8. Walker GA, Masters KS, Shah DN, Anseth KS, Leinwand LA. Valvular myofibroblast activation by transforming growth factor-beta: implications for pathological extracellular matrix remodeling in heart valve disease. *Circ Res*. **2004**;95(3):253-260. doi:10.1161/01.RES.0000136520.07995.aa
 9. Merryman WD, Youn I, Lukoff HD, et al. Correlation between heart valve interstitial cell stiffness and transvalvular pressure: implications for collagen biosynthesis. *Am J Physiol Heart Circ Physiol*. **2006**;290(1):H224-H231. doi:10.1152/ajpheart.00521.2005
 10. Bardon KM, Garelnabi M. The impact of altered mechanobiology on aortic valve pathophysiology. *Arch Biochem Biophys*. **2020**;691:108463. doi:10.1016/j.abb.2020.108463
 11. Leopold JA. Cellular mechanisms of aortic valve calcification. *Circ Cardiovasc Interv*. **2012**;5(4):605-614. doi:10.1161/CIRCINTERVENTIONS.112.971028
 12. Taylor PM, Allen SP, Yacoub MH. Phenotypic and functional characterization of interstitial cells from human heart valves, pericardium and skin. *J Heart Valve Dis*. **2000**;9(1):150-158.
 13. Rabkin-Aikawa E, Farber M, Aikawa M, Schoen FJ. Dynamic and reversible changes of interstitial cell phenotype during remodeling of cardiac valves. *J Heart Valve Dis*. **2004**;13(5):841-847.
 14. Singh S, Torzewski M. Fibroblasts and Their Pathological Functions in the Fibrosis of Aortic Valve Sclerosis and Atherosclerosis. *Biomolecules*. **2019**;9(9):472. Published 2019 Sep 10. doi:10.3390/biom9090472
 15. Goody PR, Hosen MR, Christmann D, et al. Aortic Valve Stenosis: From Basic Mechanisms to Novel Therapeutic Targets. *Arterioscler Thromb Vasc Biol*. **2020**;40(4):885-900. doi:10.1161/ATVBAHA.119.313067

16. Osnabrugge RL, Mylotte D, Head SJ, et al. Aortic stenosis in the elderly: disease prevalence and number of candidates for transcatheter aortic valve replacement: a meta-analysis and modeling study. *J Am Coll Cardiol.* **2013**;62(11):1002-1012. doi:10.1016/j.jacc.2013.05.015
17. Grimard BH, Safford RE, Burns EL. Aortic Stenosis: Diagnosis and Treatment. *Am Fam Physician.* **2016**;93(5):371-378
18. Summerhill VI, Moschetta D, Orekhov AN, Poggio P, Myasoedova VA. Sex-Specific Features of Calcific Aortic Valve Disease. *Int J Mol Sci.* **2020**;21(16):5620. Published 2020 Aug 6. doi:10.3390/ijms21165620
19. Saito Y, Lewis EE, Raval A, Gimelli G, Jacobson KM, Osaki S. The Prognosis of Elderly Patients with Aortic Stenosis after Transcatheter Aortic Valve Replacement. *Intern Med.* **2021**;15;60(4):517-523. doi: 10.2169/internalmedicine.5047-20. Epub 2020 Oct 7. PMID: 33028765; PMCID: PMC7946496.
20. Shulaw RK. Transcatheter aortic valve replacement. *Dimens Crit Care Nurs.* **2012**;31(6):311-317. doi:10.1097/DCC.0b013e31826bc60e
21. Kvaslerud AB, Santic K, Hussain AI, et al. Outcomes in asymptomatic, severe aortic stenosis. *PLoS One.* **2021**;16(4):e0249610. Published 2021 Apr 7. doi:10.1371/journal.pone.0249610
22. Doris MK, Everett RJ, Shun-Shin M, Clavel MA, Dweck MR. The Role of Imaging in Measuring Disease Progression and Assessing Novel Therapies in Aortic Stenosis. *JACC Cardiovasc Imaging.* **2019**;12(1):185-197. doi:10.1016/j.jcmg.2018.10.023
23. Rusinaru D, Malaquin D, Maréchaux S, Debry N, Tribouilloy C. Relation of Dimensionless Index to Long-Term Outcome in Aortic Stenosis With Preserved LVEF. *JACC Cardiovasc Imaging.* **2015**;8(7):766-775. doi:10.1016/j.jcmg.2015.01.023
24. Bohbot Y, Kowalski C, Rusinaru D, Ringle A, Marechaux S, Tribouilloy C. Impact of Mean Transaortic Pressure Gradient on Long-Term Outcome

- in Patients With Severe Aortic Stenosis and Preserved Left Ventricular Ejection Fraction. *J Am Heart Assoc.* **2017**;6(6):e005850. Published 2017 Jun 1. doi:10.1161/JAHA.117.005850
25. Galderisi M, Henein MY, D'hooge J, et al. Recommendations of the European Association of Echocardiography: how to use echo-Doppler in clinical trials: different modalities for different purposes. *Eur J Echocardiogr.* **2011**;12(5):339-353. doi:10.1093/ejechocard/jer051
 26. Myerson SG, Bellenger NG, Pennell DJ. Assessment of left ventricular mass by cardiovascular magnetic resonance. *Hypertension.* **2002**;39(3):750-755. doi:10.1161/hy0302.104674
 27. Lancellotti P, Moonen M, Magne J, et al. Prognostic effect of long-axis left ventricular dysfunction and B-type natriuretic peptide levels in asymptomatic aortic stenosis. *Am J Cardiol.* **2010**;105(3):383-388. doi:10.1016/j.amjcard.2009.09.043
 28. Bergler-Klein J, Klar U, Heger M, et al. Natriuretic peptides predict symptom-free survival and postoperative outcome in severe aortic stenosis. *Circulation.* **2004**;109(19):2302-2308. doi:10.1161/01.CIR.0000126825.50903.18
 29. Vahanian A, Beyersdorf F, Praz F, et al. 2021 ESC/EACTS Guidelines for the management of valvular heart disease [published correction appears in *Eur Heart J.* 2022 Feb 18]. *Eur Heart J.* **2022**;43(7):561-632. doi:10.1093/eurheartj/ehab395
 30. Yarbrough WM, Mukherjee R, Ikonomidis JS, Zile MR, Spinale FG. Myocardial remodeling with aortic stenosis and after aortic valve replacement: mechanisms and future prognostic implications. *J Thorac Cardiovasc Surg.* **2012**;143(3):656-664. doi:10.1016/j.jtcvs.2011.04.044
 31. Kapelouzou A, Tsourelis L, Kaklamanis L, Degiannis D, Kogerakis N, Cokkinos DV. Serum and tissue biomarkers in aortic stenosis. *Glob Cardiol Sci Pract.* **2015**;2015(4):49. Published 2015 Nov 13. doi:10.5339/gcsp.2015.49

32. Sun W, Julie Li YS, Huang HD, Shyy JY, Chien S. microRNA: a master regulator of cellular processes for bioengineering systems. *Annu Rev Biomed Eng.* **2010**;12:1-27. doi:10.1146/annurev-bioeng-070909-105314
33. Szemraj-Rogucka ZM, Szemraj J, Masiarek K, Majos A. Circulating microRNAs as biomarkers for myocardial fibrosis in patients with left ventricular non-compaction cardiomyopathy. *Arch Med Sci.* **2019**;15(2):376-384. doi:10.5114/aoms.2019.82919
34. García R, Villar AV, Cobo M, et al. Circulating levels of miR-133a predict the regression potential of left ventricular hypertrophy after valve replacement surgery in patients with aortic stenosis. *J Am Heart Assoc.* **2013**;2(4):e000211. Published 2013 Aug 15. doi:10.1161/JAHA.113.000211
35. Villar AV, García R, Merino D, et al. Myocardial and circulating levels of microRNA-21 reflect left ventricular fibrosis in aortic stenosis patients. *Int J Cardiol.* **2013**;167(6):2875-2881. doi:10.1016/j.ijcard.2012.07.021
36. Zhou P, Pu WT. Recounting Cardiac Cellular Composition. *Circ Res.* **2016**;118(3):368-370. doi:10.1161/CIRCRESAHA.116.308139
37. Perbellini F, Watson SA, Bardi I, Terracciano CM. Heterocellularity and Cellular Cross-Talk in the Cardiovascular System. *Front Cardiovasc Med.* **2018**;5:143. Published 2018 Nov 1. doi:10.3389/fcvm.2018.00143
38. Watson SA, Duff J, Bardi I, et al. Biomimetic electromechanical stimulation to maintain adult myocardial slices in vitro. *Nat Commun.* **2019**;10(1):2168. Published 2019 May 15. doi:10.1038/s41467-019-10175-3
39. Tkach M, Kowal J, Théry C. Why the need and how to approach the functional diversity of extracellular vesicles. *Philos Trans R Soc Lond B Biol Sci.* **2018**;373(1737):20160479. doi:10.1098/rstb.2016.0479

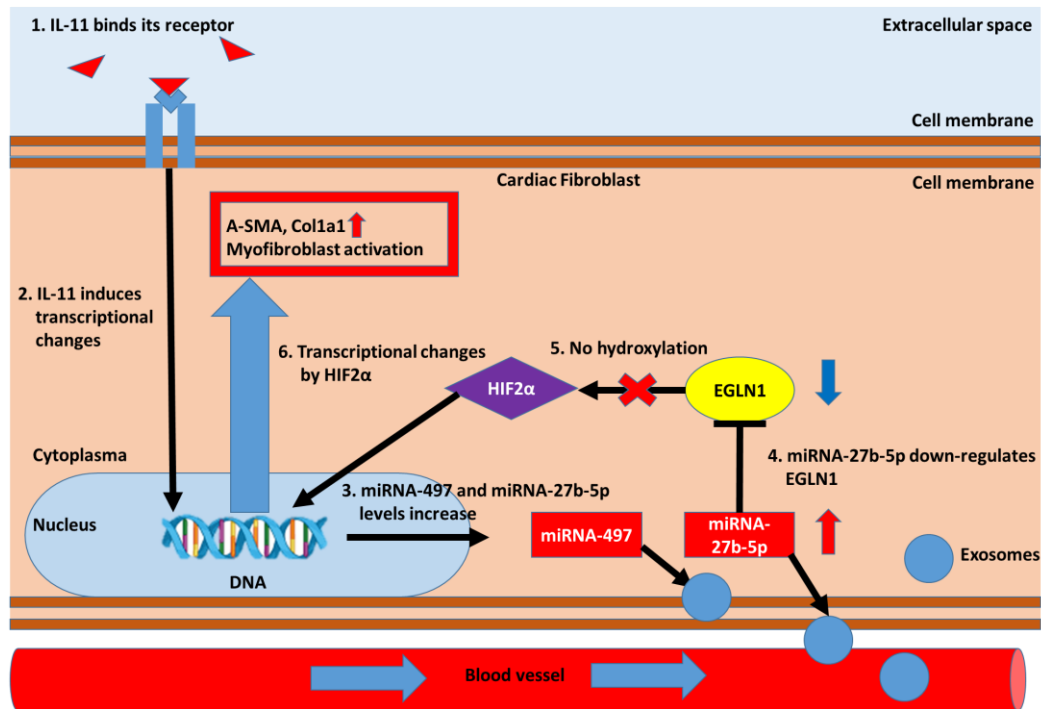
40. Lamichhane TN, Jay SM. Production of Extracellular Vesicles Loaded with Therapeutic Cargo. *Methods Mol Biol.* **2018**;1831:37-47. doi:10.1007/978-1-4939-8661-3_4
41. Wang L, Liu J, Xu B, Liu YL, Liu Z. Reduced exosome miR-425 and miR-744 in the plasma represents the progression of fibrosis and heart failure. *Kaohsiung J Med Sci.* **2018**;34(11):626-633. doi:10.1016/j.kjms.2018.05.008
42. Lim WW, Corden B, Ng B, Vanezis K, D'Agostino G, Widjaja AA, Song WH, Xie C, Su L, Kwek XY, Tee NGZ, Dong J, Ko NSJ, Wang M, Pua CJ, Jamal MH, Soh B, Viswanathan S, Schafer S, Cook SA. Interleukin-11 is important for vascular smooth muscle phenotypic switching and aortic inflammation, fibrosis and remodeling in mouse models. *Sci Rep.* **2020** ;10(1):17853. doi: 10.1038/s41598-020-74944-7. PMID: 33082445; PMCID: PMC7576123.
43. Livak KJ, Schmittgen TD. Analysis of relative gene expression data using real-time quantitative PCR and the 2^{(-Delta Delta C(T))} Method. *Methods.* **2001**;25(4):402-8. doi: 10.1006/meth.2001.1262. PMID: 11846609.
44. Bevan GH, Zidar DA, Josephson RA, Al-Kindi SG. Mortality Due to Aortic Stenosis in the United States, 2008-2017. *JAMA.* **2019**;321(22):2236–2238. doi:10.1001/jama.2019.6292
45. Baumgartner H, Falk V, Bax JJ, et al. 2017 ESC/EACTS Guidelines for the management of valvular heart disease. *Eur Heart J.* **2017**;38(36):2739-2791. doi:10.1093/eurheartj/ehx391
46. Bing R, Cavalcante JL, Everett RJ, Clavel MA, Newby DE, Dweck MR. Imaging and Impact of Myocardial Fibrosis in Aortic Stenosis. *JACC Cardiovasc Imaging.* **2019**;12(2):283-296. doi:10.1016/j.jcmg.2018.11.026
47. Treibel TA, Kozor R, Schofield R, Benedetti G, Fontana M, Bhuvana AN, Sheikh A, López B, González A, Manisty C, Lloyd G, Kellman P, Díez J, Moon JC. Reverse Myocardial Remodeling Following Valve Replacement in Patients With Aortic Stenosis. *J Am Coll Cardiol.* **2018**;27;71(8):860-

871. doi: 10.1016/j.jacc.2017.12.035. PMID: 29471937; PMCID: PMC5821681

48. Everett RJ, Tastet L, Clavel MA, Chin CWL, Capoulade R, Vassiliou VS, Kwiecinski J, Gomez M, van Beek EJR, White AC, Prasad SK, Larose E, Tuck C, Semple S, Newby DE, Pibarot P, Dweck MR. Progression of Hypertrophy and Myocardial Fibrosis in Aortic Stenosis: A Multicenter Cardiac Magnetic Resonance Study. *Circ Cardiovasc Imaging*. **2018**;11(6):e007451. doi: 10.1161/CIRCIMAGING.117.007451. PMID: 29914867; PMCID: PMC6023592
49. Saikrishnan N, Kumar G, Sawaya FJ, Lerakis S, Yoganathan AP. Accurate assessment of aortic stenosis: a review of diagnostic modalities and hemodynamics [published correction appears in *Circulation*. 2014 Oct 7;130(15):e136]. *Circulation*. **2014**;129(2):244-253. doi:10.1161/CIRCULATIONAHA.113.002310

CONCLUSIONS

Cardiac fibrosis is the pathology which accompanies various CVD (like MI, ICM, DCM and AVS) and adverse heart functions and integrity by ECM deposition. In AVS patients cardiac fibrosis is one of the key features leading to a decrease in ejection fraction, which is used to make a decision upon surgery for the patients. There is a real clinical need to establish reliable blood biomarkers of cardiac fibrosis which can help inform clinical decisions before symptoms present. This is the first study to report on potential utilization of miRNA-497-5p-5p and miRNA-27b-5p as biomarker of cardiac fibrosis in AVS patients with preserved ejection fraction. Both miRNAs activate fibroblast transdifferentiation into myofibroblasts and collagen I production in healthy and pathological MI/DCM/ICM CFs. We believe that our study provides the evidence that these miRNAs can be used in the decision making process for cardiac surgery in AVS patients. Moreover, miRNAs are released in peripheral blood encapsulated in EVs where they can be easily detected. Importantly, we found that both miRNAs are critical component of the IL-11 pro-fibrotic mechanism. In particular, we found a novel mechanism which underlies IL-11 signaling in CFs: EGLN1 suppression by miRNA-27b-5p. Thus this study may serve as a starting point for further investigation upon EGLN1 and hypoxia signaling in cardiac fibrosis. This potential mechanism is described in the schematic 1: During MI or in pressure overload TGF β 1 triggers IL-11 autocrine production. IL-11 stimulation of CFs leads to increase of miRNA-497-5p-5p and miRNA-27b-5p expression. Following this, miRNA-27b-5p is responsible for EGLN1 suppression and further HIF2 α stabilization. That leads to fibroblasts to myofibroblasts transition and increased collagen I production. In parallel, miRNAs are released in blood plasma encapsulated in EVs. Nevertheless, increase in the number of myofibroblasts during miRNA-27b-5p overexpression in human DCM and ICM CFs was not followed by EGLN1 down-regulation. That fact can indicate the pro-fibrotic role of miRNA-27b-5p is performed through another mechanism.



Schematic 1. Proposed molecular mechanism of miRNA-27b-5p and miRNA-497-5p contribution in cardiac fibrosis. During MI or in pressure overload TGFβ1 triggers IL-11 autocrine production. IL-11 stimulation of CFs leads to increase of miRNA-497-5p-5p and miRNA-27b-5p expression. Following this, miRNA-27b-5p is responsible for EGLN1 suppression and further HIF2α stabilization. That leads to fibroblasts to myofibroblasts transition and increased collagen I production. In parallel, miRNAs are released in blood plasma encapsulated in EVs.

PHD COURSE ACTIVITIES

PUBLICATIONS

- **Tikhomirov R**, Donnell BR, Catapano F, et al. Exosomes: From Potential Culprits to New Therapeutic Promise in the Setting of Cardiac Fibrosis. *Cells*. **2020**;9(3):592. Published 2020 Mar 2. doi:10.3390/cells9030592

Abstracts:

- **Tikhomirov R**, Donnell BR, Lucarelli C, Greco S, Zaccagnini G, Maryam A, Menicanti L, Leszek P, Faggian G, Srivastava P, Emanuelli C, Martelli F, Gorelik J. Identification of miRNA-497 and miRNA-27b-5p as potential diagnostic markers of cardiac fibrosis, *European Heart Journal*, Volume 42, Issue Supplement_1, October **2021**, ehab724.3344, <https://doi.org/10.1093/eurheartj/ehab724.3344>
- Greco S, Made' A, Longo M, **Tikhomirov R**, Castelvechio S, Menicanti L, Martelli F, P5398 CircRNAs deregulation in heart failure patients, *European Heart Journal*, Volume 40, Issue Supplement_1, October **2019**, ehz746.0358, <https://doi.org/10.1093/eurheartj/ehz746.0358>

Manuscripts in preparation:

- Reilly-O'Donnell B, Ferraro E, **Tikhomirov R**, Nunez-Toldra R, Shchendrygina A, Patel L, Wu Y, Mitchell AL, Endo A, Adorini, L, Chowdhury RA, Srivastava PK, Ng FS, Terracciano CM, Williamson C, Gorelik J. UDCA and INT-777 suppress cardiac fibrosis triggered by IL-11 through involvement of TGR5. *MedRxiv*, **2022**;2022.05.11.22274945. <https://doi.org/10.1101/2022.05.11.22274945>
- **Tikhomirov R**, Donnell BR, Lucarelli C, Yiu CHK, Greco S, Zaccagnini G, Mansfield C, Tessari M, Menicanti L, Dielesen J, Leszek P, Maryam A, Srivastava P, Faggian G, Emanuelli C, Martelli F, Gorelik J. Interleukin 11-induced microRNAs as functional mediators and circulating biomarkers of cardiac fibrosis

- Greco S, Made A, Bibi A, Garcia Manteiga J, Tascini AS, Piella SN, **Tikhomirov R**, Voellenkle C, Gaetano C, Leszek P, Paolin A, Castel Vecchio S, Menicanti L, Martelli F. circRNA-miRNA-mRNA deregulated network in ischemic heart failure patients

CONFERENCES

Poster sessions:

- ESC Congress 2021 – The Digital Experience, 27.08.2021, Poster presentation: Identification of miRNA-497 and miRNA-27b-5p as potential diagnostic markers of cardiac fibrosis
- National Heart and Lung Institute Research Away Day, 26.02.2021, United Kingdom, London Poster presentation: miRNA-27b and miRNA-497 as a potential diagnostics tools for cardiac fibrosis

Oral sessions:

- 3rd EU Cardio RNA meeting, 18.10.2019, Turkey, Istanbul, Oral report: Exosomes in cardiac fibrosis
- 8th EU Cardio RNA meeting, 27.05.2022, Pavia, Italy, Oral report: miRNA-27b-5p is inducing fibroblasts transdifferentiation into myofibroblasts by targeting EGLN1 in vitro

Teaching activity:

Day to day technical supervisor of MRes in Biomedical Research: Respiratory and Cardiovascular sciences, Julia Jeanette Dielesen and Kendrick Yiu. Project: “Characterizing the effect of miRNA-27b upon cardiac fibrosis”. 2020-2021, Imperial College, London.

ACKNOWLEDGMENTS

First of all, I would like to express my gratitude to Prof. Giuseppe Faggian for giving me an opportunity to join University of Verona, despite my different scientific background. I truly appreciate his infinite support in the challenging life situations. I would like to genially thank Dr. Fabio Martelli for his unbelievable patience and great impact on my knowledge and scientific progress. I would like to extremely thank Prof. Costanza Emanuelli for her constant help and for her deep knowledge in the advanced science of extracellular vesicles. It would be impossible to write this section without infinite thanks to Prof. Gorelik, who formed me not only as a scientist but also as a person. With her wise and experienced leadership, I have improved. I would like to be thankful to my technical supervisor and super-scientific friend Dr. Benedict Reilly-O'Donnell, an indispensable post-doctoral researcher in the Prof. Gorelik lab. With his gold hands almost each member of the lab learned how to do a proper research on cardiac fibroblasts. I would like to thank Dr.ssa Simona Greco and Dr.ssa Germana Zaccagnini who taught me with numbers of techniques and modern methods. I would like to give my extreme thanks to Dr. Srivastava Prashant who was my guiding light in the world of bioinformatics and prediction tools.

It is impossible to underestimate the support that Stefano Poggiolini and Prof. Giovanni Battista Luciani, people who showed themselves as reliable and helping gentlemen.

I would say huge thank to my colleagues Carla Lucarelli and Sasha Judina, who became role models for me during my PhD project. Their dedication and deep understanding of their topics influenced on me.

I want to be thankful to my friends who were always ready to give a helping hand: Zoe Kwang, Neda Mohamadi, Pragati Pandey, Vladislav Leonov, Sanchez Alonso-Mardones.

I want to say thanks for the technical assistance of the Advanced Light and Electron Microscopy BioImaging Center (ALEMBIC) in San Raffaele Hospital, and especially to Maria Carla Panzeri and Valeria Berno. I am also thankful to

Marialucia Longo for sections preparation from left ventricle of aortic valve stenosis patients.

I would like to express my gratitude to my MS students: Julia Dielesen and Yiu Chi Him Kendrick. I am extremely proud to watch over your success in the scientific field. It was a pleasure to work with you on your projects.

I would like to say special thanks to Prof. Cesare Terracciano from NHLI, Imperial College, London, who provided us with CFs from LV of human donor.

I would like to thank an important people for me, my family, all of them built me, taught me how to set my goals and how to overcome difficulties.

The last but not the least, I would like to say warm thanks to my girlfriend and future wife Sasha Korogodski. Her infinite care and love is helping me every day to get over the covid crisis and the war between our countries.